FORSCHUNGSZENTRUM ROSSENDORF FZR-179

Nuclear and Hadron Physics and Project ELBE

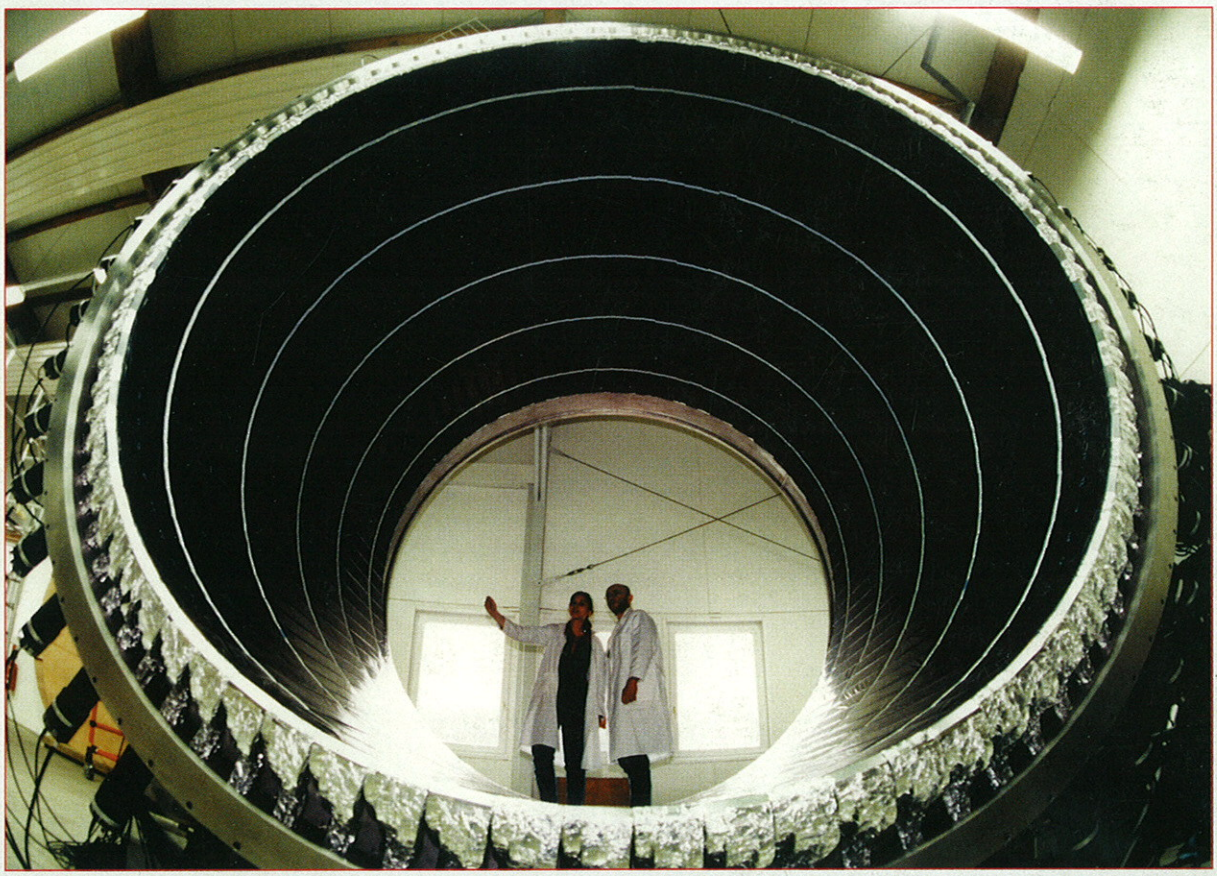

Annual Report 1996

Cover Picture:
The front cover displays the barrel hodoscope of the Time - of - Flight (TOF) Spectrometer for COSY experiments developed and assembled in Rossendorf (cf. page 95).

The use of the cover picture was permitted by Fotoagentur Zentralbild GmbH.
Photograph: Schutt Martin

Forschungszentrum Rossendorf e.V.

Postfach 51 01 19
D-01314 Dresden
Bundesrepublik Deutschland

Telefon +49 (3 51) 2 60 22 70
Telefax +49 (3 51) 2 60 37 00
E-Mail E. Grosse@fz-rossendorf.de

FZR - 179
April 1997

Annual Report 1996

Nuclear and Hadron Physics and Project ELBE

Editors:
H.W. Barz, F. Dönau, W. Enghardt, E. Grosse,
B. Kämpfer, H. Prade, M. Schlett, R. Wünsch

Explanation of special symbols:

The letters given in brackets in the following text and used as appendix in the title of the scientific contributions do express our grateful acknowledgement to the funding, sponsoring or grants provided by several institutions.

Research projects were funded by the Federal Ministry of Education, Science, Research and Technology BMBF (B), by the German Research Community DFG (D), by the GSI Darmstadt (G), by the KFA Jülich (K), were sponsored by the German Academic Exchange Service DAAD (A) or within Scientific agreements with eastern European countries (W). Several activities were funded by EC contracts (E) or INTAS contracts (I) or by the Landau-Heisenberg programme (L). All other support by special contracts or grants is indicated by (S).

CONTENTS

Preface

The Forschungszentrum Rossendorf (FZR), a research center at the outskirts of Dresden, traditionally has had - and still has - an intensive research program in the fields of nuclear and hadron physics; experimental projects at various accelerators outside of the center are pursued as well as number of theoretical investigations in this domain. This Annual Report presents the latest results of pure research performed within the Institute of Nuclear and Hadron Physics (IKH), out of which a few highlights should be mentioned here: In the Hadron Physics Department interesting results - experimental as well as theoretical - were obtained concerning the role of strangeness in hadronic and nuclear processes. The TOF spectrometer at the Jülich COSY ring - an experiment with strong Rossendorf participation - will be able to increase its role in this exciting field after the installation of the large scintillator barrel built at Rossendorf and shown on the front cover. The Department of Nuclear Physics reports new results on the study of heavy-ion collision dynamics by the observation of proton correlations and on a recently observed mode of tripartition of heavy nuclei - a fission in three nearly equal parts. The nuclear spectroscopy activites will gain heavily from the completion of EUROBALL, an European project of a large acceptance photon spectrometer which was partly built at the FZR; in that respect new rotational modes - "magnetic" and "chiral", both first predicted at Rossendorf - are of special interest.

The Annual Report also gives examples of the interesting applications of nuclear physics methods - experimental and theoretical - to other fields of science and technology, especially biomedical research. An outstanding example of such a transfer of technology developed for fundamental research in subatomic physics to various other fields is the project ELBE which was officially started at the FZR in 1996. This facility will come into operation in 1999 or 2000, its heart will be a superconducting linear accelerator with similar rf-linac-structures as developed at the particle physics laboratory DESY to become part of their future accelerator. At Rossendorf, it will bring electrons to 20 - and later 40 - MeV, i.e. to more than 99 % velocity of light. Its low emittance and thus high brilliance beam will allow the favourable use of different methods to produce electromagnetic radiation from it; as a brilliant source of photons in a wide range of wavelengths it is named Radiation Source ELBE (ELBE-Quelle). The project ELBE is part of this Annual Report as the Institute of Nuclear and Hadron Physics has initiated this project and is now heavily involved in design studies for ELBE and the related experiments.

In the first chapter some of the components of ELBE are presented as well as preparative studies performed at the electron accelerator S-DALINAC at TH Darmstadt. Among the work performed there are experiments on inelastic photon scattering from nuclei; these studies are part of the FZR nuclear spectroscopy program presented in chapter 4. The chapter on Hadron Physics (no. 2) combines meson production studies performed with heavy ion projectiles at the heavy ion synchrotron SIS at GSI Darmstadt to experiments performed with proton beams at COSY (KFA Jülich) and to related theoretical investigations. The third chapter combines theoretical and experimental results of investigations on the dynamics of nuclear reactions; the experiments were performed at the JINR at Dubna and also at the SIS. Chapter 5 is devoted to biomedical research using nuclear physics methods; it is followed by a chapter (no. 6) on technological developments, from which the contributions of the Rossendorf Detector Laboratory deserve special attention.

The traditional Holzhau-Meeting which was held in March 1996 gathered a number of well-known scientists from the fields of radiation and free electron laser physics. It thus became a milestone for the design and the research program of the Radiation Source ELBE. The second part of the meeting was devoted to nuclear structure physics with large detector arrays as well as to problems related to the role of strangeness, charm and beauty in medium energy physics; both topics are of strong interest for our institute.

The scientific activities of the Institute have benefitted from generous support from various institutions. First of all, we gratefully acknowledge the close and fruitful collaboration with the Institute for Nuclear and Particle Physics of the TU Dresden and many other scientific institutes in Germany and abroad; such contacts are of vital importance for our institute. Specific projects were financially supported by the Federal Ministry for Education, Science, Research and Technology (BMBF), the German Research Community (DFG), the Saxon State Ministry for Science and Art (SMWK), KFA Jülich and GSI Darmstadt. We express our gratitude to all these institutions as well as to the Executive Board of the Forschungszentrum Rossendorf for its essential support of the ELBE project.

Eckart Grosse

The Radiation Source ELBE

On September 25, 1996 the Supervisors of the Forschungszentrum Rossendorf (FZR) authorized the construction of a superconducting 20 MeV ELectron Source with high Brilliance and low Emittance (ELBE). This electron accelerator will be used to drive a Free Electron Laser (FEL) for the production of infrared radiation in the wavelength region of about 10μm - 200 μm and to perform experimental investigations in nuclear and radiation physics. In addition, it is planned to produce positrons and neutrons as a tool for material research purposes.
The realization of the project - which is planned to be completed by the end of 1999 - is a common task of the Central Departments Experimental Facilities & Information Technology and New Accelerators as well as the Institute for Nuclear & Hadron Physics. Project leader is Dr. F. Gabriel, head of the first department mentioned above. The activities connected to ELBE are carried out not only by the research center, there exist also close collaborations with Stanford University, DESY Hamburg, TH Darmstadt and TU Dresden, whose help is gratefully acknowledged.
The activities around the radiation source ELBE are focused on the following fields:

- *the new building*
- *the superconducting electron accelerator (electron energy $\approx$ 20 MeV; average beam current up to 1 mA; acceleration frequency 1,3 GHz)*
- *the cryogenic system*
- *the undulators and optical resonators of the IR-FEL's*
- *the laboratories to allow experiments with infrared radiation by internal as well as external users*
- *the preparation of nuclear structure investigations by means of nuclear resonance fluorescence experiments*
- *the design of radiation physics experiments with channeling and parametric X-ray radiation in the energy region between 2 keV and 50 keV*
- *the production of positrons and neutrons*

During the last year the layout of the building was elaborated where special attention was paid to the necessary radiation protection and the creation of an FEL user facility (cf. Fig. 1). The radiation shielding of the machine and the experimental caves was calculated by assuming an electron energy of 50 MeV and an average current of 1 mA.
The eight FEL laboratories and the positron laboratory do not need any shielding. The production of neutrons at ELBE as being planned by the Technical University of Dresden would require an extension of the length of the building by several meters. Up to now the so called Raumbedarfsplan (justification of the planning) and the Antrag auf Errichtungsgenehmigung (request for permission for the building) have been submitted to the responsible authorities.
The radiation source ELBE will be equipped with two different injectors: a thermionic rf-gun for continuous wave operation with the micropulse structure of 1.3 GHz and a pulsed electron gun with a time structure of 11,8 MHz for the FEL operation. The cw-gun (cf. D. Janssen, P. vom Stein) has already been built and is presently being tested (cf. A. Birnbaum et al.). The second one will be developed in connection with the gun of the Stanford University.

The cryogenic system for the radiation source ELBE (cf. Haberstroh, H. Quack) has been designed for a working temperature of 1.8 K and has already been ordered. In the contribution of H. Büttig the concept of the rf-system for ELBE is presented, where the gun test stand has been used for testing and optimizing the layout of rf-modules. In 1996 also design studies of the beam line system for ELBE have been performed (cf. P. Gippner et al.), the first aim of which is to optimize the transport of the high brillant electron beam to the nuclear and radiation physics caves as well as into the undulator of FEL 1 (the thick beam lines in Fig. 1 depict stage one of the beam line system). First considerations for an infrared FEL user facility at ELBE has been summarized and compared with existing world-wide IR-FEL user facilities (cf. W. Seidel et al.). In 1996 the preparation of nuclear resonance fluorescence as well as radiation physics investigations at ELBE has been continued by carrying out corresponding experiments at the injector ($E_e < 10$ MeV) of the superconducting electron accelerator S-DALINAC of the Technische Hochschule Darmstadt. Results of these investigations are presented in this section (cf. U. Nething et al. and R. Zahn et al.) as well as in section 4 (cf. R. Schwenger et al.). The development of a superconducting rf-gun (cf. A. Bushesev et al.) and the concept study for a slow positron source regard future options for technical improvements and enlargements of the radiation source ELBE.

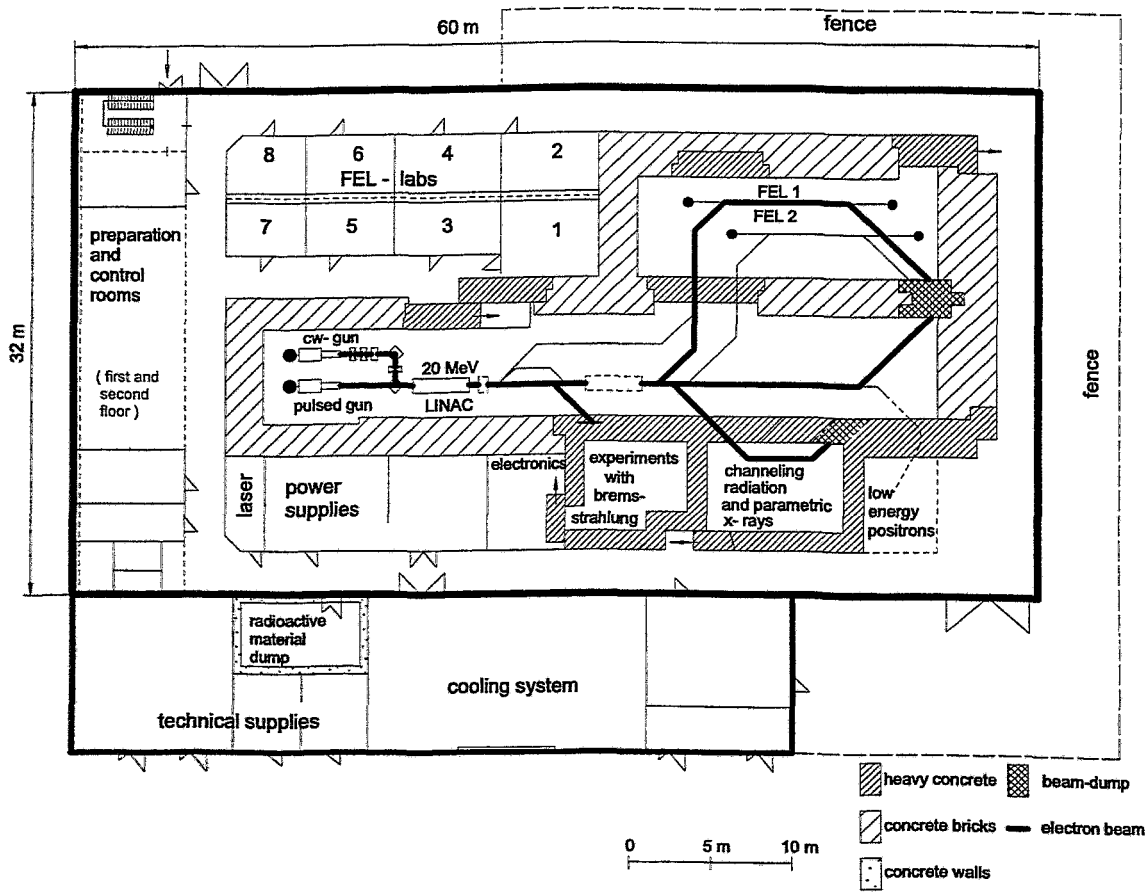

Fig. 1 *Layout of the building for ELBE*

A Low Emittance CW-Electron Injector for the ELBE Accelerator

D. JANSSEN[1], P. VOM STEIN[1]

For applications in nuclear and radiation physics there is an increasing demand for electron beams with superior brightness in the medium energy range. This work presents the injector design for the superconducting accelerator ELBE [1]. The injector consists of a thermionic rf-gun, working at a frequency of 1.3 GHz in cw-mode[2]. The superconducting section is based on the technology established at TESLA [3], modified for cw-operation. The accelerator will deliver a 20 MeV beam with an rms energy spread of 10 keV and an average current of up to 1 mA. The normalised transverse emittance remains $1\,\pi$ mm mrad. The arrangement and operating parameters of the accelerator components were settled by numerical optimization considering longitudinal beam dynamics. The result led to a nonlinear bunching scheme, which compensates the high longitudinal emittance from the thermionic rf-gun.

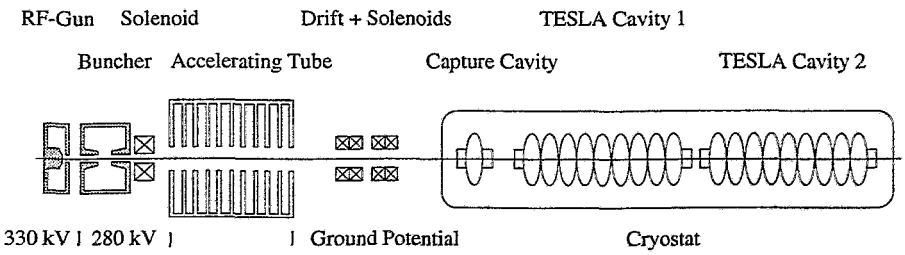

Fig. 1 *Schematic view of the accelerator arrangement*

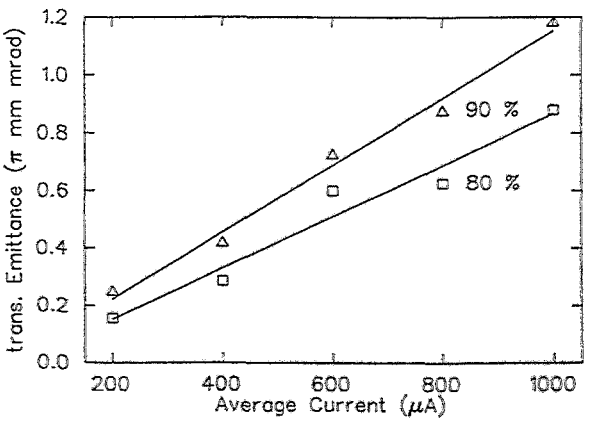

Fig. 2 *Transverse emittance versus beam current*

[1] *Zentralabteilung Neue Beschleuniger, FZR*

References

[1] F. Gabriel ed., FZR Internal Design Report (1995)
[2] D. Janssen, P. vom Stein, NIM A380 (1996) 497
[3] D.A. Edwards ed., TESLA Test Facility-Design Report, DESY, Hamburg (1995)

Calculation, Design, Manufactering and Test of a new CW-Thermionic RF Gun

A. BIRNBAUM[1], H. BÜTTIG[2], M. FREITAG, W. GLÄESER[1], H. GURATZSCH[2], H. HAUCK[1], D. JANSSEN[2], A. NOWAK[1], R. SCHLENK[1], P.VOM STEIN[2], B. WUSTMANN[1]

A new cw thermionic RF gun for the ELBE-project [1] has been built and successfully tested in a special test-facitly (see Fig.1). The corresponding design is discussed in [2]. In contrast to the pulsed thermionic RF-guns the RF-power of the gun-cavity can be limited to 100 W, so that it is possible to work in the cw-mode. The buncher at high voltage potential allows a very effective compression of the bunchlenghts (see Fig.2). The following acceleration up to 360 keV is performed by an electrostatic acceleration tube.

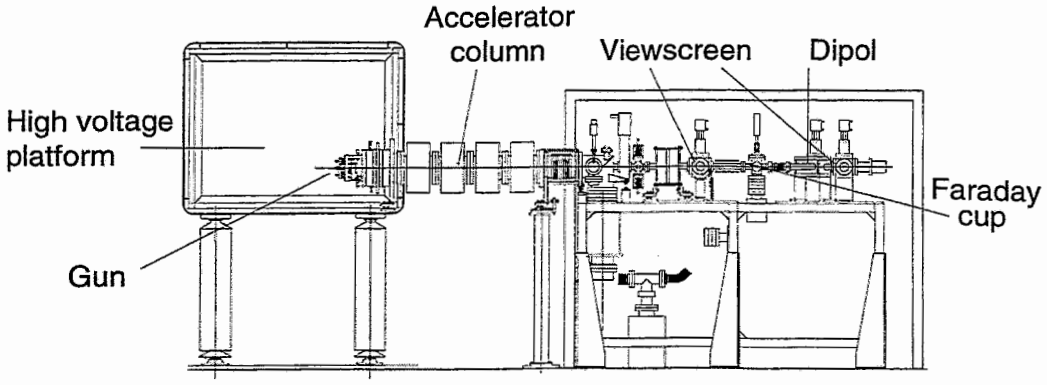

Fig. 1 *The gun-testfacility*

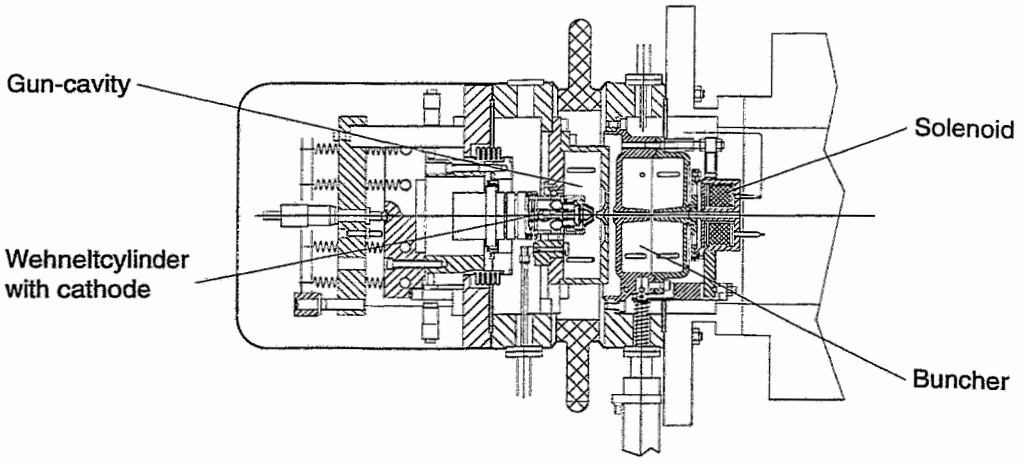

Fig. 2 *The thermionic RF-gun and the buncher*

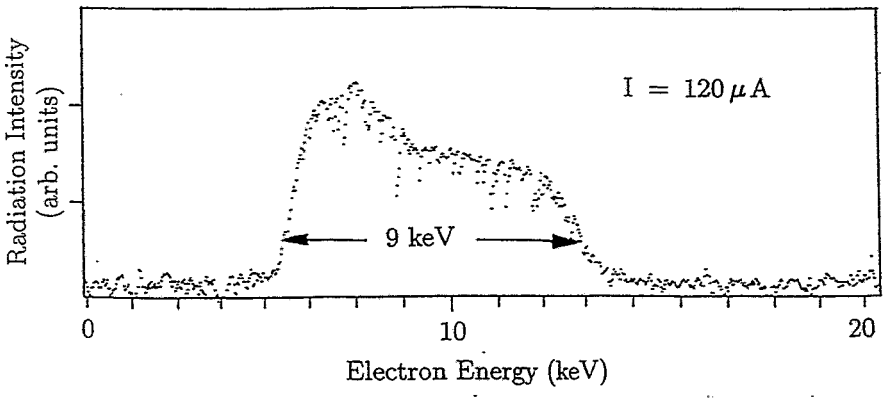

Fig. 3 *Energy distribution of the electron beam*

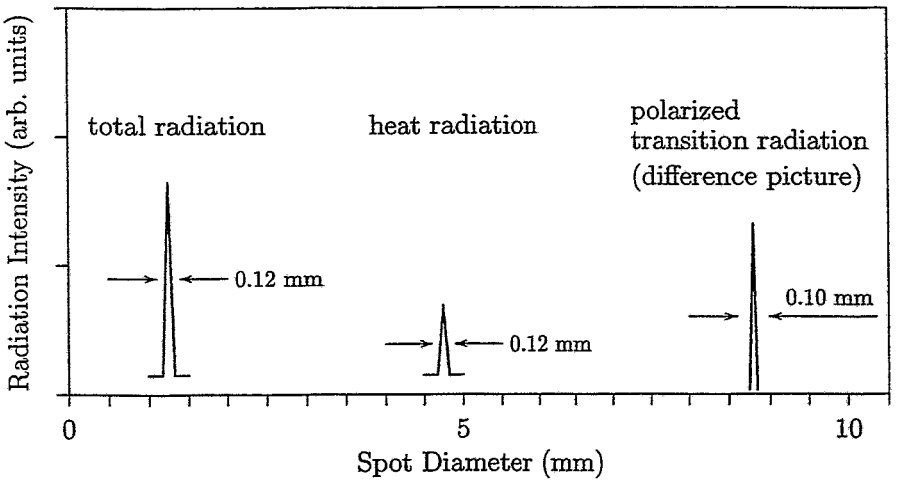

Fig. 4 *Profiles of the electron beam, measured by optical transition radiation. The heat radiation background has been separated from the optical transition radiation by means of a polarization filter and image processing.*

The current, the energy, the emittance and the energy spread of the electron beam has been measured the test facility. Due to radiation safety the current is limited to 100 A at the energy of 330 keV. For these values the emittance $\varepsilon = 0.2\ \pi$ mm mrad has been obtained. The energy spread is a function of the buncher phase and amplitude. Its maximal value is about 10 keV. Fig. 3 and Fig. 4 show some examples for the beam profile and the energy spread, measured by the intensity of the transition radiation, which is emitted from an aluminium foil target.

[1] *Zentralabteilung Forschungs- und Informationstechnik, FZR*
[2] *Zentralabteilung Neue Beschleuniger, FZR*

References

[1] F. Gabriel ed., FZR Internal Design Report (1995)

[2] D. Janssen and P.vom Stein, NIM A380(1996)497

Cryogenic System for the Radiation Source ELBE

CH. HABERSTROH[1], H. QUACK[1]

In order to maintain a working temperature of 1.8 K for the superconducting cavities bath cooling with superfluid helium is required. Despite superinsulation of all components and the introduction of an 80 K thermal shield inside the helium cryostat heat loads at 1.8 K total in $\approx$ 113 W, mainly due to the high dissipation energy connected with the cw-regime of the superconducting cavities. Additional 150 W at 80 K are required. The helium plant as it will be realized for ELBE is based on a modified Claude cycle, specified for 200 W at 1.8 K and 200 W at 80 K, respectively.

Compressed helium gas at 1.3 MPa and ambient temperature is cooled down to 4.4 K by passing a combination of counterflow heat exchangers and work extracting expansion turbines. A minor part of the cold helium is branched off and, after passing a further heat exchanger placed directly at the cavity cryostats, expanded to 1.6 kPa (helium vapor pressure corresponding to 1.8 K).

Recompression to atmospheric pressure partially is done by a two stage "cold compression", i. e. the helium gas is partly compressed at low temperatures ($\approx$ 4 K) by means of two centrifugal machines in series. The application of these "cold compressors" implies a lot of sophisticated techniques and therefore up to now was used only in large scale helium plants as e.g. for CERN. Benefits of this solution are savings in size and expenses for the ambient temperature vacuum system and for the low density heat exchangers inside the cold box. Since the superconducting cavities are extremely sensitive to microphonics, all components are placed in a separate building with own foundations. The helium cycle compressor is split into a 226 kW and a 60 kW unit thus allowing a flexible adaptation to the actual refrigeration demands (e.g. for stand by / full load mode of the accelerator). Additionally the operation of the plant as liquefier is possible. An outstanding feature of the helium plant for ELBE is the possibility of a later upgrade to 400 W at 2.1 K in case of increasing refrigeration demand in the future. Even so the cryogenic system represents the fourth in size of this kind all over Germany.

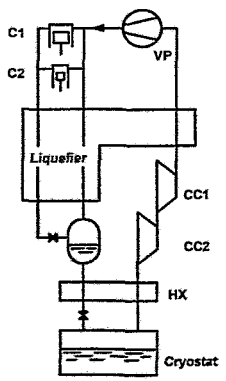

The figure shows the simplified flow scheme of the cryogenic system consisting of the cycle compressors C1, C2, the liquefier with additional heat exchangers, the subcooling heat exchanger HX and the 1.8 K cryostat. On the low pressure side the two stage "cold compression" CC1, CC2 and the vacuum pump system at ambient temperature (VP) are indicated.

[1] *Institut für Energiemaschinen und Maschinenlabor, TU Dresden*

ELBE - Radio Frequency System

HARTMUT BÜTTIG[1]

For the Radiation Source ELBE [1] the rf-system (details see Fig. 1 and Table 1) has to provide a total rf-power of 20 kW (cw) , to meet the design values (energy 20 MeV, average current 1 mA). The activities within the ELBE rf-project during 1996 cover the design work for the rf-system and the development of an experimental set-up for a gun test stand . The gun test stand has been built to study the performance and the handling of an electron beam, emitted by a thermal cathode, mounted inside a microwave resonator [2]. This experimental set-up has also been used for testing and optimizing the layout and the performance of rf-modules, which we are going to use for the linac, too.

Table 1 *RF-parameters for ELBE*

Component	RF-Power(cw)	Remarks
Pulses GUN (FEL-mode)	100 W	wide band 10-500 MHz
Buncher 1 (FEL-mode)	250 W	260 MHz
Buncher 2 (FEL-mode)	500 W	520 MHz
cw-GUN	100 W	1.3 GHz
cw-Buncher 1	100 W	1.3 GHz
cw-Buncher 2	max 1 kW	1.3 GHz
TESLApower amp.	10 kW (cw)	klystron VKL 7811ST

Based on the key decision to use TESLA-cavities for the superconducting part of the cw- linac, the frequency of the system has to be 1.3 GHz. To obtain 10 MeV / m energy gain per cavity and 1 mA cw-beam current, each power amplifier has to provide 10 kW. The working point of the Klystrons has to be within the linear part of its characteristics. Klystrons available are the K3320R (15 kW, EEV-Chelmsford) and the VKL 7811ST (10kW, CPI - Palo Alto). We have chosen the VKL 7811ST because of its permanent magnet system. A problem that has not been solved yet is the power capability of the rf-main couplers to the helium cryostat. We try to learn from Stanford University, putting a cw-linac into operation, based on the same cavities and couplers. Two injectors are forseen to serve the experiments. The design of a pulsed mode injector used for FEL operation has not been fixed yet. The cw-mode pre- accelerator (1.3 GHz) has been performed and optimized at the test stand (rf- modules covered by a dotted line in Fig.1). The system for the test stand is driven by a 1.3 GHz PLL- oscillator, that allows frequency tuning to study the temperature stability of the copper resonators and several working points depending on the coupler performance. A phase stable glass-fiber link (Thomson CSF, analog bandwith 3 GHz) is used to feed the sinusoidal 1.3 GHz signal to the rf-amplifiers on top of a 300 kV terminal [3]. All low-level rf-modules are of equal design, and consist of a phase and amplitude leveling unit , buffer amplifiers and power modules [4]. The piezoelectric cavity tuner of the gun is controlled by a dc voltage in dependence of the mismatch between power amplifier and input coupler. The system was put into operation in august 1996. Failures during first tests, performed in early spring 1996, were a melted rf-antenna of the gun, melted contact-fingers inside the gun-resonator (delivery of tin-plated fingers instead of silver-plated ones) and some selfexcitations of high-gain rf- amplifiers caused by ground loops. All these problems have been solved.

[1] *Zentralabteilung Neue Beschleuniger, FZR*

References

[1] F. Gabriel; ELBE-Quelle, Interner Projektvorschlag; FZ-Rossendorf 1995
[2] D. Janssen and P. vom Stein, NIM A380(1996)497
[3] St. Scheurer, Diplomarbeit, HWT (FH) Dresden 1996
[4] H. Büttig; FZR-141 (1996) 62

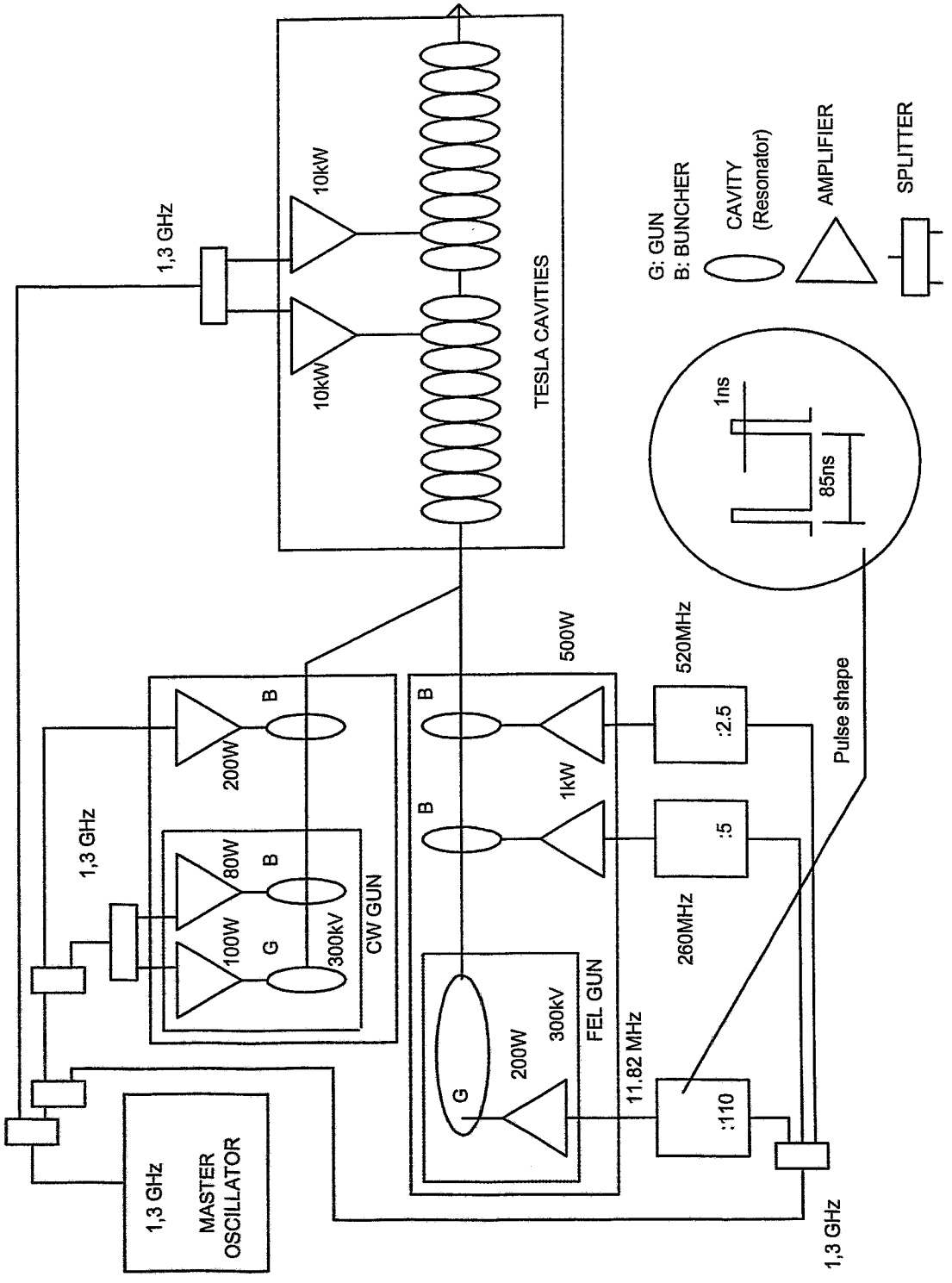

Fig. 1 *RF - System for the Radiation Source ELBE*

The Status of the Beam Transport System for the ELBE Project

P. GIPPNER, U.NETHING, R. ZAHN

The most essential group of elements of the electron beam transport system for the ELBE project consists of two s-formed double arc's with deflection angles of two times 90° [1]. They guide the beam from the accelerator hall into the room of the Free Electron Laser (FEL). Furthermore, they should be (i) achromatic, (ii) isochronous and (iii) possibly able to compress the beam bunches within the longitudinal phase space. Part of the two systems, until now taken into consideration, were shown in Fig. 1.

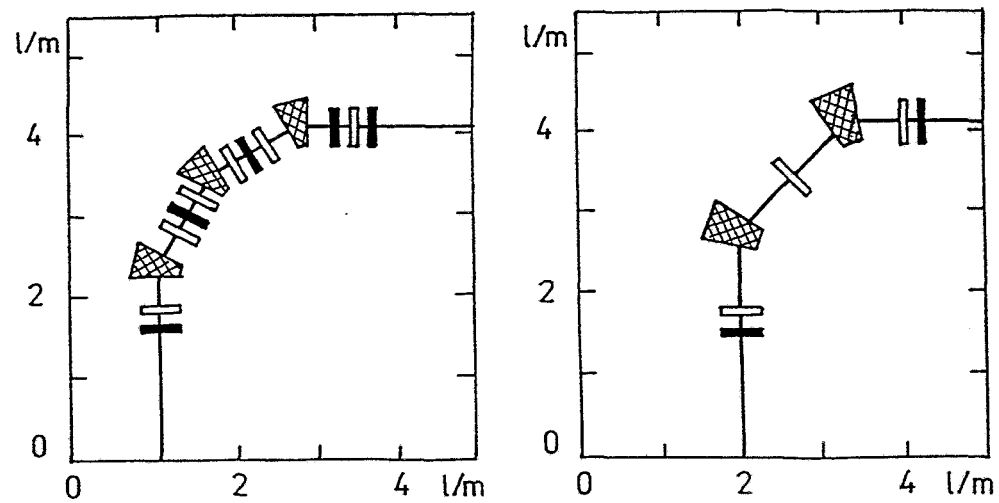

Fig. 1
Part of two different electron beam transport systems. The trapezoids represent the bending magnets, whereas black and white boxes are vertically and horizontally focusing quadrupoles, respectively.

The calculations were performed with the programs MIRKO [2] and TRANSPORT [3] based on the formalisms of transport (T) and beam (σ) matrices. MIRKO allows an interactive work, especially an interactive fitting of beam envelopes, T-matrix elements and coefficients of the beam ellipses in the transversal phase space. It is well suited for getting the field parameters of quadrupoles, which can easily be introduced into the input file of TRANSPORT for calculations of higher orders. The system shown in Fig. 1 (left side) fulfills the mentioned conditions (i) - (iii) and can supply the FEL equipment with a beam of less than 1 mm diameter [4]. Its disadvantage is the large number of quadrupoles and 30° dipoles needed. Therefore, the simpler system of Fig. 1 (right side) is under investigation presently.

References

[1] this Annual Report
[2] B. Franczak, GSI Darmstadt, Mirko, Version 5.13, 1989
[3] D.C. Carey, K.L. Brown, F. Rothacker, SLAC-R-95-462
[4] U. Nething, R. Zahn, Annual Report 1995, FZR - 130, p. 133

Considerations for an Infrared FEL at the Radiation Source ELBE

W. SEIDEL, K.D. SCHILLING, F. GABRIEL[1], P. GIPPNER, E. GROSSE, U. NETHING, H. PRADE, R. ZAHN

The scientific program at ELBE concentrates mainly on the usage of the high-brilliant 20 MeV electron beam to drive two free-electron lasers (FEL) in the far-infrared region. The first of them has been designed to be based on an electromagnetic undulator, comparable with that of the FIREFLY FEL at Stanford. Its radiation spectrum will cover the region of about 30-150 μm wavelengths. The second FEL will be realized on the basis of an undulator with permanent-magnet (hybrid) structure and will produce intense picosecond light pulses in the shorter wavelength region. Both FEL's will be driven in parallel with subsequent beam bunches to allow pump-probe experiments with independently tunable wavelengths. They will serve as a user facility for potential users inside and outside of our institute.

In the review period, several conceptual design studies have been performed. They comprise the beam transport calculations and the choice of the individual beam-line components (dipole and quadrupole magnets,diagnostic elements), in order to optimize the beam line for the efficient transport of the high-quality electron microbunches into the undulators. Also, the conceptual plan of the optical (FEL) laboratory complex has been realized. The present activities aim at the elaboration of future research lines and experimental requirements: what kind of experiments can be done at an IR-FEL, which wavelengths are of particular interest and what kind of performance is needed for future applications. Special attention is given to the extension of the spectral range below 30 μm and beyond 150 μm, the intensity requirements and the time structure. For final decisions we need the information about the state-of-the-art of the already existing IR-FEL user facilities in the world. Therefore, a compilation of these facilities has been made, which is presented in Table 1.

Each FEL is identified by its location or name. The electron beam energy and peak current as provided by the accelerator are listed in the second and third columns in units of MeV and Amperes. The fourth column τ_{micro} presents the electron micropulse length in picoseconds and the bunch separation in nanoseconds. The next column τ_{macro} of the table contains the macropulse duration in microseconds and macropulse repetition rate in Hz for the electron beam. The average current $\langle I \rangle$ in microamperes (μA) is shown in the sixth column. The seventh column of the table summarizes the operating wavelength range λ in micrometers (μA). The large range of operating wavelength, four orders of magnitude, indicates the flexible design characteristics of the FEL mechanism. The optical output power for the average in Watt and for the micropulse in Megawatt are given in the eighth column. In the last column, the main undulator parameters are compiled. *"Electr."* stands for electromagnetic, *Ha* for Halbach type, *Hy* describes the hybrid undulators. The usally applied permanent magnets are Sm-Co or NdFeB. The conventional periodic undulators are characterized by the length L in meters, the undulator period length λ_u in centimeters, the number of undulator periods N, the minimum magnetic field gap g in millimetres and the undulator parameter K.

[1] *Zentralabteilung Forschungs- und Informationstechnik, FZR*

FEL USER FACILITIES

Institute	Energy	I_{peak}	τ_{micro}	τ_{macro}	<I>	λ	Optical Power	Undulator					
	[MeV]	[A]	[ps/ns]	[μs/Hz]	[μA]	[μm]	Av.[W]/Mic.[MW]	Type	l_u[m]	λ_u[cm]	N	g[mm]	K
Stanford (USA)	25 - 36	10	0.7 - 3 / 84.6	5000/20	<200	3 - 12	1.2 / $\leq$1.5	Ha/Sm	2.30	3.2	72	11	1
	12 - 25	6	2 - 10 / 84.6	5000/20	<200	15 - 65	1.2 / 0.3	Electr.	1.50	6.0	25	20	0.8-1.2
UCSB (USA)	4 - 6	2	Van-de-Graaff	20/4	<160	30 - 66	<0.4 / <0.01	Hy/Nd	2.26	1.85	122	7	.7756
	2.5 - 6	2		20/4	<160	63 - 300	<0.8 / <0.01	Hy/Nd	3.0	2.0	150	18.6	.13205
	2 - 6	2		20/4	<160	338 - 2500	<0.2 / <0.02	Hy/Sm	3.0	7.14	42	35.9	.7071
Duke Univ. (USA)	25 - 45	40	0.5 - 3 / 0.35	8/1 - 15	$\leq$60	1.9 - 9.1	<2 / <10	Hy/Sm	1.08	2.3	47	6	1 - 1.7
FELIX (Netherl.)	25 - 46	70	3 / 40 or 1	10/10	<20	5 - 30	$\leq$0.5 / $\leq$20	Ha/Sm	2.47	6.5	38	16	0.9 - 1.9
	15 - 25	70	3 / 40 or 1	10/10	<20	16 - 110	$\leq$0.5 / $\leq$20	Ha/Sm	2.47	6.5	38	27	0.9 - 1.3
CLIO	24-32-40-50	50 -80	10/4, 8, 16 or 32	10/50	<100	3 - 40	$\leq$1 / <80	Ha/Sm	1.92	5.04	38	18	0 - 2.2
FELI (Japan)	$\leq$165	80	5/44.8 or 5.6	24/10	<20	0.23 - 1.2	$\leq$2 / 10	Ha/Sm	2.68	4.0	67	16	0.5 - 2.3
	$\leq$75	60	7/44.8 or 5.6	24/10	<20	1 - 6	$\leq$3 / 15	Ha/Sm	3.0	3.8	78	20	0.5 - 1.4
	$\leq$30	40	10/44.8 or 5.6	24/10	<20	5 - 22	$\leq$1 / 5	Ha/Sm	2.0	3.4	58	15	0.5 - 1.5
	$\leq$30	40	10/44.8 or 5.6	24/10	<20	20 - 60	$\leq$1 / 5	Hy/Sm	2.7	9.0	30	30	1 - 2.7
	$\leq$30	40	10/11.2	10/10	<20	50 - 100	$\leq$1 / 5	Ha/Sm	2.24	8.0	28	30	1 - 2.3
Darmstadt (Germany)	30 - 50	2.7	2 / 100	cw	<60	2.6 - 7.5	$\leq$ 3 / $\leq$0.3	Hy/Sm	2.56	3.2	80	15	0.4 - 1.26

Table 1: *Characteristic accelerator and laser properties of existing world-wide IR-FEL user facilities.*

Channeling Radiation - Continuum State Contributions to the Spectral Density [B,D,S]

U. Nething, J. Freudenberger[1], H. Genz[1], V.L. Morokhovskii[2], A. Richter[1], H. Prade, J.P.F. Sellschop[3], R. Zahn

Investigations have been performed at the superconducting electron accelerator S-DALINAC of the Technische Hochschule Darmstadt to explore the continuous part of planar channeling radiation produced by bombarding a natural diamond crystal (55 μm thick) with electrons of 6.8 and 8.3 MeV kinetic energy. The bound state regime corresponds to the electrons being guided by a single lattice plane, while the free state regime corresponds to electrons crossing the lattice planes. The bound-to-bound transitions (bb) cause the discrete channeling radiation lines. The free-to-free transitions (ff) can be interpreted as coherent bremsstrahlung, especially the $\Delta N = 2$ transitions [1]. Finally, the free-to-bound transitions (fb) are lying in between these two pictures where electrons crossing the lattice plane will be trapped by a single plane after the emission of a photon.

The later two types are majorly responsible for the continuous part of the channeling radiation and were analyzed at three different photon energy ranges as a function of the tilt angle with respect to the electron beam direction and the crystallographic plane [2]. The intervals were selected between 9.5 and 14.5, 20 and 25 as well as 25 and 30 keV, respectively. The observed photon energy corresponds to the energetical difference of the states involved. The calculated contributions of the initial states for the energy windows used are listed in table 1. As the energy window is shifted to higher photon energies, the group of states are also shifted to higher continuum states. In the case of channeling along the (111) plane the density of the initial states is larger in comparison with the (110) plane. In the range between 9.5 and 14.5 keV the number of the ff and fb transitions are nearly equal for all cases (8.3 MeV, 6.8 MeV, (110), (111) plane). The contributions of the ff transitions are dominant for the (111) plane in the energy range of 20 to 30 keV. For the (110) plane even at the highest photon energy the number of ff and fb transitions are of the same order. For channeling along the (111) plane the main contribution in the energy range between 20-30 keV is the coherent bremsstrahlung. For all other cases the observed spectra can be described by assuming a mixture of coherent bremsstrahlung and the free-to-bound type radiation.

Table 1: *Calculations of the initial states (IS) denoted by their quantum numbers (N) for the different energy windows. For $N > 2$ at 6.8 MeV and $N > 3$ at 8.3 MeV the states are free. The number of fb transtions are labeled with #fb and the number of ff transitions with #ff, respectively.*

Photon Energy	*(110) 6.8 MeV*			*(111) 6.8 MeV*			*(111) 8.3 MeV*		
	IS	*#fb*	*#ff*	*IS*	*#fb*	*#ff*	*IS*	*#fb*	*#ff*
9.5 - 14.5 keV	*3-6*	*3*	*2*	*4-15*	*5*	*6*	*3-12*	*6*	*7*
20 - 25 keV	*5-6, 8-10*	*2*	*2*	*10-14*	*0*	*3*	*6-13, 17-21*	*2*	*10*
25 - 30 keV	*6-7, 10-12*	*1*	*3*	*11-17*	*0*	*7*	*10-14, 22-30*	*1*	*8*

[1] *Institut für Kernphysik, Technische Hochschule Darmstadt, Darmstadt, Germany*

[2] *Kharkov Institute of Physics and Technology, Kharkov, Ukraine*

[3] *University of Witwatersrand, Johannesburg, South Africa*

References

[1] *Coherent Radiation Sources*, ed. A.W. Sáenz and H. Überall, Springer-Verlag (1985)

[2] L. Groening, Diploma Thesis, TH-Darmstadt, (1995)

Coherent Bremsstrahlung Production under Channeling Condition [B,D,W]

R. ZAHN, J. FREUDENBERGER[1], H. GENZ[1], V.V. MOROKHOVSKII[1], U. NETHING, H. PRADE, A. RICHTER[1], J.P.F. SELLSCHOP[2]

Coherent bremsstrahlung (CB) is emitted when a charged particle is traversing a crystal and the momentum transfer to the crystal corresponds to a reciprocal lattice vector τ. Two kinds of coherent bremsstrahlung are distinguished [1]. Type A is radiated if τ is lying in the reciprocal lattice plane, which is approximately normal to the direction of incidence and contains the origin of the reciprocal lattice space. In contrast, coherent bremsstrahlung of type B arises if this plane does not contain the origin.

Charged particles can be trapped by a plane or a row of atoms of a crystal [2]. This effect is called channeling and is due to the electrostatic potential which is built up by the planes or rows. If the particle is trapped by a plane, one speaks of planar channeling. If the particle spirals around a row of atoms, the effect is called axial channeling.

The spectral density of coherent bremsstrahlung depends on the structure factor S, which describes the interference conditions in a unit cell of the crystal. In our experiment a diamond crystal has been used. Since in the case of diamond the structure factor amounts to $S = 0$ for τ=(110), one expects to observe no coherent bremsstrahlung due to $S = 0$. But, this holds only if the electrons in the crystal can be described by a plane wave (first Born approximation). However, under channeling condition the electrons have to be described by Bloch waves and the cross section for τ=(110) is not zero.

A first test experiment concerning CB of type B under axial channeling condition has been performed at the super conducting linear accelerator S-DALINAC at the TH-Darmstadt with electrons of about 3 MeV kinetic energy. The diamond crystal has been bombarded with electrons in the direction of the [110] axis. In figure 1 the ratio of two spectra is shown. The spectrum under axial channeling condition has been divided by a non-coherent bremsstrahlung spectrum, which has been measured for an arbitrary direction of incidence. The peak of coherent bremsstrahlung type B at 350 keV is clearly visible suggesting the description of the channeling electrons by Bloch waves.

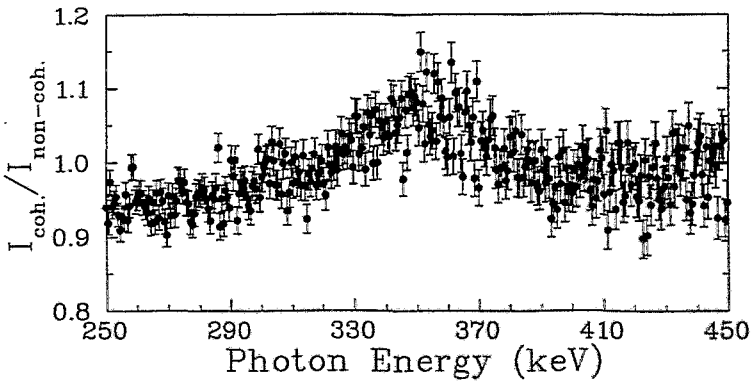

Fig. 1 *Intensity ratio of coherent bremsstrahlung type B under axial channeling condition to non-coherent bremsstrahlung. The measured spectra have been normalized by the accumulated electron beam charge.*

[1] *Institut für Kernphysik, Technische Hochschule Darmstadt, Darmstadt, Germany*
[2] *University of the Witwatersrand, Johannesburg, South Africa*

References

[1] A.W. Sáenz and H. Überall, Phys. Rev. B **25** (1982) 4418
[2] J. Freudenberger, H. Genz, L. Groening, P. Hoffmann-Stascheck, W. Knüpfer, V.L. Morokhovskii, V.V. Morokhovskii, U. Nething, A. Richter, J.P.F. Sellschop, Nucl. Instr. and Meth. **B 119** (1996) 123

The Development of a Superconducting RF Gun: Status of the Drossel Collaboration

A. Bushuev[1], D. Janssen, M. Karliner[1], S. Konstantinov[1], J. Kruchkov[1], V. Petrov[1], I. Sedlyarov[1], P. vom Stein, A. Tribendis[1], V. Volkov[1]

In the beginning of 1996 the Drossel collaboration was established between the FZR and the BINP Novosibirsk for the development of a new electron injector. The injector combines the principle of a photocathode rf gun[1] with the use of superconducting (sc) accelerating cavities. The objective of this development is a sc rf gun, which delivers a bunched electron beam in current wave (cw) mode. The beam parameters should fulfill the requirements of the ELBE accelerator[2,3] to run both an IR FEL and nuclear physics, radiation physics experiments.
First a new design was developed to insert a high quantum efficiency photocathode (Cs_2Te) into the sc cavity. The cryogenic and rf problems, caused by the heat load of the photocathode, were solved by a cooling insert with an independent liquid nitrogen circuit (fig. 1). This insert also integrates the function of a multistaged rf filter.
In parallel the cavity shape of of the rf gun was optimized. The conical back wall of the first half cell focusses the beam at low energy and compensates beam blow up due to space charge effects. Beam dynamics simulations (PARMELA[4]) show a transverse emittance of 1.7 π mm mrad for 200 pC bunch charge and a gradient of 20 MV/m at the cathode. The full cell cavities of the rf gun have the TESLA geometry to simplify production by using existing sc cavity technology. The low gradient allows both single bunch and cw mode of operation without exceeding present field limits for sc cavities.

Table 1 *Beam Parameters of the Prototype Gun*

	Nuclear Physics Mode	FEL Mode
E_{peak}@ Cathode	14.5 MV/m	19.6 MV/m
Bunch charge	1 pC	200 pC
Injection angle ϕ	5.0 deg	34.6 deg
Laser pulse length (FWHM)	5 ps	10 ps
Laser spot size	3 mm	3mm
Energy	4.2 MeV	5.7 MeV
Energy spread (100% rms)	$1 * 10^{-4}$	$3 * 10^{-3}$
trans. emittance (100% rms)	0.06 π mm mrad	1.7 π mm mrad
long. emttance (100% rms)	0.040 deg keV	6.1 deg keV

To generate an electron beam with low energy spread for the nuclear physics experiments, the injection angle ϕ is set to 5^o. This effects a bunch compression of the electron pulse by a factor of four. The resulting short bunch length of less than 1.5 ps diminishes the energy spread increasing influence of the rf field in the main accelerator. In the FEL mode ϕ is 34.6^o with slightly higher electrical peak field. The higher momentarilly cathode field $E_{peak} * \sin(\phi)$ allows the extraction of bunch charges up to 500 pC from the cathode, which is necessary to achieve high peak currents for FEL operation.
First tests with a 1.3 GHz half cell to prove the feasibility of our design concepts are scheduled for the middle of 1997. At present the production of the test cavity is under way at the workshops of BINP. First design considerations and price estimations for the laser system were done by the Max Born Institute, Berlin. For the design of the cryogenic system we are in contact with the TU Dresden and JINR Dubna.

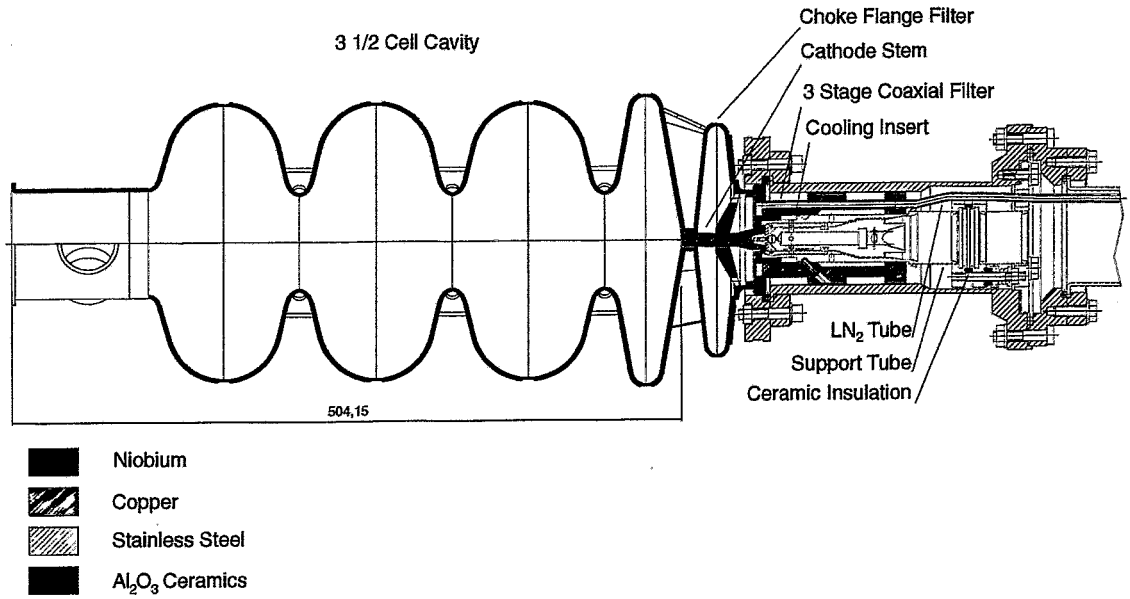

Fig. 1 *Draft of the Prototype Rf Gun*

[1] *Budker Institute for Nuclear Physics, Novosibirsk, Russia*

References

[1] C.Travier, Nucl. Instr.& Meth. A304(1991) 285-296
[2] F. Gabriel ed., FZR Internal Design Report (1995)
[3] D. Janssen, P. vom Stein, Nucl. Instr.& Meth. A380(1996) 497-504
[4] J. Billen, L. Young, Proc. of the 1993 PAC, Vol.2 790-792

Concept Study for a Slow Positron Source at the ELBE Facility

R. Ley[1], G. Werth[1], G. Brauer[2], W. Wendler[3]

The superconducting electron accelerator for the radiation source ELBE has a projected average current of 1 mA and energy of 20 MeV. This facility is well suited to produce a monoenergetic beam of at least 10^8 positrons/s. The high energy electrons hit a cooled tantalum or tungsten target (which probably has to be a rotating wheel) and create the positrons in a shower of bremsstrahlung and pair production. The number of positions energing from the conversion target reaches a maximum at a target thickness of 2.5 mm tantalum. The positron spectrum has its maximum at very low energies and has a half width of about 9 MeV. Immediately in front of the conversion target a positron moderator is positioned which consists of an array of well annealed polycrystalline thin tungsten vanes. The nearly monoenergetic slow positrons are extracted from the moderator by electrostatic lenses and are guided inside a bent 0.01 Tesla solenoid over a distance of about 10 m to an experimental area which lies well screened behind a concrete wall. From the following figures the optimum target thickness (Fig. 1) and the conversion efficiency (Fig. 2) can be obtained as a function of the primary electron energy E_- [1]. For 14, 36 and 100 MeV the experimental conversion efficiencies in $e^+/10^9 e^-$ amount to: 2,3 [2], 50 [3,4] and 1500 [5,6]. For 20, 25 and 40 MeV the interpolated conversion efficiencies are: 25, 35 and 80, respectively.

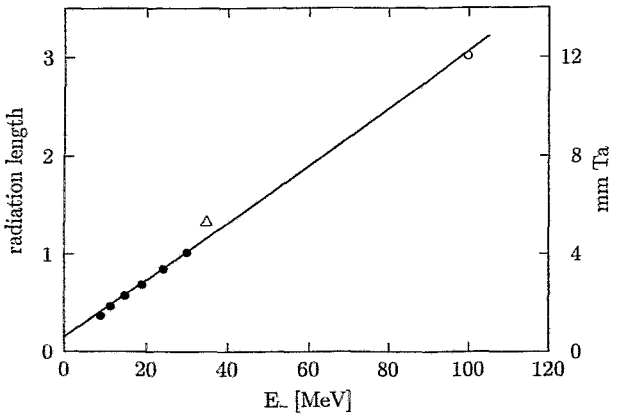

Fig. 1 *Optimum target thickness*

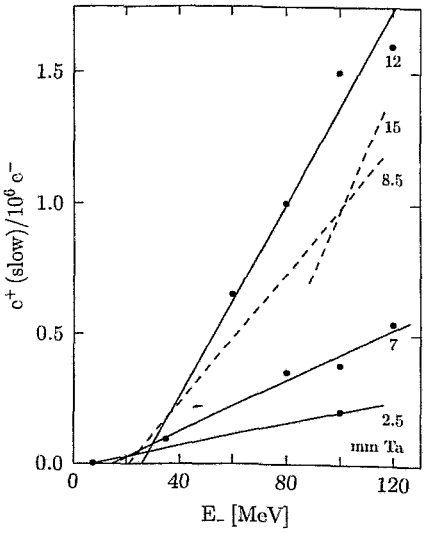

Fig. 2 *Conversion efficiency for different tantalum thicknesses*

1 *Institut für Physik, Johannes Gutenberg-Universität, Mainz*
2 *Institut für Ionenstrahlphysik und Materialforschung, FZR*
3 *Vorstandsbereich, FZR*

References

[1] J. Dahm et al., Hyp. Interact. 44 (1988) 151
[2] M. Begemann et al., Nucl. Instr. Meth. 201 (1982) 287
[3] W. Faust et al., Nucl. Instr. Meth. B 56/57 (1991) 575
[4] D. Hagena et al., Phys. Rev. Lett. 71 (1993) 2887
[5] R.H. Howell et al., Nucl. Instr. Meth. B 10/11 (1985) 373
[6] R.H. Howell et al., in "SLOPOS-7", Paul Scherrer Inst., 1996, Contribution B 12

Abstracts of publications

Experimental Determination of the Linewidth of Parametric X-ray Radiation at Electron Energies Below 10 MeV
(Nucl. Instr. Meth. B 115 (1996) 408)

Freudenberger, J., M. Galemann, H. Genz, L. Groening, P. Hoffmann-Stascheck, V.L. Morokhovskii, V.V. Morokhovskii, U. Nething, H. Prade, A. Richter, J.P.F. Sellschop, R. Zahn

Abstract: The linewidth of parametric X-ray radiation has been determined experimentally applying an absorption technique. Using a copper foil of 27.7 μm thickness and tuning the energy of the PXR peak across the K-absorption edge of copper by tilting a 55 μm thick diamond crystal, the variance of the PXR line at 8.98 keV photon energy was found to be $\sigma = 48$ eV. The diamond crystal has been bombarded with electrons of 6.8 MeV kinetic energy delivered by the superconducting linear accelerator S-DALINAC at Darmstadt. The experimental yield of the intensity amounts to $N = 0.91 \times 10^{-5}$ photons/(electron sr). From the measured variance the spectral density in the peak is deduced to be $J = 0.95 \times 10^{-7}$ photons/(electron sr eV).

Channeling Radiation and Parametric X-radiation at Electron Energies below 10 MeV
(Nucl. Instr. Meth. in Phys. Res. B 119 (1996) 123)

Freudenberger, J., H. Genz, L. Groening, P. Hoffmann-Stascheck, W. Knüpfer, V.L. Morokhovskii, V.V. Morokhovskii, U. Nething, A. Richter, J.P.F. Sellschop

Abstract: The intensity of channeling radiation (CR) was compared for diamond and ruby crystals and also with the intensity of parametric X-radiation (PXR) originating from the same diamond. The investigations were carried out with relativistic electrons provided by the injector of the S-DALINAC at energies between 3.0 and 9.0 MeV. Both types of radiation were observed by means of Si(Li) detectors placed at 0° and 44° with respect to the electron beam axis for CR and PXR, respectively. The highest photon flux $\Phi = 2 \times 10^8$ photons/(s mm^2) was found to result from CR of diamond crystals. Ruby crystals exhibit somewhat narrower X-ray lines but less intensity. A comparison with PXR reveals that - against predictions - its intensity is three orders of magnitude weaker than CR under the same conditions. The possibility to use the CR and PXR as intense tunable photon sources is discussed.

Channeling Radiation of Electrons in Natural Diamond Crystals and their Coherence and Occupation Lengths
(Phys. Rev. B 53 (1996) 8922)

Genz, H., L. Groening, P. Hoffmann-Stascheck, A. Richter, M. Höfer, J. Hormes, U. Nething, J.P.F. Sellschop, C. Toepffer, M. Weber

Abstract: Measurements have been performed at the superconducting Darmstadt electron linear accelerator (S-DALINAC) to investigate systematically channeling radiation produced by bombarding natural diamond crystals with thicknesses of 13, 20, 30, and 55 μm with electrons at 5.2 and 9.0 MeV. Planar channeling from the (110) and (111) planes was studied for a variety of transitions with respect to their energy, intensity, and linewidth. Axial channeling from the 110 axis could be detected as well. It was found that the intensity increases as a function of

the crystal thickness, and values up to 7.7×10^{-2} photons/esr could be obtained, which is the highest intensity at low electron energies achieved so far. The intensity increases with electron energy as $\gamma^{5/2}$. The $1/e$ occupation length deduced from the photon yield as a function of the crystal thickness was found to be $l_{occ} \approx 29$ and 85 μm for planar and for axial channeling, respectively. These values are by far the largest ever observed. Comparison with a quantum mechanical theory of channeling radiation exhibits fairly good agreement for the intensity and linewidth provided that contributions caused by electronic scattering and Bloch wave broadening, which actually are largest for diamond, are properly taken into account. It turns out that multiple scattering dominates in the planar case and single scattering for the axial channeling. The coherence length could be deduced to be of the order of $0.7\,\mu$m, which is about a factor of 2 larger than observed before in silicon.

Hadron Physics

This section deals with those aspects of strongly interacting systems, where hadronic properties are investigated. Such hadron degrees of freedom can become relevant in heavy-ion collisions and hadron-nucleus interactions and, of course, in hadron-hadron collisions as well.

The present theoretical activities cover studies of in-medium modifications of hadrons up to estimates of conditions achievable in ultrarelativistic heavy-ion collisions. Also electromagnetic (photons and dileptons) radiation of dense and hot hadron matter is considered. Many of the presented results are obtained in close collaboration with visiting scientists and our students.

On the experimental side new and stimulating results on kaon production are reported from the KaoS collaboration. The K^+/K^- ratio in heavy-ion collisions at equivalent beam energies yields experimental evidence for an enhanced K^- production, which seems to indicate a significant in-medium K^- mass reduction. The other experimental efforts are related to the experiments with proton beams from the cooler synchotron COSY at Jülich. The first experimental runs with the time-of-flight spectrometer TOF have been analyzed (not described here in detail), and the bremsstrahlung signal is now extracted from the background. There is a big deal of progress in completing TOF and in finalizing the design of the magnetic spectrometer ANKE.

The future experimental activities will focus on investigations of the strangeness degrees of freedom. Since in proton or nucleus induced reactions there is no net strangeness in the entrance channel, the production of strange hadrons can serve as sensitive probe of the nuclear environment and/or the strangeness content of nucleons. Experiments on kaons at KaoS will be continued, and ANKE will measure the subthreshold kaon production in proton-nucleus collisions. The possibility to measure near threshold the associated $K\,\overline{K}$ production in proton-proton reactions at one of the above mentioned detectors is under intense discussion. Certainly, the efforts of the theoreticians will accompany the experimental activities on strangeness exploration.

Temperature and Density Dependence of the Self-Consistent Mean Field of the NJL Soliton[B]

M. SCHLEIF AND R. WÜNSCH

To study the behaviour of nucleons in nuclear matter at finite values of temperature T and density ρ we have considered the hedgehog soliton of the bosonized Nambu & Jona-Lasinio (NJL) model [1] embedded in a gas of constituent quarks. The soliton is defined by the self-consistent solution of the NJL Lagrangian in mean-field approach.
Within our restrictions to spherical hedgehog configurations and to the chiral circle the mesonic σ and π fields are uniquely described by the constituent quark mass M^* and by the profile function $\Theta(r)$ with $\sigma(r) = M^* \cos\Theta(r)$ and $\pi(r) = M^* \sin\Theta(r)$. Quark states are defined as eigenstates of the Dirac equation with the fields σ and π. Expressing energies in units of M^* and distances in units of $1/M^*$, the quark energies and wave functions are independent of the constituent quark mass and hence independent of T and ρ. The self-consistent profile function $\Theta(r)$ is given by a complicated combination of quark energies and wave functions. A part of these contributions is controlled by temperature and density dependent occupation numbers. As a result the self-consistent meson profiles do not exactly scale with the constituent quark mass in the medium but exhibit an additional dependence on T and ρ. Solitonic fields in a medium at higher temperatures and/or densities are slightly more narrow (in scaled units) than the corresponding field in vacuum. Fig. 1 displays the deviation from the scaling behaviour.

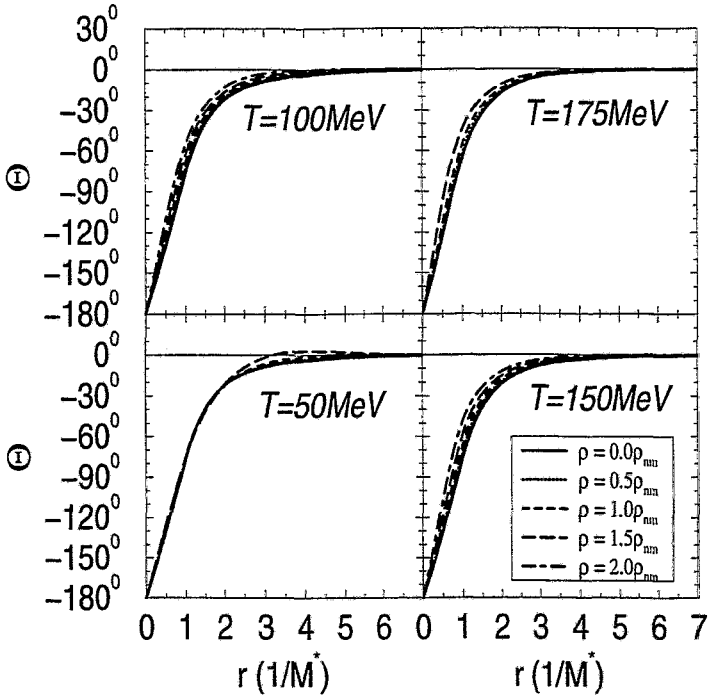

Fig. 1
Self-consistent meson profiles $\Theta(r)$ for various values of temperature T and nuclear density ρ in units of the normal nuclear density $\rho_{\rm nm} = 0.16\,{\rm fm}^{-3}$. The radius r is scaled in units of the inverse constituent quark mass M^* in the hot matter. The constituent quark mass in the vacuum at $T = 0$ was chosen to be 420 MeV.

The valence level plays the crucial role for the stability of the NJL soliton. If it is well bound by the meson field it produces a σ field with a hole around the center of the soliton ($r=0$). At some critical values of temperature and density the meson field is too shallow to bind the valence quarks and the soliton dissolves (*deconfinement transition*). This happens at $T = 175\,{\rm MeV}$ and $\rho = 2.0\rho_{\rm nm}$ where $\Theta \equiv 0$ is the only self-consistent solution.
The dissolutions of the soliton appears if the constituent quark mass in the hot medium is reduced to roughly half of its vacuum value. This point is still far away from the restoration of chiral symmetry where the constituent mass reduces to the current mass.

References

[1] R. Wünsch, K. Goeke and Th. Meißner, *Z. Phys.* **A348** (1994) 111

The Exclusive Deuteron Break-up Reaction[B]

L.P. KAPTARI[1], B. KÄMPFER, S.M. DORKIN[2], S.S. SEMIKH[1]

In a recent study [1] the static properties of the deuteron have been calculated within the Bethe-Salpeter (BS) approach. Satisfactory results are achieved which let us trust the numerical solution method employed. The relation between different representations of the BS aplitudes is clarified.

We now exploit the numerical solution of the BS equation and calculate the exclusive deuteron break-up by protons. This reaction will be measured in near future in the experiment #20 with the ANKE magnet spectrometer at COSY. Our predictions [2] are displayed in fig. 1 for the kinematics as planned in this experiment. Our interest in this reaction is stimulated by two deficits of previous investigations of the inclusive deuteron break-up [3]: (i) the cross section shows a broad shoulder which is not described within the BS approach in impulse approximation, and (ii) the tensor analyzing power changes the sign at larger values of the momentum of the outgoing fast proton, in contrast to data. We hope that the inclusive measurement at COSY allows firm conclusions, e.g., whether other non-mesonic degrees of freedom (such as Δ excitations) are needed to describe the data more precisely.

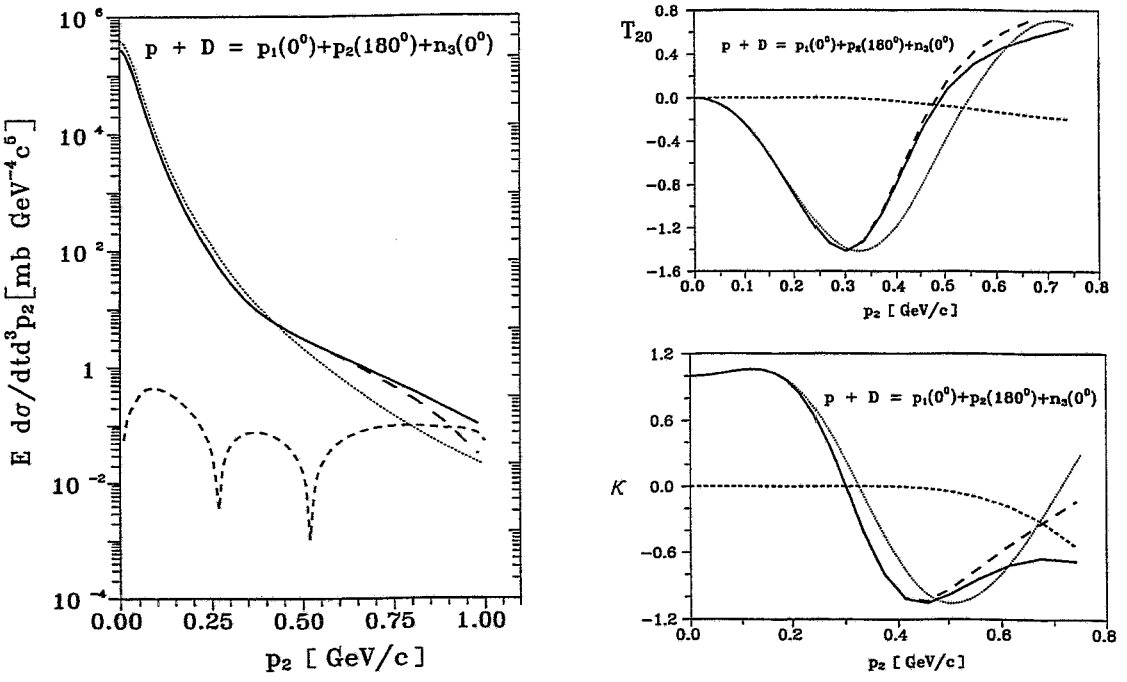

Fig. 1 *The spin averaged differential cross section without flux factor (left panel), tensor analyzing power T_{20} (right upper panel), and polarization transfer κ (right lower panel). Dashed curves: positive wave contributions, short-dashed curves: relativistic corrections, full curves: the net result within the BS approach, dotted curves: non-relativistic calculations with Bonn potential. For more details cf. [2].*

[1] *Bogoliubov Institute of Theoretical Physics, JINR Dubna, Russia*
[2] *Far-Eastern State University, Vladivostok, Russia*

References

[1] L.P. Kaptari, A.Yu. Umnikov, S.G. Bondarenko, K.Yu. Kazakov, F.C. Khanna, B. Kämpfer, Phys. Rev. C 54 (1996) 986
[2] L.P. Kaptari, B. Kämpfer, S.M. Dorkin, S.S. Semikh, FZR-161 (1996)
[3] L.P. Kaptari, A.Yu. Umnikov, F.C. Kahanna, B. Kämpfer, Phys. Lett. B 351 (1995) 400

In-Medium Kaon Properties[B]

E.E. KOLOMEITSEV, B. KÄMPFER

The recent measurement of K^+ and K^- spectra in the reaction Ni + Ni at equivalent beam energies in the subthreshold region [1] shows the striking fact that both yields are roughly the same, despite a large difference in the elementary cross sections $NN \to X\,K^+$ and $NN \to X\,K^-$ near threshold. Different in-medium properties of kaons and anti-kaons are thought to be the key for understanding this remarkable experimental finding.

We have therefore improved our previous estimates [2] of the in-medium K^- properties [3]. Starting from a general formulation of the KN interaction in vacuum we derived the scattering lengths by relying on (i) interpolating fields, (ii) constrains on the hadron current from weak interaction currents, (iii) reduction formulas together with current algebra and PCAC relations. This yields the sigma term, the Weinberg-Tomozawa term and the resonance terms contributing to the Cheng Dashen amplitude. Remaining contributions to the full amplitude are obtained by adjusting them to available experimental data. With this parametrization of the vacuum amplitude we derive the in-medium kaon self energy. Additionally we take into account effective baryon masses in medium, kaon scattering on virtual pions, and correlations. The corresponding excitation spectrum is displayed in fig. 1. As in our previous approach [2] again the additional branch of excitations with quantum numbers of the kaon is built up by correlated states of a Λ with a proton-hole. The different behavior of kaons and anti-kaons can be traced back to the isospin asymmetry of the Weinberg-Tomozawa term in the scattering amplitude. The present K^- dispersion relation can be used to calculate the spectrum resulting in heavy-ion collisions within a fireball model and a suitable procedure for transforming the in-medium excitations to vacuum particles [4]. Due to the occurrence of the Λ branch our spectra are in agreement with experimental data.

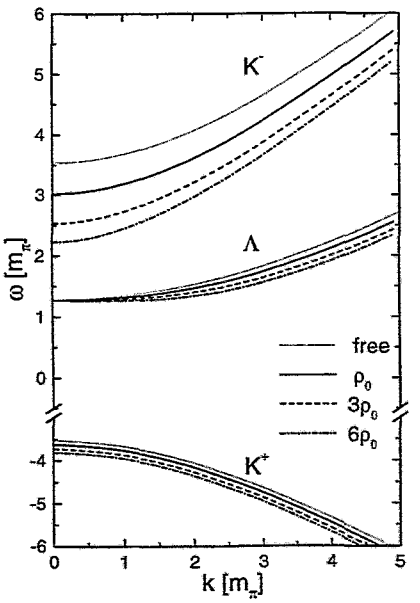

Fig. 1 *Dispersion relations of the in-medium kaons and anti-kaons at various densities of nuclear matter. The excitations with negative energies correspond to kaons, while positive energies belong to the anti-kaon excitations.*

References

[1] R. Barth et al. (KAOS collaboration), Phys. Rev. Lett. (1997) in print
[2] E.E. Kolomeitsev, D.N. Voskresensky, B. Kämpfer, Nucl. Phys. A 588 (1995) 889
[3] E.E. Kolomeitsev, Ph.D. thesis, Dresden (1997)
[4] E.E. Kolomeitsev, D.N. Voskresensky, B. Kämpfer, Int. J. Mod. Phys. E 5 (1996) 313

Asymmetry and Anisotropy of the Dilepton Emission Rates[B]

A.I. TITOV[1], T.I. GULAMOV[1], B. KÄMPFER

Recently we have pointed out [1] that the dilepton rate from a hot pion gas shows a directional dependence. Due to different contributions of the decaying transverse and longitudinal virtual photons, the lepton pairs with total momentum parallel or orthogonal to the relative momentum behave differently. We call this effect the dilepton asymmetry.

Intuitively it is clear that there must be a relation to the previously defined anisotropy of the dilepton emission rate [2]. It turns out that the definition of the anisotropy in ref. [2] is related to a very special kinematical situation, which occurs rather seldom in a thermalized system. With appropriate averaging we find that our asymmetry [1] and the anisotropy [2] agree.

We reanalyzed the pion annihilation and η Dalitz decay and find indeed that they obey different effective asymmetries as seen in fig. 1. Therefore, as proposed originally [2], this observable might be useful in disentangling various sources in the total dielectron rate.

Our studies show that a substantial part of the asymmetries stem from kinematics and not from a specific dynamics of the photon self-energy. This can be seen, e.g., in fig. 2 where the averaged asymmetry in the pion annihilation process is calculated either with a complicated dynamics of a $\pi\rho$ gas [1] or within pure kinematical considerations. This might help to estimate the net asymmetry to be expected at HADES, where the involved nucleon-meson-resonance dynamics can be replaced in a first step by our kinematical averaging procedure. The averaged asymmetry factor for the η Dalitz decay is opposite to the one for the pion annihilation process.

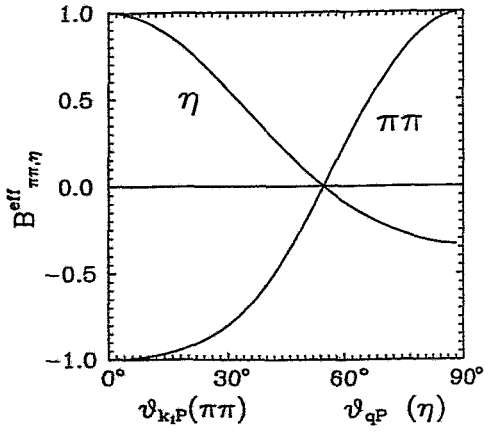

Fig. 1 *The effective asymmetry factor $B^{eff}_{\pi\pi}$ (B^{eff}_{η}) as a function of the angle between one of the incoming pions (or outgoing real photon) and the total pair momentum for pion annihilation (η Dalitz decay).*

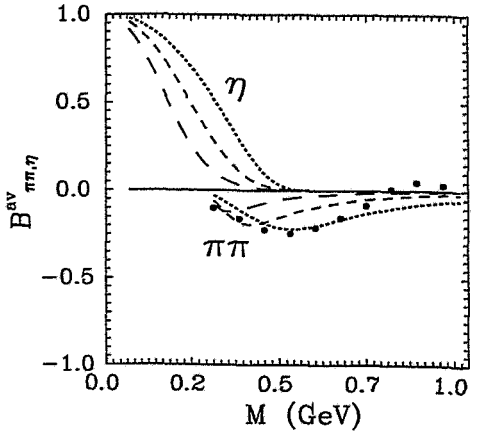

Fig. 2 *The averaged asymmetry factors $B^{av}_{\pi\pi}$ and B^{av}_{η} as function of the dielectron invariant mass M. The full, long-dashed, dashed, dotted curves are for total pair momenta $|\mathbf{P}| = 0,\ 0.2,\ 0.4,\ 0.8$ GeV. The heavy dots depict the result of [1] for $|\mathbf{P}| = 0.8$ GeV.*

[1] *Bogoliubov Institute of Theoretical Physics, JINR Dubna, Russia*

References

[1] T.I. Gulamov, A.I. Titov, B. Kämpfer, Phys. Rev. D 53 (1996) 3770, Phys. Lett. B 372 (1996) 187

[2] E.L. Bratkovskaya et al., Phys. Lett. B 348 (1995) 283, 325

Parametrizing the Transverse Momentum Spectra of Hadrons in Central Collisions Pb + Pb at 158 AGeV[B]

B. KÄMPFER

Recently the transverse hadron spectra at midrapidity in central reactions of Pb + Pb at 158 AGeV, measured by the NA 44, NA49 and WA98 collaborations, became available and have been analyzed [1]. The data from NA49 [2] can be conveniently parametrized by

$$\frac{dN^i}{m_\perp\, dm_\perp\, dy} = \mathcal{N}_i \int_0^1 d\xi\, \xi\, m_\perp I_0\left(\frac{p_\perp \mathrm{sh}(\rho)}{T}\right) K_1\left(\frac{m_\perp \mathrm{ch}(\rho)}{T}\right), \qquad (1)$$

where $\rho = \mathrm{arcth}(v_\perp(\xi))$, $v_\perp(\xi) = \frac{3}{2} v_\perp^{aver}\, \xi$, and $v_\perp^{aver}$ is the averaged transverse flow velocity; $m_\perp = \sqrt{m_i^2 + p_\perp^2}$ denotes the transverse mass of the hadron species i; I_0 and K_1 are Bessel functions. The normalization constants $\mathcal{N}_i$ depend on the chemical potentials, phase space occupation factors and particle degeneracies. This model relies on boost-invariant scaling hydrodynamics and a unique freeze-out time in both longitudinal and transverse directions. As optimum parameters we find $T = 120$ MeV and $v_\perp^{aver} = 0.43$ (see fig. 1). The π^0 spectrum up to $p_\perp = 3$ GeV can also perfectly be described by these values [3]. The NA44 data have been fitted also by the model (1) but with taking into account additional feeding by resonance decays. A maximum temperature parameter of 140 MeV (at $v_\perp^{aver} = 0.40$) is claimed [4], and an optimum fit seems to be centered at $T \leq 100$ MeV. More ambitious fits of the single particle spectra together with two-body observables by U. Heinz and the NA49 collaboration also points to rather low temperature parameters [5].

These data parametrizations can be interpreted as hint to low thermal freeze-out temperatures and large unique collective transverse expansion. Interestingly, at AGS energies one also finds similar values for heavy systems [6].

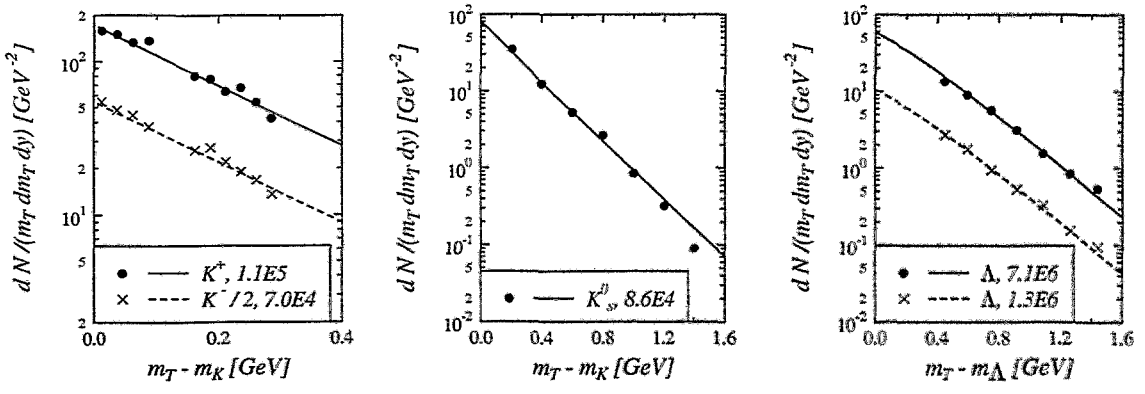

Fig. 1 *Transverse momentum spectra of strange hadron species according to eq. (1). Data from [2].* Normalizations $\mathcal{N}_i$ are given in the keys.

References

[1] B. Kämpfer, FZR-141 (1996)
[2] P.G. Jones et al. (NA49), Nucl. Phys. A (1997) in print
[3] T. Peitzmann, invited talk at Workshop Hirschegg (1997)
[4] I.G. Bearden et al. (NA44), Phys. Rev. Lett. (1997) in print
[5] D. Röhrich, invited talk at Workshop Hirschegg (1997)
[6] C. Müntz, invited talk at Workshop Hirschegg (1997)

Diphoton Production in a Chemically Equilibrating, Expanding and Hadronizing Quark-Gluon Plasma[B]

M. HENTSCHEL[1], B. KÄMPFER, O.P. PAVLENKO[2], G. SOFF[1], K. REDLICH[3]

Diphoton production is considered within a complete dynamical framework for thermalized matter assumed to be formed in ultra-relativistic heavy-ion collisions [1]. Our model [2] includes (i) chemical equilibration processes in the initially gluon-enriched plasma, (ii) longitudinal and transverse expansion, and (iii) hadronization. Besides the electromagnetic pion and quark - antiquark annihilation processes, $\pi^+\pi^- \to \gamma\gamma$ and $q\bar{q} \to \gamma\gamma$, we also take into account the process $gg \to \gamma\gamma$ via the quark box diagram. Contrary to the expectation the latter gluon driven process turns out as not so important even in an initially strongly gluon dominated quark-gluon plasma if we assume fast chemical equilibration. An example of an invariant mass spectrum is displayed in fig. 1 for the following assumed initial conditions of the thermalized era: temperature $T_0 = 550$ MeV, gluon fugacity $\lambda_g^0 = 0.5$, quark fugacity $\lambda_q^0 = 0.1$, time $\tau_0 = 0.32$ fm/c. One observes that the thermal diphoton yield is determined by the quark fusion process; it outshines the Drell Yan background (DY) (here with Duke Owens parton distribution functions, set 1.1, without K factor; dashed lines).

This is in contrast to SPS energies. The presently measured pion rapidity densities are so large that the use of Bjorken's formula points to high initial temperatures: either 191 MeV for the standard bag model or 204 MeV for a resonance gas model which includes all resonances up to 2 GeV. Despite these comparatively high initial temperatures the thermal signal shows no clear dominance above the down-extrapolated Drell Yan background, see fig. 2.

In future studies we plan to figure out procedures to suppress the combinatorial background from π^0 decays.

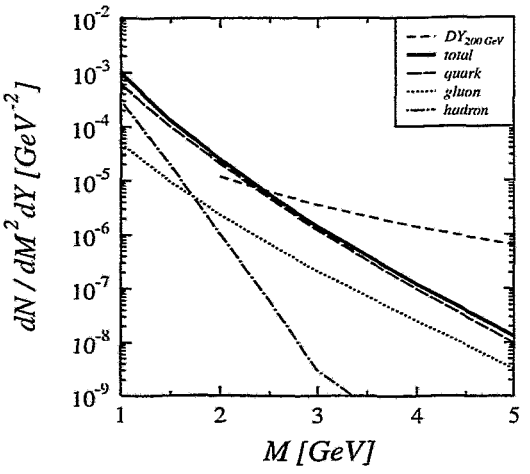

Fig. 1 *Different contributions to the diphoton spectrum for RHIC conditions.*

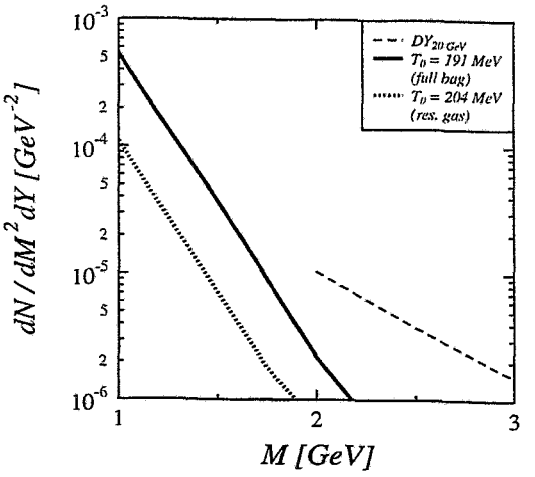

Fig. 2 *The diphoton spectrum for SPS conditions, either in hadronic scenario (dotted curve) or a scenario with deconfined matter (full curve).*

[1] *Institut für Theoretische Physik, TU Dresden*
[2] *Institute for Theoretical Physics, Kiev, Ukraine*
[3] *GSI, Darmstadt*

References

[1] M. Hentschel, B. Kämpfer, O.P. Pavlenko, G. Soff, K. Redlich, Z. Phys. C (1997), in print
[2] B. Kämpfer, O.P. Pavlenko, A. Peshier, G. Soff, Phys. Rev. C 52 (1995) 2704

Estimates of Dilepton and Charm Yields in Ultrarelativistic Heavy-Ion Collisions[B]

B. KÄMPFER, O.P. PAVLENKO[1]

In a recent attempt [1] we calculated the following hard initial processes on equal footing at RHIC and LHC energies: (i) mini-jets at midrapidity, (ii) dileptons, and (iii) open charm. Suitable factorization and renormalization scales are chosen for the MRS D-' parton distribution functions and effective cross sections. From the mini-jet distribution the possible initial conditions of a thermalized quark-gluon plasma are derived and the subsequent thermal history is followed. In doing so the thermal production rates of dileptons and open charm are accessible. The results are displayed in figs. 1 and 2. One observes that at RHIC energies the thermal dilepton signal strongly competes with the down-extrapolated Drell Yan background, but at LHC energies there are favorable conditions for the thermal signal to outshine the hard initial signal. This situation is contrary to the charm signal: here the initial hard processes dominate anywhere.

The copious charm production can represent a huge combinatorial background due to leptons from correlated and uncorrelated semileptonic decays of D mesons. In a further study we try to find suitable cuts for suppressing this competing source of dileptons and estimate the chances for observing the thermal signal.

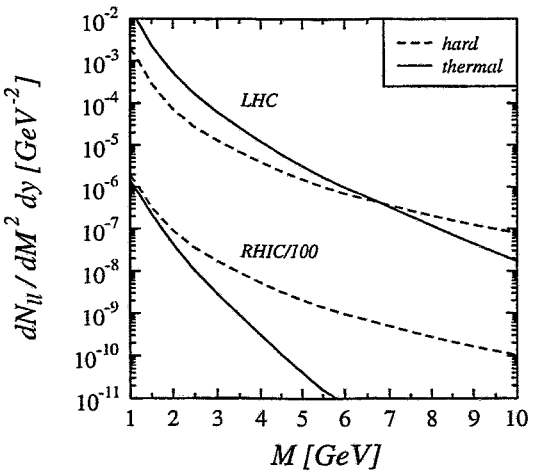

Fig. 1 *The invariant mass spectrum of dileptons.*

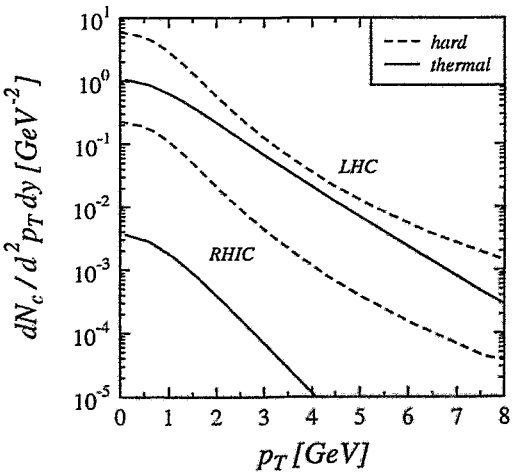

Fig. 2 *The transverse momentum spectrum of open charm.*

[1] *Institute for Theoretical Physics, Kiev, Ukraine*

References

[1] B. Kämpfer, O.P. Pavlenko, Phys. Lett. B 391 (1997) 185

Is Perturbative QCD useful for the Quark-Gluon Plasma near T_c?[B]

A. Peshier, B. Kämpfer, O.P. Pavlenko[1], G. Soff[2]

Recently the contributions to the partition function Z of the quark-gluon plasma (QGP) have been calculated within perturbative QCD (pQCD) up to fifths order in the coupling constant g [1]. While for small values of g the sub-leading terms give small corrections to the leading-order term, they dominate for larger values of g, say $g \geq 0.1$. In the latter region, the renormalization scale independence is violated, and therefore in the strong-coupling regime any perturbative expansion is suspected to be not well-behaved. However, the QGP once created in a heavy-ion collision is expected to stay in the strong coupling regime, i.e. near the confinement temperature T_c. Therefore, the applicability of pQCD to the QGP is questionable. Here we extend a reasoning [2] concerning the divergence of perturbative series, and we discuss the range of validity of pQCD. The background for our argument is the observation that the gluon thermodynamics [3] down to T_c can be described by a modified leading-order term from pQCD [4].

Consider the model function $Z(g^2) = (2\pi)^{-1/2} \int_{-\infty}^{\infty} dx \exp\{-\frac{1}{2}x^2 - g^2x^4\}$ which resembles the path integral form of the partition function of a system with a kinetic and an interaction term $\propto g^2$. As for realistic partition functions, $Z(g^2)$ cannot be expressed in closed form. However, the term $\exp\{-g^2x^4\}$ can be expanded and yields a perturbative series representation $\tilde{Z}(g^2) = \sum z_k g^{2k}$, with $z_k = (-\frac{1}{4})^k (4k)!/(k!(2k)!)$. The obviously divergent behavior of this expansion, due to $z_{k+1}/z_k \sim k$, follows from the integral representation of $Z(g)$: Z, considered as a function of the complex variable g^2, has a branch cut along the negative real axis and thus no convergent Laurent expansion at $g^2 = 0$. The same argument is expected to hold for realistic partition functions, i.e., there is no convergent power expansion in g of Z around the free limit $g = 0$ because a change of the sign of g does not smoothly change the physics.

Nevertheless, perturbative expansions are still useful. For the above toy model, the residual part $R_n(g^2) = |Z(g^2) - \sum_0^n z_k g^{2k}|$ is estimated as $R_n \leq |z_{n+1} g^{2(n+1)}| \sim (ng^2)^n$, so there is an optimal order $n^\star \sim g^{-2}$ to perform the expansion. Interestingly, with growing g^2 *less* terms of the expansion should be used to get an optimum approximation of Z!

A similar behavior is found in hot SU(3) gauge theory. Near T_c the sub-leading terms do not improve the leading order result as seen in fig. 1. We assert that this is a general feature of perturbative series and conclude that even for larger couplings the leading-order calculations might give reliable estimates, as exercised in [4].

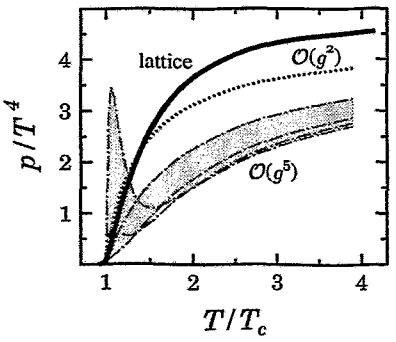

Fig. 1 *Comparison of SU(3) pQCD results, where g is fixed at T_c, with lattice data [3]. The shaded area depicts the range uncovered by the order g^5 due to the renormalization scale dependence.*

[1] *Institute for Theoretical Physics, Kiev, Ukraine*
[2] *Institut für Theoretische Physik, TU Dresden*

References

[1] Ch. Zhai, B. Kastening, Phys. Rev. D 52 (1995) 7232
[2] C. Itzykson, J.B. Zuber, Quantum Field Theory, McGraw-Hill, New York 1980
[3] G. Boyd et al., Phys. Rev. Lett. 75 (1995) 4169
[4] A. Peshier, B. Kämpfer, O.P. Pavlenko, G. Soff, Phys. Rev. D 54 (1996) 2399

Kaon Production in Dense and Hot Hadronic Matter [B]

R. BARTH[1], D. BRILL[3], M. DĘBOWSKI[5], E. GROSSE, P. KOCZOŃ[1], B. KOHLMEYER[4], F. LAUE[1], M. MANG[1], CH. MÜNTZ[2], L. NAUMANN, H. OESCHLER[2], F. PÜHLHOFER[4], E. SCHWAB[1], Y. SHIN[3], P. SENGER[1], J. SPEER[2], H. STRÖBELE[3], CH. STURM[2], A. WAGNER[2], W. WALUŚ[5]

The production of kaons in nucleus-nucleus collisions and their propagation in the nuclear medium is sensitive to both the nuclear equation of state and the modification of hadron properties in the medium. We have studied medium effects on kaon production with the magnetic spectrometer KaoS installed at the heavy ion synchrotron SIS at GSI Darmstadt [1]. The large proton to kaon ratio (10^4 : 1) requires an efficient kaon trigger which is based on a simultaneous time-of-flight and momentum measurement and, for high momentum kaons, on threshold Cherenkov detectors. High accuracy trajectory reconstruction (important for off-line background suppression) is based on two large area multi-wire chambers. The centrality of the collision is determined by the multiplicity of charged particles (p, d, π) measured in the range $12^o < \Theta_{lab} < 48^o$ by a plastic scintillator hodoscope consisting of 96 modules.

The kaon production probability increases strongly with increasing centrality as demonstrated in Fig. 1. The data are measured around midrapidity in Ni+Ni collisions at 1.8 GeV/nucleon (left panel) and at 1.0 GeV/nucleon (right panel). For comparison the K^- data taken at 1.8 GeV/nucleon are superimposed on the data taken at 1.0 GeV/nucleon. The meson multiplicities per solid angle around midrapidity are given by $dM/d\Omega_{c.m.}=(d\sigma/d\Omega_{c.m.})/\sigma_R$ with $d\sigma/d\Omega_{c.m.}$ the energy integrated cross section for meson production in the c.m. system and σ_R the reaction cross section. The collision centrality is tagged by the number of charged particles measured with the large-angle hodoscope. The values of A_{part} are determined by a Monte Carlo simulation for each centrality bin. The calculation is based on measured yields of protons, deuterons and pions and reproduces the charged particle multiplicity as measured by the scintillator hodoscope.

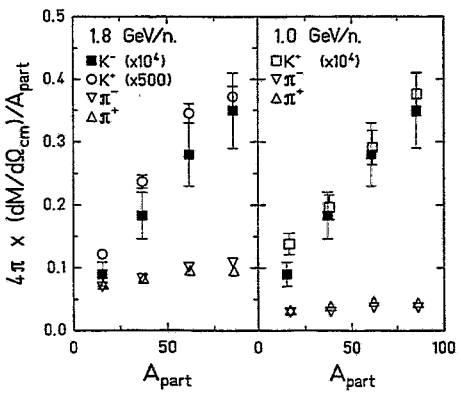

Fig. 1 *Kaon and pion multiplicities per c. m. solid angle and per number of participating nucleon*

The pion multiplicities per solid angle and per A_{part} increase only slightly with A_{part}, whereas the K^+ and K^- multiplicities per A_{part} increase strongly. This effect was first found in Au+Au collisions at 1.0 GeV/nucleon and interpreted as a signature of multiple collisions contributing dominantly to subthreshold K^+ production [2]. To systematically investigate K^- production in the nuclear medium, we want to compare the K^- yield measured in nucleus-nucleus collisions to the K^- yield from free nucleon-nucleon collisions. However, this comparison cannot be performed at the same bombarding energy, as we study subthreshold K^- production in order to amplify a possible effect. Therefore, we introduce an intermediate step: we determine the K^+/K^- ratio at equivalent bombarding energies both in nucleus-nucleus and in nucleon-nucleon collisions. The concept of equivalent beam energies corrects for the different production thresholds: For example, a set of equivalent beam energies is 1 GeV/nucleon for K^+ production and 1.8 GeV/nucleon for K^- production. The resulting Q-values are identical: $\sqrt{s} - \sqrt{s_{thres}} = -0.23$ GeV for both processes $NN \rightarrow K^+\Lambda N$ at 1.0 GeV and $NN \rightarrow K^+K^-NN$ at 1.8 GeV. The study of K^+/K^- ratios at equivalent beam energies has the advantage that trivial medium effects like Fermi motion or multiple collisions largely cancel. According to Fig. 1 the K^+ yield at 1 GeV/nucleon agrees roughly with the K^- yield at 1.8

GeV/nucleon and also the dependence on A_{part} is equal for K^+ and K^- observed at equivalent energies. The corresponding K^+/K^- ratio is found to be 1±0.4. This result for nucleus-nucleus collisions is quite different from the K^+/K^- ratio for proton-proton collisions. Fig. 2 shows the available data on inclusive cross sections for K^+ and antikaon production in proton-proton collisions as a function of the energy above threshold. The K^+ data are taken from [3]. Data on K^- production in pp collisions are very rare. The antikaon data points at $\sqrt{s}$-$\sqrt{s_{thres}}$ = 0.48 and 0.63 GeV in Fig. 2 are determined by taking the sum of the measured cross section for pp→ $K^+\bar{K}^o$pn and pp→ $K^o\bar{K}^o$pp [3]. This is an upper limit for pp→ K^+K^-pp but should correspond to K^- production in pn and nn collisions. The lines in Fig. 2 represent a parametrization of the elementary kaon and antikaon cross sections performed within the framework of a quark statistical phase space calculation [4]. The calculation is in rough agreement to a new experimental value of σ(pp→ppK$^+\Lambda$)=8.2±1.8 nb measured at COSY for $\sqrt{s}$ -$\sqrt{s_{thres}}$ = 2 MeV [5]. According to Fig.2 the elementary K^+ cross section is larger than the K^- cross section by about one order of magnitude for equivalent proton energies close to threshold. When assuming σ(pp→K$^+$+X)≈ σ(pn→K$^+$+X) and neglecting K^+ production via neutron-neutron collisions, the K^+/K^- ratio reduces from 10 for proton-proton collisions to about 7 for nucleon-nucleon collisions at equivalent beam energies. As shown above we find a K^+/K^- ratio of 1±0.4 in Ni+Ni collisions at equivalent beam energies: this corresponds to an enhanced in-medium K^- production by a factor of 7±3. This enhancement of the K^- yield is unexpected, as K^- mesons are strongly absorbed in the nuclear medium by strangeness exchange reactions and, on the contrary, the K^+ meson can hardly be absorbed due to its anti-strange quark.

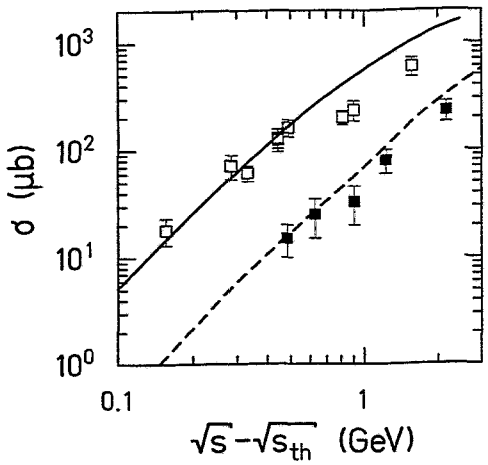

Fig. 2 *Inclusive K^+ and K^- cross section in p+p collisions as a function of the energy above threshold*

There is one important in-medium effect which might cause an enhanced K^- production in nucleus-nucleus collisions with respect to nucleon-nucleon collisions: A reduction of the effective masses of antikaons in the medium will strongly enhance the K^- production. Using the measured K^+ excitation function and the in-medium enhancement factor of 7±3, the reduction of the K^- threshold can be estimated from our data. Assuming a similar beam energy dependence of the K^+ and K^- production cross sections in nucleus-nucleus collisions, the enhancement factor results in a difference of available energies $\sqrt{s_2}$-$\sqrt{s_1} = 270^{+55}_{-90}$ MeV. This value can be considered a first estimate for the in-medium K^- mass reduction from our experimental data.

[1] *GSI Darmstadt*
[2] *TH Darmstadt, Institut für Kernphysik*
[3] *Universität Frankfurt, Institut für Kernphysik*
[4] *Universität Marburg, Physikalisches Institut*
[5] *Jagiellonian Cracow, Institute of Physics*

References

[1] P. Senger et al., Nucl. Instr. Meth. **A 327** (1993) 393
[2] D. Miskowiec et al., Phys.Rev.Lett. **72** (1994) 3650
[3] CERN HERA Report 84-01 (1984)
[4] H. Müller, Z.Phys. **A 353** (1995) 103
[5] J. Balewski et al., Phys.Lett. **B** (1996) in print

Proton Proton Bremsstrahlung at Beam Momentum 797 MeV/c [B,K]

P. Hermanowski[1], E. Kuhlmann[2], S. Dshemuchadse, P. Michel, K. Möller[2], B. Naumann, L. Naumann, A. Schamlott, A. Schülke, M. Steinke[1], U. Zielinski[1], A. Böhm[2], K.T. Brinkmann[2], H. Freiesleben[2], B. Hübner[2], S. Lange[2] and the COSY-TOF-Collaboration

In October 1996 we had our second dedicated run on pp-bremsstrahlung. The beam momentum was chosen as 797 MeV/c. Thus the 2-particle reaction $pp \to d\pi^+$ which opens at 789 MeV/c as well as the $pp\pi^0$ channel (p_{thr} = 777 MeV/c) were accessible; both were wanted as a source for useful calibration data. In order to identify bremsstrahlung events, the main principle of the experiment was to detect the two accompanying protons and to reconstruct the 4-momentum of the photon from the combined information on the protons' points of impact, their energy losses dE/dx and their time-of-flight-values Δt. A large amount of data has been collected which is presently being analysed. First preliminary results will be given in the following. The COSY-TOF spectrometer has extensively been described previously [1]. Additionally to the "traditional" set-up in this particular experiment the central hole of the "Quirl" was filled with a segmented 12-part scintillator device called PAD-detector thus reducing the blind hole around the beam axis to an area with radius less than 15 mm. It ensured the detection of deuterons from the $d\pi^+$ reaction. Four separate scintillator strips at a mean angle of $\theta = 50°$ and covering an azimuthal range of $\Delta\phi = 15°$ served as luminosity monitors. In combination with the "Quirl" they allowed the coincident detection of elastically scattered protons in a limited angular range. The trigger for recording bremsstrahlung events was based on requiring 2 hits in the start detector system, additional 2 hits in at least 2 of the 3 "Quirl"-layers and no hit in either of the veto detectors. In the ensuing analysis these conditions were tightened by applying moderate QDC and narrow TDC cuts, and by requiring 2 reconstructed pixel elements in the "Quirl" together with 2 geometrically corresponding elements in the start unit. Thus rather clean data samples were extracted in the first sweep of the analysis. Data were taken with full and empty target. Proton induced reactions on nuclei of the foil material (mainly carbon and oxygen) could thus be isolated and after suitable normalization be subtracted. As an example fig. 1 shows distributions of the square of the reconstructed missing mass of the unobserved particle X. The two top curves represent full (left) and empty (right) target measurements, the one on the bottom left shows both curves overlayed and the bottom right one the result after subtraction. Two narrow structures representing $pp\pi^0$ and $pp\gamma$ events are visible in all but the empty target distributions and they alone remain after subtraction (fig. 1, bottom right).

After further enlargement of the spectrometer through "Ring" and "Barrel" sections, scheduled for summer 1997, and first successful extraction of a polarized proton beam the experiment will be continued.

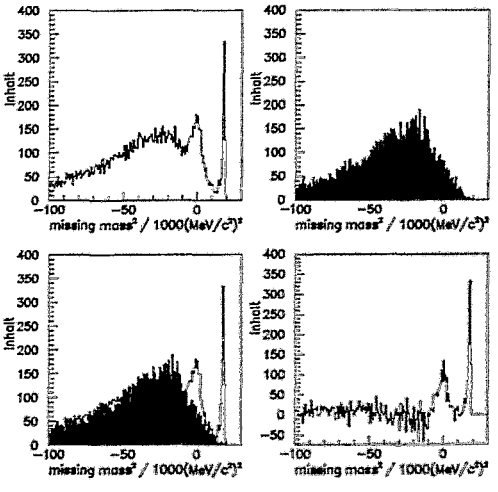

Fig. 1 *Proton pair events as a function of the missing mass squared (see text).*

[1] *Institut für Experimentalphysik I, Ruhr Universität Bochum*
[2] *Institut für Kern- und Teilchenphysik, TU Dresden*

References

[1] U. Bechstedt et al., Annual Report 1995 Jül-3200 p. 5 and earlier volumes

Neutron Time-of-Flight Measurements at the COSY-TOF-Spectrometer [B,K]

A. Böhm[1], K.-Th. Brinkmann[1], H. Freiesleben[1], J. S. Lange[1], K. Hebbel[2], W. Scobel[2], S. Dshemuchadse, P. Michel, K. Möller[1], B. Naumann, L. Naumann, A. Schamlott, A. Schülke and the COSY-TOF Collaboration

A large area neutron detector has been built in Hamburg and Dresden as a supplement to the COSY-TOF-spectrometer. Fig. 1 shows the schematical setup of one of the four Dresden modules. The array, called COSYnus (COSY neutron spectrometer), was successfully tested during several beamtimes at the TOF spectrometer. In October 1995, it was used with a short version of the TOF (only the inner part of the end cap, the Jülich quirl, 86 cm behind the liquid hydrogen target), at 350 MeV proton beam energy. A clean signal for the $pp \rightarrow pn\pi^+$ reaction was obtained from the proton signal in the quirl and the neutron detected in COSYnus, so that the missing mass of the undetected pion could be reconstructed as shown in Fig. 2. The overall time-of-flight start signal was delivered by the Rossendorf start detector MARS which is routinely used at low beam energies.

Beamtime has been allocated [1] for a thorough investigation of the $pn\pi^+$ channel near threshold. The experiment will be the first at COSY to make use of the barrel section of the TOF spectrometer which was recently completed in Rossendorf [2]. Pions from the channel under investigation as well as particles from other reaction channels, in particular elastic scattering, will be detected in the barrel. The simultaneous measurement of elastic scattering is crucial for the normalization of measured pion production cross sections.

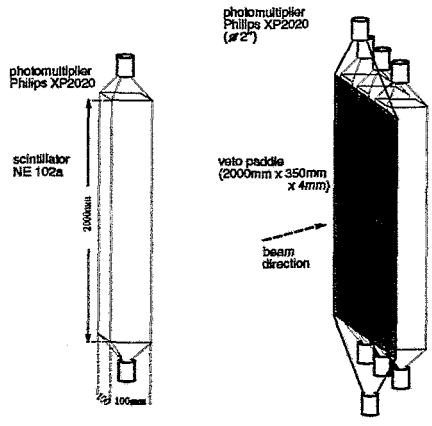

Fig. 1 *Schematic view of one module of the Dresden neutron detector.*

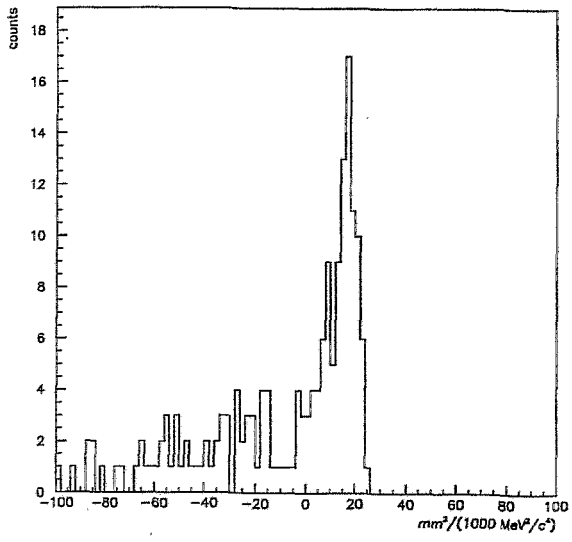

Fig. 2 *Missing-mass spectrum $pp \rightarrow pn\pi^+$ at 350 MeV incident beam energy.*

[1] *Institut für Kern- und Teilchenphysik, TU Dresden*
[2] *Institut für Experimentalphysik, Universität Hamburg*

References

[1] K.-Th. Brinkmann et al., COSY Proposal 39
[2] S. Dshemuchadse et al., this Annual Report

Are Missing-Mass Measurements the Key for Understanding Subthreshold Particle Production?[B]

T. KIRCHNER, H. MÜLLER, CHR. SCHNEIDER, CHR. SCHNEIDEREIT, O.W.B. SCHULT[1], K. SISTEMICH[1]

The term "subthreshold particle production" is applied to the energy region between the threshold for the production of a definite particle in a nuclear reaction and the corresponding threshold in a free nucleon-nucleon (NN) collision. Below the NN threshold, nuclear phenomena must be the reason for subthreshold particle production. The increasing interest in understanding these phenomena is the reason why the investigation of subthreshold production became an important research area in recent years. Different physical pictures are used to interpret the experimental results. High-momentum components of the nuclear wave function, clusters of several target nucleons, two-step processes, or medium effects (like lower effective masses of the hadrons due to the restoration of chiral symmetry) might be responsible for the abundant subthreshold production observed (for references see [1]).
The determination of the number a of target nucleons participating in the interaction process will be a decisive tool to decide between the various approaches. This will be discussed in the following for the case of subthreshold K^+ and K^- production, because there are plans [2, 3] to investigate these processes at the spectrometer ANKE [4] at COSY-Jülich.
In the case of K^- production

$$p + [aN] \rightarrow (a+1)N + K^+ + K^- \qquad (a = 1 \ldots A), \tag{1}$$

with a being the number of participants, an energy of about 1 GeV is transferred. Most of this energy is necessary to create the kaon pair. Only a small amount of the available energy remains as relative energy between the $(a+1)$ nucleons and the two kaons in the rest system of this particle group. Thus, the velocity of all particles originating from the participant interaction is in the laboratory system quite close to the (high) velocity of their rest system itself. Because the energy transfer to the remaining $(A-a)$ spectator nucleons is small, their relative velocities as well as the velocity of their rest system in the laboratory remain small, too. Therefore, a kinematic distinction between these two groups of particles is possible. The recipe for fixing the number of participants is thus quite obvious: one has to measure all fast particles (kaons, nucleons, fragments), which at subthreshold energies are emitted under small angles in the laboratory system. In the missing-mass spectra peaks must appear, which correspond to the

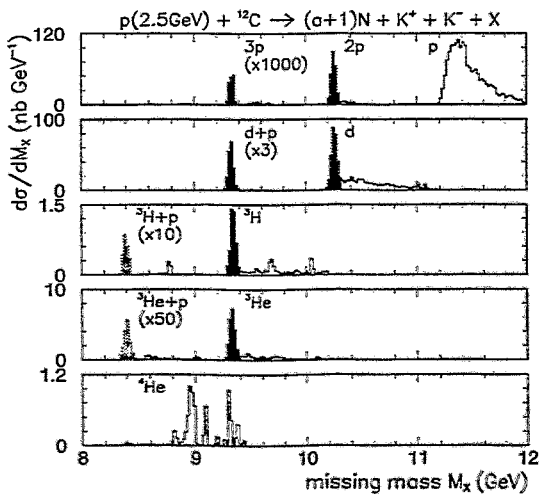

Fig. 1 *Calculated missing mass spectra for the reaction $p\,^{12}C$ at 2.5 GeV for the production of K^+/K^- pairs in the interaction with a participants (see Eq.(1)). Type and number of the nucleonic ejectiles are indicated.*

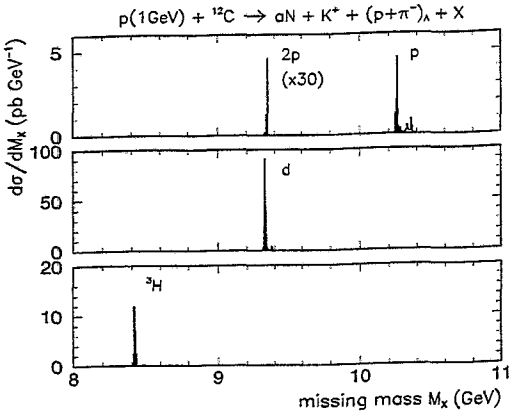

Fig. 2 *Calculated missing mass spectra from the reaction $p^{12}C$ at 1.0 GeV for the production of K^+ mesons in the interaction with a participants (see Eq.(2)). Type and number of the nucleonic ejectiles are indicated.*

masses of the spectator system consisting of the residual $(A-a)$ nucleons, if all fast particles are measured. If one or several of the fast particles are missed then they increase the corresponding missing mass and the peaks are accompanied by tails at the high-mass side.
As an illustration, missing-mass spectra calculated with the ROC model [5] (and references therein) for p^{12}C interactions at 2.5 GeV are plotted in Fig. 1. It is assumed that all charged particles emitted under angles $\Theta \leq 10°$ are detected with a momentum resolution of $\Delta p/p = 1.5\%$. There are peak positions at about 10.2, 9.3 and 8.4 GeV, which correspond to spectator systems consisting of eleven to nine nucleons, respectively.
K^+ meson production (see Fig. 2) is associated with the creation of an unstable Λ baryon, which can be detected via its decay into charged particles according to

$$p + [aN] \rightarrow K^+ + (p + \pi^-)_\Lambda + aN \qquad (a = 1 \ldots A). \tag{2}$$

The π^- meson is rather light and will be emitted into a wide angular region contrary to the heavier particles, which are strongly forward peaked. This fact diminishes the detection efficiency. Therefore, an additional detection system with large angular acceptance at ANKE would be desirable and is under discussion (for details see [6]). So far, subthreshold particle production has been investigated by inclusive measurements. In such experiments the various subprocesses cannot be identified in a model-independent way, because inclusive momentum spectra contain no peculiarities which would allow this. In contrast, the positions of the expected peaks in the missing-mass spectra are clearly model independent, while the calculation of the relative intensity of the various subprocesses is a critical measure, which depends on the model approach. Thus, by comparing experimental missing-mass spectra with theoretical results a more definite verification or falsification of the different model approaches and, consequently, a deeper understanding of particle production becomes possible.

[1] *Forschungszentrum Jülich GmbH, Institut für Kernphysik, 52428 Jülich, Germany*

References

[1] H. Müller, Z. Phys. A **355**, 223 (1996)
[2] W. Borgs et al., COSY Proposal #18. Jülich (1990)
[3] T. Kirchner et al., COSY Proposal #21. Jülich (1996)
[4] O. W. B. Schult et al., Nucl. Phys. A **583**, 629 (1995)
[5] H. Müller, Z. Phys. A **353**, 237 (1995)
[6] Chr. Schneider, Ph.D. thesis, Technische Universität Dresden (1997)

Abstracts of publications

Study of the Out-Of-Plane Emission of Protons and Light Fragments in Symmetric Heavy-Ion Collisions
(Z. Phys. A 355 (1996) 61)

Brill, D., P. Beckerle, C. Bormann, E. Schwab, Y. Shin, R. Stock, H. Ströbele, P. Baltes, C. Müntz, H. Oeschler, C. Sturm, A. Wagner, R. Barth, M. Cielak, M. Debowski, E. Grosse, P. Koczo, M. Mang, D. Mikowiec, R. Schicker, P. Senger, B. Kohlmeyer, F. Pühlhofer, J. Speer, K. Völkel, W. Waluś

Abstract: Midrapidity protons from ^{209}Br + ^{209}Bi collisions were measured with the Kaon Spectrometer at SIS at incident energies of E_{Lab}/A = 400, 700 and 1000 MeV. Additionally, light fragments were analysed at 400 MeV. We have investigated the azimuthal emission pattern of the particles relative to the reaction plane as function of transverse momentum, bombarding energy and impact parameter. We observe an enhanced emission of particles perpendicular to the reaction plane at all bombarding energies. The ratio of the number of particles emitted out-of-plane/in-plane increases strongly with the particles transverse momentum. The anisotropy decreases with increasing beam energy. Composite particles show a much stronger effect than protons.

K $^+$-Meson Production in pBe Interactions at T_p = 2.9 GeV
(Z. Phys. A 355 (1996) 93)

Büscher, M., R. Eßer, A. Franzen, L. v. Horn, D. Kopyto, H. Ohm, H. Seyfarth, K. Sistemich, H. Müller, B. Prietzschk, B. Rimarzig, C. Schneider, C. Schneidereit, A. Akindinov, M. Chumakov, V. Demechin, V. Ergakov, A. Gerasimov, V. Goryachev, Y. Kiselev, V. Kostromin, A.A. Sibirtsev, V. Sopov, V. Tchernyshev, V. Kruglov, A. Petrus, V. Koptev, S. Mikirtychyants

Abstract: The production of K^+ and π^+ mesons and protons in pBe collisions at T_p = 2.9 GeV has been studied at the ITEP proton synchrotron. Ejectiles with a momentum of p = 545 MeV/c were observed under an emission angle $\vartheta = 17°$. The detectors which have been developed for the identification of kaons out of a six orders of magnitude more intense background of pions and protons are described. A cross-section ratio $d^2\sigma_{K+}/d\Omega dp$: $d^2\sigma_{\pi+}/d\Omega dp$: $d^2\sigma_p/d\Omega dp$ of (1±0.34):(85±1):(31±1) has been measured. Normalization with existing pion data yields an invariant differential cross section $E \cdot d^3\sigma_{K+}/d^3p$ = (3.1± 1.2) mb GeV^{-2}c^{3}sr^{-1}and a total cross section of $\sigma_{tot}(p\text{Be})$ = (3.7±1.5) mb. These cross sections are compared with existing data and theoretical predictions. The A dependence of K^+ production in the few-GeV range is analyzed.

Subthreshold K$^+$ Production in Proton-Nucleus Collisions
(Z. Phys. A 356 (1996) 313)

Debowski, M., R. Barth, M. Boivin, Y. Le Bornec, M. Cieślak, M.P. Comets, P. Courtat, R. Gacougnolle, E. Grosse, T. Kirchner, J.M. Martin, D. Miśkowiec, C. Müntz, E. Schwab, P. Senger, C. Sturm, B. Tatischeff, A. Wagner, W. Waluś, N. Willis, R. Wurzinger, J. Yonnet, A. Zghiche

Abstract: Double differential K^+ cross sections have been measured in p+C collisions at 1.2, 1.5 and 2.5 GeV beam energy and in p+Pb collisions at 1.2 and 1.5 GeV. The K^+ spectrum taken at 2.5 GeV can be reproduced quantitatively by a model calculation which takes into account first chance proton-nucleon collisions and internal momentum with energy distribution of nucleons according to the spectral function. At 1.2 and 1.5 GeV beam energy the K^+ data excess significantly the model predictions for first chance collisions. When taking secondary processes into account the results of the calculations are in much better agreement with the data.

K^+ Emission in Symmetric Heavy Ion Reactions at Subthreshold Energies
(Phys. Rev. Lett. 77 (1996) 4884)

Elmér, R., M. Berg, L. Carlén, B. Jakobsson, B. Norén, A. Oskarsson, G. Ericsson, J. Julien, T.-F. Thorsteinsen, M. Guttormsen, G. Løvhøiden, V. Bellini, E. Grosse, C. Müntz, P. Senger, L. Westerberg

Abstract: Subthreshold K^+ production cross sections have been measured in symmetric Ne + NaF, Ni + Ni, and Au + Au collisions at 1.0A GeV. The mass dependence is strong, close to A^2. The angular distributions are nonisotropic in the center-of-mass system. Introducing rescattering seems to explain this effect to a large extent.

Heating of Nuclei with Energetic Antiprotons
(Phys. Rev. Lett. 77 (1996) 1230)

Goldenbaum, F., W. Bohne, J. Eades, T. v. Egidy, P. Figuera, H. Fuchs, J. Galin, Ye.S. Golubeva, K. Gulda, D. Hilscher, A.S. Iljinov, U. Jahnke, J. Jastrzebski, W. Kurcewicz, B. Lott, M. Morjean, G. Pausch, A. Péghaire, L. Pienkowski, D. Polster, S. Proschitzki, B. Quednau, H. Rossner, S. Schmid, W. Schmid, P. Ziem

Abstract: The annihilation of energetic (1.2 GeV) antiprotons is exploited to deposit maximum thermal excitation (up to 1000 MeV) in massive nuclei (Cu, Ho, Au, and U) while minimizing the contribution from collective excitation such as rotation, shape distortion, and compression. Excitation energy distributions $d\sigma/dE^*$ are deduced from eventwise observation of the whole nuclear evaporation chain with two 4π detectors for neutrons and charged particles. The nuclei produced in this way are found to decay predominantly statistically, i.e., by evaporation.

Asymmetry of the Dielectron Emission Rate in an Isospin-Asymmetric Pion Medium
(Phys. Lett. B 372 (1996) 187)

Gulamov, T.I., A.I. Titov, B. Kämpfer

Abstract: The dielectron emission by pion annihilation in an isospin asymmetric pion gas at finite temperature is considered. Due to the difference between the longitudinal and transverse parts of the in-medium ρ meson self-energy a specific asymmetry of the rates is caused for electron pairs with relative momenta perpendicular or parallel to the total pair momentum. This asymmetry may be considered as a sensitive signal of in-medium modifications of the ρ properties.

Neutral ρ-Meson Properties in an Isospin-Asymmetric Pion Medium
(Yad. Fiz. 59 (1996) 727)

Gulamov, T.I., A.I. Titov, B. Kämpfer

Abstract: We evaluate the ρ-meson self energy at finite temperature T and charged-pion chemical potential μ_Q as well by utilizing a conventional π-p effective Lagrangian and functional integral representation of the partition function in the one-pion loop order (i.e., second order in the $g_{p\pi\pi}$ coupling constant). We find an increase of both the p-meson mass and the width with increasing temperature and chemical potential μ_Q. At large value of μ_Q these increases may be about two times larger as compared with the pure temperature shift of Gale and Kapusta at vanishing μ_Q.

Production and Decay of Hot Nuclei Following Antiproton Annihilation at Rest and in Flight
(Yad. Fiz. 59 (1996) 1625)

Jahnke U., W. Bohne, J. Eades, T. von Egidy, P. Figuera, H. Fuchs, J. Galin, F. Goldenbaum, K. Gulda, Ye.S. Golubeva, F.J. Hartmann, D. Hilscher, A.S. Iljinov, J. Jastrzebski, W. Kurcewicz, B. Lott, M. Morjean, G. Pausch, A. Peghaire, L. Pienkowski, D. Polster, S. Proschitzki

Abstract: The decay modes of highly excited nuclei have been studied using energetic antiprotons. The excitation energy distributions are in very good agreement with predictions from the intranuclear cascade model.

Bethe-Salpeter Amplitudes and Static Properties of the Deuteron
(Phys. Rev. C 54 (1996) 986)

Kaptari, L.P., A.Yu. Umnikov, S.G. Bondarenko, K.Yu. Kazakov, F.C. Khanna, B. Kämpfer

Abstract: Extended calculations of the deuteron's static properties, based on the numerical solution of the Bethe-Salpeter equation, are presented. A formalism is developed, which provides a comparative analysis of the covariant amplitudes in various representations and nonrelativistic wave functions. The magnetic and quadrupole moments of the deuteron are calculated in the Bethe-Salpeter formalism and the role of relativistic corrections is discussed.

The Impact of Kaon Polarization in Nuclear Matter on the K^- Production in Heavy-Ion Collisions
(Int. J. Mod. Phys. E5 (1996) 313)

Kolomeitsev, E.E., D.N. Voskresensky and B. Kämpfer

Abstract: The impact of the kaon polarization in nuclear matter on the K^- yield in intermediate-energy heavy-ion collisions is investigated. Our scenario of the strange particle production and dynamics is based on an expanding fireball model. This allows for a proper account of in-medium effects. A relation between observed K^+ and K^- yields is derived. Differential K^- cross sections are calculated and compared with available experimental data taken at various collision energies. It turns out that in-medium effects can modify the K^- yields by factors 2 to 5 at beam energies between 2 and 1 AGeV.

Hot and Dense Pion Gas with Finite Chemical Potential
(Acta Physica Polonica B 27 (11) (1996) 3263)

Kolomeitsev, E.E., D.N. Voskresensky, B. Kämpfer

Abstract: A dense and hot pion system with a dynamically fixed particle number and an arbitrary charge is investigated with respect to ultra-relativistic heavy-ion collisions. The Lagrangian for describing such a system is derived from Weinberg's chiral Lagrangian for the pion-pion interaction. Pion polarization operators are calculated within the Hartree approximation. The pion spectrum in the isospin symmetrical gas is presented. The effective in-medium pion gap depends sensitively on the density and the temperature, and it is found to exceed both the free pion mass and the corresponding value for the pion gas in chemical equilibrium. The possibility of a Bose-Einstein condensation is also discussed.

Are Missing-Mass Measurements the Key for Understanding Subthreshold Particle Production?
(Z. Phys. A 355 (1996) 223)

Müller, H.

Abstract: By measuring the fast particles emerging from a proton-nucleus interaction the number of participants can be determined. This might be the key quantity for understanding subthreshold particle production.

Massive Quasiparticle Model of the SU(3) Gluon Plasma
(Phys. Rev. D 54 (1996) 2399)

Peshier, A., B. Kämpfer, O.P. Pavlenko, G. Soff

Abstract: Recent SU(3) gauge field lattice data for the equation of state are interpreted by a quasiparticle model with effective thermal gluon masses. The model is motivated by lowest-order perturbative QCD and describes very well the data. The proposed quasiparticle approach can be applied to study color excitations in the nonperturbative regime. As an example we estimate the temperature dependence of the Debye screening mass and find that it declines sharply when approaching the confinement temperature from above, while the thermal mass continuously rises.

Studies of *pp* and *pd* Interactions with the Time of Flight Spectrometer at COSY
(Acta Physica Polonica B Vol.27 (1996))

Roderburg, E., R. Bilger, A. Böhm, K.-T. Brinkmann, H. Clement, P. Cloth, M. Dahmen, M. Dellert, V. Drüke, H. Dutz, W. Eyrich, H. Freiesleben, D. Filges, M. Fritsch, R. Geyer, A. Hassan, J. Hauffe, J. Hays, P. Hermanowski, B. Hübner, P. Jahn, K. Kilian, H. Koch, R.A. Kraft, J. Krug, J. Kress, E. Kuhlmann, S. Lange, H. Matthäy, A. Metzger, W. Meyer, P. Michel, K. Möller, M. Moosburger, H.P. Morsch, C. Nake, B. Naumann, L. Naumann, N. Paul, M. Rogge, C. Rohloff, A. Schamlott, A. Schülke, T. Sefzick, E. Sinde, R. Sperl, M. Steinke, F. Stinzing, P. Turek, G.J. Wagner, D. Wallom, S. Wirth, U. Zielinsky

Abstract: First results of measurements with the Time of Flight spectrometer are shown. Reconstructed missing mass distributions of the reactions $pp \to d\pi^+$, $pp \to pp\pi^0$, and $pp \to pK^+\Lambda$ are given.

ρ-Meson Self-Energy and Dielectron Emissivity in an Isospin-Asymmetric Pion Medium
(Phys. Rev. D 53 (1996) 3770)

Titov, A.I., T.I. Gulamov, B. Kämpfer

Abstract: The ρ-meson self-energy in an isospin-asymmetric pion gas at finite temperature and charged-pion chemical potential is evaluated. We utilize a conventional effective $\pi-\rho$ Lagrangian and the functional integral representation of the partition function in the second order in the $\rho\pi\pi$ coupling constant. We analyze the ρ-meson polarization operator and its dependence on the invariant mass M and spatial momentum $\mid \mathbf{p} \mid$ of the ρ-meson. The pole positions and the values of the imaginary parts of the self-energy for different polarization states have different functional dependences on M and $\mid \mathbf{p} \mid$. The corresponding dielectron rate (calculated from the imaginary part of the in-medium ρ-meson propagator) shows a distinctive asymmetry when the momentum $\mathbf{t} = \mathbf{p}_+ - \mathbf{p}_-$ is perpendicular or parallel to $\mathbf{p}_\pm$, where $\mathbf{p}_\pm$ are the $e^\pm$ momenta of the electron pair.

The Reaction $NN \to NN \to_\gamma$ in the 1 GeV Region within an Effective One-Boson Exchange Model
(Phys. Lett. B 372 (1996) 15

Titov, A.I., B. Kämpfer, B.L. Reznik, V. Shklyar

Abstract: Within an effective one-boson exchange parametrization of the T matrix of NN interactions we calculate cross sections for the reactions $pp \to pp\gamma$ and $pn \to pn\gamma$ for proton incidence energies in the order of 1 GeV. Besides bremsstrahlung processes we consider photons from Δ decays and contributions from the $\eta \to \gamma\gamma$ process, where the η is excited via the N_{1535} resonance. At beam energies above 700 MeV the Δ decay channel dominates for large photon energies, while above the η threshold the η decay photons show up only in a narrow window. The low energy photons stem from pure bremsstrahlung processes.

Heavy-Ion Reactions

Theoretical work aimed for investigating the effects of mean field and in-medium cross-section on the observables in heavy-ion collisions. The sensitivity of the cross-section to the directed side flow was demonstrated in the molecular dynamics approach. In various energy regions new data became available quantifying the influence of the electric charge of the combined system on spectra of positively and negatively charged particles. The observed difference between these spectra delivers information on the source properties and supplements the Hanbury-Brown and Twiss analysis.

The FOPI collaboration proceeded successfully with their programme towards higher bombarding energies where meson production becomes essential. New data are taken for collisions of the four target-projectile combinations of ^{96}Zr and ^{96}Ru to investigate equilibration and collective flow as a function of the isospin between 400 A·MeV and 1.5 A·GeV. Still there are open questions for energies around a few hundreds of MeV. The amount of pre-equilibrium emission could be studied by analysing the ^{3}He to ^{4}He ratio which is larger than predicted by the statistical model although partly of ^{3}He could come from coalescence. As in the GeV region fragments are becoming rare proton-proton correlations are the proper mean to extract the source size. The analysis of the reaction Ni on Ni gives an example how time and spatial extension can be disentangled by means of the method developed by S. Koonin.

Since the 4π-spectrometer FOBOS went into operation at the U-400M synchrotron in Dubna at the end of 1995, the FOBOS group was very active in taking data for intermediate heavy-ion reactions. ^{197}Au and ^{232}Th targets were bombarded with ion beams of ^{7}Li and ^{14}N of 43 A·MeV and 53 A·MeV, respectively. This energy is just below the threshold of the transition from fission to multifragmentation. Several 10^7 binary and 10^5 ternary events were collected. The kinetic energies of very asymmetric fission events were compared with the Viola systematics. A calculation of the energy landscape supports the experimental findings of preferred emission of deeply bound clusters. Surprisingly small fragment-mass spreadings were found at high excitation energies. Their interpretation requires a detailed analysis of the cooling mechanism along the fission path. The transition from binary to ternary decay were studied on the basis of velocity-velocity correlations. Emissions of light fragments from the neck as well as nearly mass-symmetric three-body decays were observed. The system decays preferentially from a linear configuration. A theoretical analysis is in preparation to extract the pre- and post-scission contributions to the light charged particle emission.

Study of Freeze-Out Time by Means of Pionic Charge Ratio in Ultrarelativistic Heavy Ion Collisions [B]

H.W. BARZ[1], J.P. BONDORF[2], J.J. GAARDHØJE[2] AND H. HEISELBERG[3]

In heavy ion collisions at ultrarelativistic energies, nuclear systems with a total net positive charge of around 160 can now be studied. In central Pb+Pb collisions at CERN-SPS energies a significantly increased ratio of negative pions to positive pions has been observed at low transverse masses.
We investigate this effect as a consequence of the strong Coulomb field of the source which accelerates the pions essentially during their free motion after freeze-out. The freeze-out scenario is described by a longitudinally and transversally expanding fireball in thermal equilibrium. Pion trajectories are calculated in the field of the fireball. Initially formed charge asymmetries turn out to be unimportant since they are washed out by thermal motion.

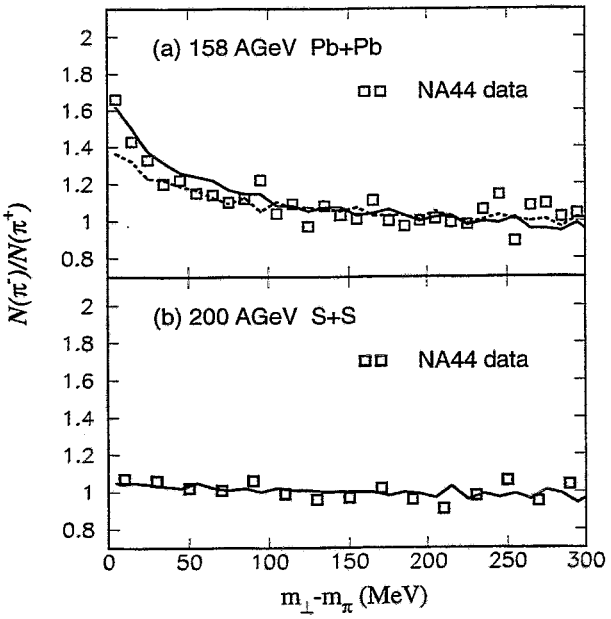

Fig. 1 *Calculated $N(\pi^-)/N(\pi^+)$ ratios for the reactions (a) $Pb+Pb$ and (b) $S+S$ as a function of transverse mass compared to data [1]. The solid lines are calculated using a freeze-out time of τ_0= 7 fm/c while the dashed line in (a) shows the result for τ_0 = 15 fm/c.*

Our investigations show that an increase of temperature, transversal expansion velocity or freeze-out time diminishes the difference between positive and negative pions. On the other hand the effect has turned out to be proportional to the rapidity density of the net positive charge. Taking a temperature of 120 MeV, a mean transverse velocity of 0.42 of light velocity and a net charge rapidity density of 35, which are compatible with recent measurements of the NA44 and NA49 group, we can adjust the freze-out time parameter of the source to be 7 fm/c in order to reproduce the data (see Fig.1).

[1] *Institut für Theoretische Physik, TU Dresden and Institut für Kern- und Hadronenphysik, FZR*
[2] *Niels Bohr Institute, Copenhagen, Denmark*
[3] *NORDITA, Copenhagen, Denmark*

References

[1] H. Bøggild et al., NA44 collaboration., Phys. Lett. **B372**, 343 (1996)

Effect of the Nucleon-Nucleon Cross Section on Directed Sideflow in Heavy Ion Collisions [B]

H.W. Barz[1], J.P. Bondorf[2], D. Idier[2] and I.N. Mishustin[2]

A molecular dynamical model has been developed to describe heavy-ion collisions at intermediate energies up to 400 MeV per nucleon. Nucleons are represented by wave packets with time independent widths. Using Skyrme-forces an effective classical Hamiltonian is derived which governs the motion of the nucleons. In addition two-particle collisions are included using an effective nucleon-nucleon cross-section. We have compared Skyrme interactions Skm* with SKIII which gives incompressibility moduli of 230 MeV and 360 MeV, respectively, when applied to matter. Both types of forces reproduce rather well the production of intermediate mass fragments (IMFs) with charges larger than two [1].

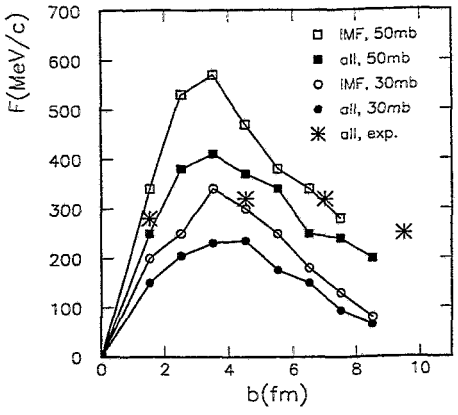

Fig. 1 *Calculated average side flow F of all fragments and IMFs as a function of the impact parameter b for Au on Au collisions at 150 MeV per nucleon for two values of 30 mb and 50 mb of the effective cross section. Data (stars) are taken from [2].*

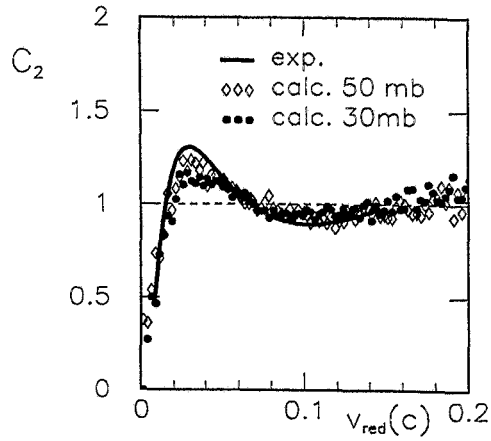

Fig. 2 *Effect of the nucleon-nucleon cross-section on the peak in the IMF-IMF correlation function C_2 as a function of the reduced velocity v_{red} for Au on Au collisions at 250 MeV per nucleon. Data are taken from [3].*

Especially, we have studied the effect of the in-medium cross-section on the amount of side flow $F = (1/A_{IMF})d\langle p_x\rangle/dy$. A strong rise has been found with increasing cross section. Fig. 1 shows the side flow calculated with the force Skm* for IMFs and its average over all produced particles. The side flow affects also the peak in the velocity-correlation function C_2 measured in semi-peripheral Au on Au collisions [3]. Larger side flow causes larger asymmetry in the azimuthal angular distribution and shifts therefore the maximum of the mixed correlation function towards larger relative velocities which increases the peak in the function C_2 as shown in Fig. 2.

[1] *Institut für Theoretische Physik, TU Dresden and Institut für Kern- und Hadronenphysik, FZR*
[2] *Niels Bohr Institute, Copenhagen, Denmark*

References

[1] H.W. Barz, J.P. Bondorf, D. Idier and I.N. Mishustin, Phys. Lett. **B382** (1996) 343
[2] H.A. Gustafsson et al., Mod. Phys. Lett. **A3** (1988) 849
[3] R. Kotte et al., Phys. Rec. **C51** (1995) 2686

Proton-Proton Correlations in Central Collisions of Ni+Ni at 1.93 A·GeV and the Space-Time Extent of the Emission Source[B,G]

R. KOTTE, J. BIEGANSKY, J. MÖSNER, W. NEUBERT, C. PLETTNER AND D. WOHLFARTH
FOPI COLLABORATION

We have studied experimental small-angle correlations of proton pairs produced in central collisions of Ni+Ni at 1.93 A·GeV. The present analysis [1] uses a subsample of the data, taken with the outer Plastic Wall/Helitron [2] combination of the FOPI detector system [3] at the heavy-ion synchrotron SIS at GSI Darmstadt. For the first time the difference between transverse and longitudinal correlations has been derived in heavy-ion reactions in the beam energy region of $1 - 2A$·GeV. This difference can be explained as a result of the finite source lifetime. The additional information allows to unravel the space-time ambiguity of the emission process. We have fitted simultaneously the longitudinal and transverse correlation functions with the predictions of the Koonin-Pratt formalism [4]. The fast collective expansion of the participant zone introduces a reduction of the extracted source radius of more than 30%. Correcting for this effect and taking into account the finite experimental resolution the extracted r.m.s. radius and emission time parameters of the source amount to $R_{rms} = (4.2 \pm 1.2)$ fm and $t_{rms} = (11^{+7}_{-5})$ fm/c, respectively. In contrast, the analysis of the angle-integrated correlation function gives an upper limit $R_{rms} = (7.0 \pm 1.4)$ fm of the source radius. The estimated characteristic source emission time is the shortest one determined with the method of directional cuts on the two-proton correlation function known so far. It does well compare with the typical expansion time of the source of about 10 fm/c.

References

[1] R. Kotte et al., Proc. Int. Workshop "Heavy Ion Physics at Low, Intermediate and Relativistic Energies using 4π Detectors", Poiana Brasov, Romania, 1996, in press.
[2] Y. Leifels, GSI Nachrichten, GSI 08-95, 4 (1995); S. Mohren et al., GSI 96-1, 183 (1996).
[3] A. Gobbi et al., Nucl. Instr. Meth. **A324**, 156 (1993).
[4] S.E. Koonin, Phys. Lett. **70B**, 43 (1977); W. Bauer, C.K. Gelbke and S. Pratt, Ann. Rev. Nucl. Part. Sci. **42**, 77 (1992), and references cited therein.

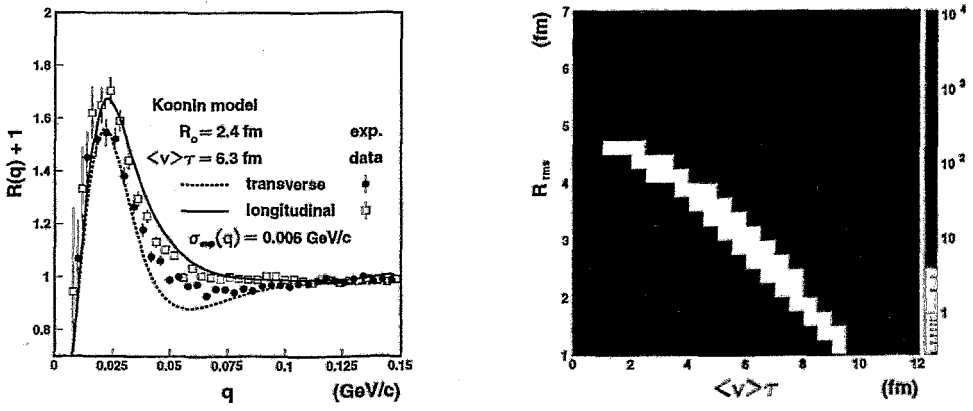

Fig. 1 *Left panel: The transverse (dots) and longitudinal (squares) two-proton correlation functions in dependence of the relative momentum* $q = \frac{1}{2}|\mathbf{p}_1^{cm} - \mathbf{p}_2^{cm}|$ *for central events which comprise about 8% of the total cross section. Dashed and full lines are the corresponding results of Koonin model calculations using the Gaussian source parameters given in the figure. The results of the model are folded with an experimental resolution of* $\sigma_{exp}(q) = 6$ *MeV/c. Right panel: The distribution of* χ^2 *per degree of freedom as determined by simultaneously comparing measured longitudinal and transverse correlation functions (over the range* $q = 12 - 32$ *MeV/c) with the correlation functions predicted by the Koonin model. The quantity is given in dependence of the r.m.s. radius* $R_{rms} = \sqrt{3/2}R_0$ *and the Gaussian lifetime parameter* $\langle v \rangle \tau$.

Light Charged Particle Emission in Central Au+Au Collisions [B,G]

W. NEUBERT, A.S. BOTVINA[1], J.BIEGANSKY, R. KOTTE, J. MÖSNER, C.PLETTNER AND D. WOHLFARTH

A modified statistical multifragmentation model which considers the emission of neutrons and light charged particles (LCP) prior to thermalization has been recently presented in ref. [1]. The essential quantities to parametrize the thermal source are the excitation energy E^*, the number of nucleons A_s and the energy of the radial flow E_f. These parameters have been derived from the steepness of the charge distributions of intermediate mass fragments (IMF, $Z \geq 3$) and the IMF multiplicities as described in [1]. The corresponding values at 250 AMeV are $E^* = (11.5 \pm 1.5)$ AMeV, $A_s \simeq 217$ and $E_f = 34$ AMeV (taken from ref.[2]). The proton, deuteron and triton yields solely generated by this thermal source are underestimated compared to the experimental data, refs. [2,3]. Protons are the dominating particles in the preequilibrium component which are expected to contribute also to the central event samples. Therefore, we donot relate the hydrogen and helium isotopic yields to the proton intensity (as originally done in [3]) but we consider the ratios shown in fig. 1. The other preequilibrium LCP's are lower in abundance and we expect that they are strongly suppressed in the telescope setup [3] with limited polar angle $60^o \leq \Theta_{c.m.} \leq 90^o$ and small azimuthal coverage. Therefore, thermal source simulations should be reasonable. The above parameters provide yield ratios which slightly deviate from the data. How much have these parameters to be changed to reproduce the LCP yield ratios devoid of preequilibrium admixtures? Since the calculated equilibrium yield ratios have been found to be independent of the source size only the excitation energy has been varied to remove the remaining deviations of the yield ratios. Fig. 1 shows that a good reproduction can be achieved with slightly increased E^*. However, the reproduction of the ratios which involve ^3He require an excitation energy beyond the error limits of E^* given at the beginning. In this context we mention the enhancement of the ^3He yield by coalescence [4] by which the ratio $^3He/^4He$ comes closer to the data using a low E^*. Thus, reasons of hitherto existing discrepancies between statistical model simulations and data mentioned in ref. [3] have been enlightened.

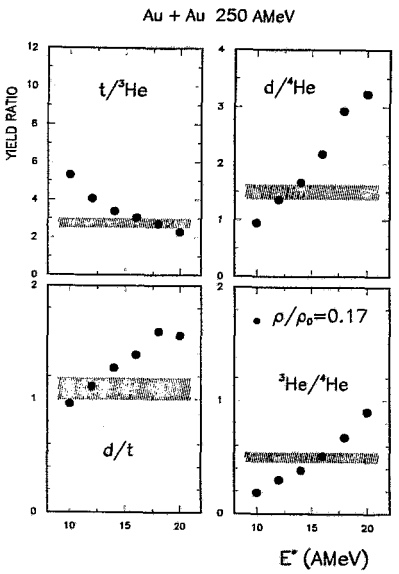

Fig. 1 *Isotopic yield ratios vs. excitation energy E^*. Hatched bands: data obtained from central event samples [3], dots: thermal source simulations filtered for $60^o \leq \Theta_{c.m.} \leq 90^o$ with lower and upper detection thresholds [3] of the given particle species.*

[1] *Hahn-Meitner-Institut Berlin GmbH, Glienicker Str. 100, 14109 Berlin*

References

[1] W. Neubert et al., FOPI collaboration, Proc. Int. Workshop "Heavy Ion Physics at Low, Intermediate and Relativistic Energies using 4π Detectors", Poiana Brasov, Romania, 1996, in press.
[2] W. Reisdorf et al., FOPI collaboration, Nucl. Phys. **A612** (1997) 493
[3] G. Poggi et al., FOPI collaboration, Nucl. Phys. **A324** (1993) 177
[4] W. Neubert et al, this report

A Possible Reason of the ^{3}He -^{4}He Anomaly Observed in Central Heavy Ion Collisions [B,G]

W. NEUBERT, A.S. BOTVINA[1], J. BIEGANSKY, R. KOTTE, J. MÖSNER, C.PLETTNER AND D. WOHLFARTH

In various reactions (Nb+Nb [1], Au+Au [1,2,3], Ar+Ca [4], Ar+Ni [5] and p+Ag [6]) the mean kinetic energy $\langle E_{kin} \rangle$ of ^{3}He fragments has been found to be larger than that of ^{4}He. This observation is opposite to predictions of statistical equilibrium models and radial flow considerations [7]. Moreover, we have found that statistical calculations for the Au+Au system underestimate the Z=2 multiplicity which has been obtained in experimental central event samples. Here we probe an approach which considers preequilibrium emission from a central source prior to equilibration followed by secondary particle evaporation. The calculations with the code *SMMFC* are performed for 250 AMeV Au+Au with a parameter set adjusted by available data. The excitation energy and the size of the equilibrated source have been found from the abundances of intermediate mass fragments ($Z \geq 3$). Such calculations favour ^{3}He production in the preequilibrium stage. However, these yields are still too low to compensate the missing portion of the Z=2 multiplicity.

Additionally, ^3He fragments may be produced if a preequilibrium proton and a $p-n$ pair combine after scattering independently into small phase space. In the present code version such coalescence processes are treated in momentum space, a realization in coordinate space is under consideration. We have generated energy spectra of ^{3}He and ^{4}He by superposition of preequilibrium admixtures to the thermal component. Whereas the mean kinetic energy of ^{4}He remains nearly constant, that of ^{3}He increases with increasing preequilibrium content (see fig.1). The enhanced kinetic energy of ^{3}He can be reproduced if we assume that about 35 % of the total ^{3}He yield is formed by coalescence in the preequilibrium stage. We note that just this surplus of both He isotopes is able to account for the missing part of the measured Z=2 multiplicity.

Preliminary calculations performed with similar assumptions for the system Ar + Ca at 400 AMeV show a satisfactory agreement with the data [4] too.

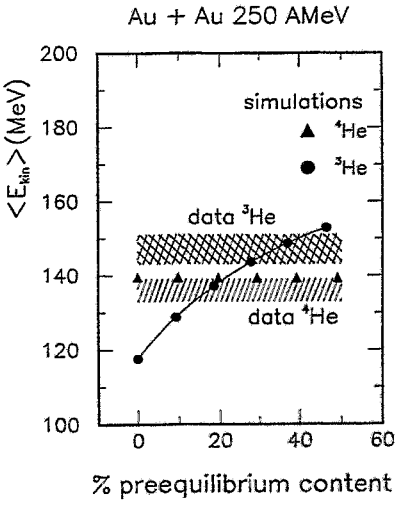

Fig. 1 *Mean kinetic energy vs. preequilibrium content of the ^3He and the ^4He yields, respectively*

[1] *Hahn-Meitner-Institut Berlin GmbH, Glienicker Str. 100, 14109 Berlin*

References

[1] K. G. R. Doss et al., Mod. Phys. Lett. **A3** (1988) 849
[2] G. Poggi et al., FOPI collaboration, Nucl.Phys. **A324** (1993) 177
[3] M. Lisa et al., Phys. Rev. Lett. **75** (1995) 2662
[4] S. Mohren, PHD Thesis, Universität Heidelberg (1996)
[5] B. Borderie et al., Proc. Int. Workshop "Heavy Ion Physics at Low, Intermediate and Relativistic Energies using 4π Detectors", Poiana Brasov, Romania, in press.
[6] E. N. Volnin et al., preprint LNPI Nr.101, Gatchina 1974
[7] W. Reisdorf et al., FOPI collaboration, Nucl.Phys. **A612** (1997) 493

Simulations of Pre- and Post-Scission Components of Light-Charged-Particles in the Reaction of 53 A MeV $^{14}N + ^{197}Au^{B}$

R. YANEZ AND THE FOBOS COLLABORATION

Events measured with the 4π detector FOBOS in which two fission fragments and one or several light-charged-particles (LCP) are detected in coincidence are currently being analyzed. The kinetic energy spectra of LCP allow a decomposition into pre- and post-scission multiplicities by fitting the experimental spectra at different angles with a moving source parametrization [1]. The magnitude of the components are determined by the time of scission and can therefore be used to derive the dynamics of the fission process by comparison with model simulation. Currently, emission from five distinct sources is considered: *i*) pre-equilibrium, *ii*) the equilibrated compound nucleus inside the saddle point, *iii*) the neck-in region of the compound nucleus beyond the saddle point towards scission, *iv*) and *v*) the two fully accelerated fission fragments. Sources *ii*) and *iii*) are considered pre-scission, while sources *iv*) and *v*) are considered post-scission. The contribution from source *i*) is estimated with the aid of simulations of the initial stages of the reaction, prior to thermalization, with the Boltzmann-Uehling-Uhlenbeck (BUU) model [2]. To roughly reproduce the experimental linear momentum transfer the in-medium nucleon-nucleon cross section is reduced by $\left(1 + a\frac{\rho}{\rho_0}\right)$, where ρ is the local nucleon density, ρ_0=0.168 is the nucleon density at normal conditions and a=-0.2. In fitting this component independently it is imminent that two sources, with ~70 and 25 % of the beam velocity and similar multiplicities, are needed to reproduce the spectra, showing that, after the 130 fm/c the simulation runs, the compound nucleus is in thermal equilibrium.

The later stages of the reaction, when thermal equilibrium is reached, are simulated by the statistical evaporation code SIMON [3] using as input the physical quantities of the compound nucleus (A, Z, P, J, E^*) derived from the BUU simulations. SIMON has been modified in several respects, incorporating temperature-dependent level densities [4] and retardation. The retardation, which mimics the effect of nuclear dissipation along the path towards scission, is accomplished by reducing the transition-state-model decay width Γ^{BW} by Kramers factor [5],

$$\Gamma_f(t) = \Gamma^{BW}\left(\sqrt{1+\gamma^2} - \gamma\right)\left[1 - exp\left(ln(0.1)\frac{t}{\tau}\right)\right] \quad (1)$$

including the correct form of the time dependence. γ is the nuclear friction coefficient, which determines the magnitude of the dissipation, and τ is the time at which the fission flux across the barrier is 90% of its quasi-stationary value calculated with Fokker-Planck equation [5]. Furthermore, near-scission emission is allowed during the time required for the flux to propagate from the saddle to the scission point [6], once the compound nucleus is committed to fission.

The simulations are moreover needed to estimate the uncertainties introduced by several features of the experimental data. For example, the large detection threshold for LCP (~3.5 MeV/u) causes some indefinitions in the parameters of post-scission emission, especially when the particle is emitted opposite to the source direction. An experimental filter to the simulated events has therefore been developed to mimic the response of FOBOS in order to *a*) estimate the uncertainties in the post-scission emission parameters, to *b*) estimate to what extent the forward arrays have a pre-equilibrium component and to *c*) estimate the quality of the fitting procedure.

References

[1] J.P. Lestone et al., Nucl. Phys. **A559**, 277 (1993).
[2] W. Bauer, Phys. Rev. **C40**, 715 (1989).
[3] D. Durand, (private communication).
[4] J.P. Lestone, Phys. Rev. **C52**, 1118 (1995).
[5] P. Grange et al., Phys. Rev. **C34**, 209 (1986).
[6] H. Hofmann, J.R. Nix, Phys. Lett. **122B**, 117 (1983).

Different Three-Body Decay Modes of Hot Heavy Nuclei [B]

C.-M. Herbach, H.-G. Ortlepp[1], A.A. Aleksandrov[2], I.A. Aleksandrova[2], L. Dietterle[1], V.N. Doronin[3], P. Gippner, S.A. Ivanovsky[3], D.V. Kamanin[1], A. Matthies[3], Yu.E. Penionzhkevich[3], Yu.V. Pyatkov[2], G. Renz, K.D. Schilling, D.I. Shishkin[3], O.V. Strekalovsky[3], V.G. Tichtchenko[3], I.P. Tsurin[3], C. Umlauf[3], W. Wagner[1], M. Wilpert[4], and V.E. Zhuchko[3]

The 3-body decay of hot heavy nuclei at excitation energies up to 3.5 MeV/amu has been investigated in the reactions ^{14}N(53AMeV)+^{197}Au and ^{232}Th by using the fragment spectrometer FOBOS [1]. In both runs, intermediate-mass fragments (IMF: Z>2) in coincidence with fission fragments (FF) have been identified. The separation of IMFs from different sources was achieved by means of gates within the distribution of the relative velocity V_{IMF-FF} between the IMF and the center-of-mass of the two FFs versus the IMF emission angle Θ_{IMF-FF} relative to the fission axis (Fig.1): The dominant isotropic yield with V_{IMF-FF}=2.5-3.5 cm/ns corresponds to the Coulomb repulsion from a target-like nucleus. In contrast to this, IMFs observed within the range of V_{IMF-FF}=1.5-2.3 cm/ns are focused close to 90°, thus confirming the neck emission mechanism recently reported in [2,3] for IMFs up to Z=8. A further ternary decay mode with V_{IMF-FF}=0.9-2.0 cm/ns turns out to be not focused. However, both groups of low-energy IMFs exhibit much flatter charge distributions and relative yields that are less dependent on excitation energy than those for IMFs of the sequential mode (Fig.2). This observation indicates a slow decay mechanism at the end of the de-excitation process, when the primary excitation energy is almost completely removed by particle evaporation - as known from binary fission [4].

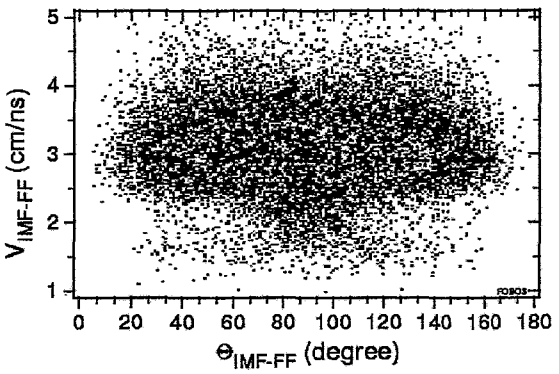

Fig. 1 *Relative IMF velocity versus IMF emission angle with respect to the fission axis*

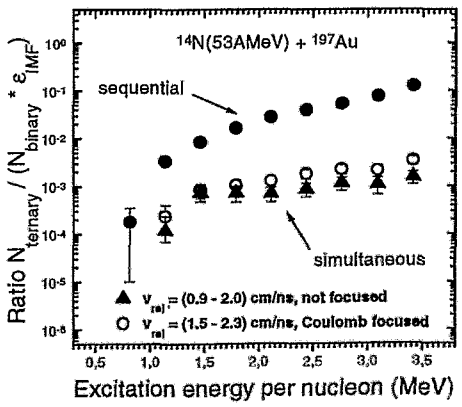

Fig. 2 *Relative yields of ternary decay modes in dependence on the excitation energy*

[1] *Institut für Kern- und Hadronenphysik , FZR and Flerov Laboratory of Nuclear Reactions, JINR Dubna, Russia*
[2] *Moscow Engineering Physics Institute, Moscow, Russia*
[3] *Flerov Laboratory of Nuclear Reactions, JINR Dubna, Russia*
[4] *Freie Universität Berlin, Germany*

References

[1] H.-G. Ortlepp *et al.*, Proc. Int. School-Seminar on Heavy Ion Physics, Dubna, Russia, 1993; JINR E7-93-274, vol.2 (1993) 466.
[2] D.E. Fields *et al.*, Phys. Rev. Lett. **6**, 3713 (1992).
[3] S.L. Chen *et al.*, Phys. Rev. **C 54** , 2114 (1996).
[4] D.Hilscher and H.Rossner, Ann. Phys. Fr. **22**, 471 (1992).

Mass-Symmetric Collinear Tripartition of Hot Heavy Nuclei [B]

C.-M. Herbach, H.-G. Ortlepp[1] and the FOBOS Collaboration

The reactions ^{14}N(53AMeV)+^{197}Au and ^{232}Th have been used to study the decay of equilibrated compound-like systems into three fragments at excitation energies up to 3.5 MeV/amu - well below the multifragmentation threshold. The event-by-event analysis of the angular and velocity correlations between the fragments allows to distinguish between different modes of ternary disintegration [1]. Due to the near cancelation of the Coulomb forces parallel to the scission axis of two separated fragments, a third fragment simultaneously formed in between the two others can be identified by its reduced kinetic energy and by its emission perpendicular to the scission axis of the outer fragments [1]. For the following analysis, the three fragments are sorted according to their masses, which were determined from TOF-E measurements. The charge distribution of the lightest fragments is shown in fig.1 for different decay modes. The yield of the focused simultaneous component is nearly constant for Z>10 up to charges, which correspond to a decay into three fragments of comparable mass. Selected events from [1] of nearly mass-symmetric tripartitions have been further analyzed with respect to relative fragment velocities (fig.2): (i) between the lightest fragment and the center-of-mass of the two heavier fragments V_{IMF-FF}, and (ii) between the two heavier fragments V_{FF}. The data for the simultaneous decay agree with estimates that take into account the Coulomb energy at scission of a collinear three-fragment configuration assuming the same distance between neighbors as for the binary case [2]. This is a signature, that our results indicate a transition from the 'neck'-emission of intermediate-mass fragments [3] to the mass-symmetric ternary fission, which has been predicted within the framework of the liquid-drop model [4], but has not yet confirmed experimentally.

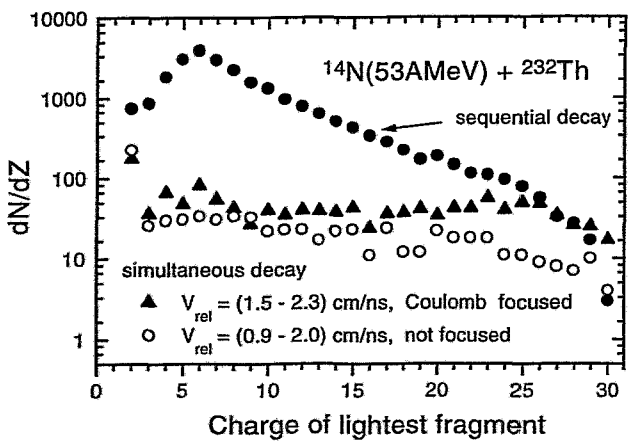

Fig. 1 *Charge distributions of the lightest fragment class for different decay modes, the yields for Z<6 are decreased by efficiency*

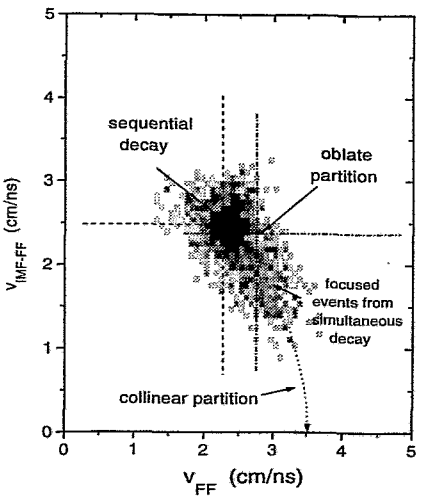

Fig. 2 *Relative velocity correlations for events from the ternary decay into fragments of nearly equal masses*

[1] *Institut für Kern- und Hadronenphysik , FZR and Flerov Laboratory of Nuclear Reactions, JINR Dubna, Russia*

References

[1] C.-M. Herbach *et al.*, this Annual Report, p.
[2] V.E. Viola *et al.*, Phys. Rev. **C 31**, 1550 (1985).
[3] S.L. Chen *et al.*, Phys. Rev. **C 54**, 2114 (1996).
[4] H. Diel and W. Greiner, Phys. Lett. **B 45**, 35 (1973).

Angular Distribution of LCP Emitted in Binary Fission [B]

T. MÖHLENKAMP, C.-M. HERBACH, D. KAMANIN[1] AND THE FOBOS COLLABORATION

The angular distributions of light-charged particles (LCPs) in the reaction ^{14}N(53AMeV)+^{197}Au have been analyzed. The LCP were measured by the CsI scintillator shell of the FOBOS spectrometer in coincidence with binary fission. The folding angle between the two fission fragments was used to deduce the portion of linear momentum transfer (LMT) as a measure of the excitation energy of the composite system. It was calculated event-by-event from the center-of-mass velocity V_{CM} relative to the velocity V_{max} of a completely fused projectile and target.
The number of the detected LCPs, separated for charges Z=1 and Z=2, was normalized to the effective solid angle and to the number of fission events. Both angular distributions for H (Fig.1) and for He exhibit a nearly constant behaviour in the backward hemisphere and a strong rise towards smaller polar angles. The error bars in Fig.1 indicate the discrepancy of the results obtained from several CsI-detectors at the same polar angle and therefore include some non-uniformity of the azimuthal angular distribution of LCP with respect to the fission plane. In order to separate the yield of isotropic LCP evaporation, the mean value of the distribution at Θ>100° was integrated over the entire angular range. The pre-equilibrium LCP emission, which preferably occurs in the forward direction $\Theta \leq 90°$, was estimated by an exponential fit of the difference between the total yield and the yield from evaporation.
Before the LCPs can be detected, they have to pass through the layers of the FOBOS set-up: the gas of the ionization chamber ($\eta \approx 16 mg/cm^2$ $Ar(90\%)+CH_4(10\%)$) and a supporting grid ($\eta \approx 47 mg/cm^2$ Ni) of 75% transparency. The portions below the corresponding energy thresholds for protons and α-particles were estimated to be 4% and 40% for LCP from evaporation and 2% and 25% for the pre-equilibrium component. The resulting efficiencies ε were used to correct the absolute yields, displayed in Fig.2 for different bins of $LMT = V_{CM}/V_{max}$. Except for the lowest LMT bin, the yields of LCP evaporation (left panel) are linearly increasing with excitation energy. They amount up to 2.6 and 1.5 for H and He, respectively, while the ratio N_H/N_{He} is decreasing from 2.8 to 1.7. The yields from pre-equilibrium LCPs have a weaker dependence on LMT (right panel). The number of H per fission increases with LMT from 1.2 to 1.9, while the He yield at about 0.7 turns out to be independent of LMT. Corresponding to the measured value of <LMT>=0.47 both pre-equilibrium contributions add to about 50% of the ^{14}N projectile charge.

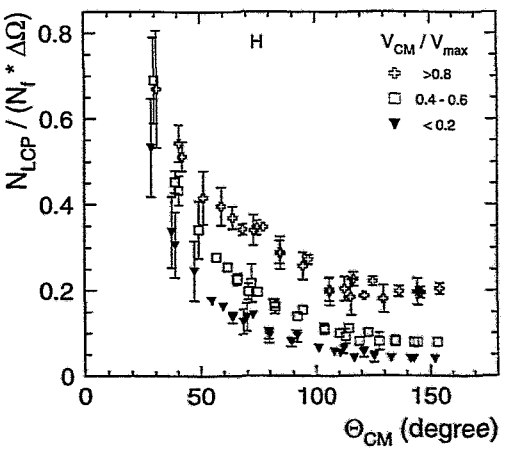

Fig. 1 *Mean number of emitted H per fission event as a function of the polar angle.*

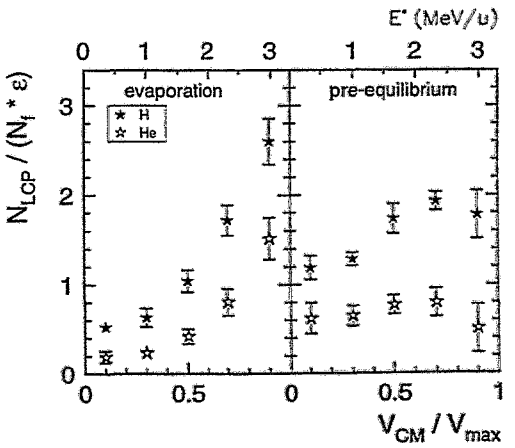

Fig. 2 *N_{LCP} per fission event from evaporation and pre-equilibrium emission.*

[1] *Institut für Kern- und Hadronenphysik , FZR and Flerov Laboratory of Nuclear Reactions, JINR Dubna, Russia*

Effect of the Saddle-to-Scission Cooling on the Fragment Mass Dispersion in the Fission of Hot Nuclei [B]

H.-G. ORTLEPP[1], C.-M. HERBACH, W. WAGNER[1], and the FOBOS Collaboration

One of the goals of the presently running physical programme at the FOBOS spectrometer are new fragment-spectroscopic data about the fission of hot nuclei [1]. The main experimental problem at high E* - the deterioration of the measured parameters due to the emission of many particles [2] - has been overcome by the principles applied at the FOBOS detector [3]. The further interpretation of the data taken for the reaction ^{7}Li (43 AMeV) + ^{232}Th, however, showed up a new error source not taken into account in [1] and [3]. As the fragment masses and also the linear momentum transfer (LMT, used as measure of the excitation energy E*) are derived from the same raw data, considerable covariances occur in their uncertainties. In the present re-analysis mass disributions without unphysical correlations have been achieved deriving LMT and mass from different raw parameters. By additional selection conditions also geometrical acceptance effects have been excluded. The fragment mass dispersions in dependence on the LMT, deduced in this way, are shown in Fig.1. They fall far below a systematics derived in [4] on the basis of many heavy ion induced fission data, thus demonstrating the effect of suppression of the upper mentioned experimental errors in the present re-analysed FOBOS data.

For E* = 50-90 MeV many measured mass dispersions are well understood as proportional to the square root of the temperature [5]. The rise of the dispersion predicted by this proportionality using the mass asymmetry stiffness parameter from the systematics [5] is also shown in fig. 1. The considerably slower rise of the measured dispersion at E* above 80 MeV can be understood as a new effect of the particle evaporation during the long descent from saddle to scission. The effective temperature exciting the mass-asymmetry mode becomes substantionally lower than the initial one. The extreme assumption that the mass distribution is "created" near scission yields too small values. The whole process from the primary excitation up to the scission influences the fragment creation. For the description of the underlying dynamical evolution of the system presently a three-dimensional model on the basis of the Langevin formalism is being developed.

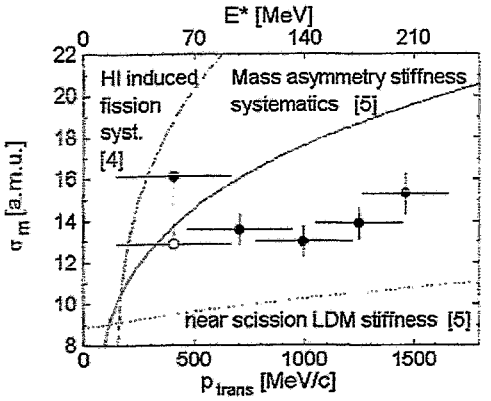

Fig. 1
Fission fragment mass dispersion in dependence on the transferred momentum for ^{7}Li + ^{232}Th. The increase at low E is due to a double-humped component which was separated out by a TKE cut. Open circle - dispersion of remaining symmetric distribution. Lines - see text.*

[1] *Institut für Kern- und Hadronenphysik, FZR and Flerov Laboratory of Nuclear Reactions, JINR Dubna*

References

[1] H.-G. Ortlepp et al., Proc. Int. Conf. LEND '95, St. Peterburg, April 1995, World Scientific 1995, p. 231; Preprint FZR-102 (1995)
[2] G. Casini et al., Nucl. Inst. and Meth in Phys. Res. A277 (1989) 445
[3] C.-M. Herbach, Proc. FOBOS workshop Cracow '94, FZR-65 (1995) 87
[4] W.U. Schröder and J.R. Huizenga, Nucl. Phys. A502 (1989) 473c
[5] M. G. Itkis et al., Fiz. Elem. Chastits At. Yadra 19 (1988) 701

Manifestation of Clustering in Spontaneous Fission of ^{252}Cf [B]

Yu.V. Pyatkov[1], V.V. Pashkevich[2],
Yu.E. Penionzhkevich[2], V.G. Tishchenko[2], A.V. Unzhakova[2],
P. Gippner, C.-M. Herbach, H.-G. Ortlepp[3], K.D. Schilling, W. Wagner[3],
and the FOBOS Collaboration

In ref. [1] a ^{252}Cf spontaneous fission measurement performed at the FOBOS detector [2] is reported. On the basis of the same data a new special analysis was performed with the aim of searching for manifestations of cluster effects in total-kinetic-energy - mass (TKE-M) distributions. To visualize the gross structure of the experimental two-dimensional TKE-M spectrum it was transformed into the conditional distribution $P(M|E^*)$, where $E^* = Q - TKE$ and Q is the energy released in the reaction for a given mass splitting. The transformation can be done by normalization to unit area of every cross section at given E^* of the $P(M, E^*)$ distribution. The contour map of the $P(M|E^*)$ distribution is presented in Fig. 1. One can clearly see two components (modes) in the plot at mass splits 106/146 and 118/134.

To analyze the data presented here potential energy surface (PES) calculations were performed using the method of Ref. [3]. Two distinct valleys on the PES predicted for the descent presumably give rise to the modes shown in Fig. 1. Two constituents (clusters), which are close to magic spherical and deformed nuclei are responsible for the shape of the fissioning system in each fission mode (inserts A and B).

Further conclusions drawn are as follows. The available experimental and theoretical results give evidence for the existence of fission modes caused by clustering of the fissioning nuclei. One of the modes in ^{252}Cf can be treated as a heavy-cluster decay involving the formation of two fragments close to magic Sn nuclei. A sharp drop of the proton odd-even effect is discovered at an excitation energy above $E^* \approx 40\,MeV$ in the scission point, which is presumably associated with the complete clusterization of the fissioning nucleus.

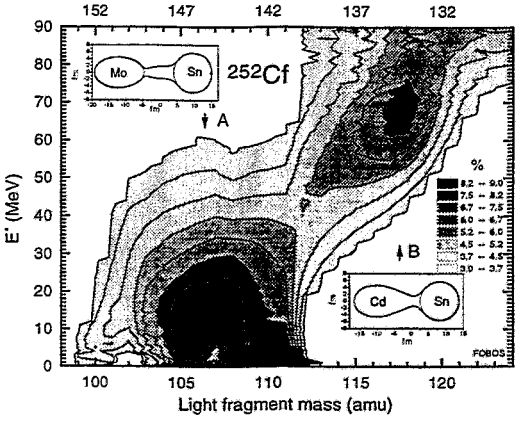

Fig. 1 *The contour maps of the conditional distribution $P(M|E^*)$. The panels depict the shapes of the fissioning system following from the PES calculations ascribed to the two dominant structures.*

[1] *Moscow Engineering Physics Institute, 115409 Moscow, Russia*
[2] *Joint Institute for Nuclear Research, 141980 Dubna, Russia*
[3] *IKH, FZR and Flerov Laboratory of Nuclear Reactions, JINR Dubna*

References

[1] Yu.V. Pyatkov et al., Annual Report 1995, FZR-130 (1996) 99
[2] M. Andrassy et. al. (FOBOS collaboration)
Communication of JINR, Dubna, Russia E7-95-148, 1995.
[3] V.V. Pashkevich, Nucl. Phys. A 477 (1988) 1.

Parametrization of the Kinetic Energy Release in Two-Fragment Decays of Hot Nuclei

W. WAGNER AND H.-G. ORTLEPP

Evaluations of the total kinetic energy release (TKE) in fission [1, 2] are widely used for prediction and interpretation purposes of nuclear-reaction data. The TKE-formula of ref. [2], which bases on a simple two-spheres approximation of the scission configuration, well describes the measured mean TKE of mass-symmetric as well as medium-asymmetric fission, if a correction for the charge split and the actual fragment radii is applied. At large fragment mass (A_i) asymmetries ($R = \frac{A_2}{A_1}$) observed in the binary fragmentation of hot compound systems produced by incomplete fusion reactions (e.g. in refs. [3, 4, 5]), however, the scaling of the effective scission distance ($\sim (A_1^{1/3} + A_2^{1/3})$) becomes incorrect. The TKE smoothly approaches to the energy value of the Coulomb barrier. This means that the fission path of the nucleus from the saddle towards scission becomes successively shorter, and the collective motion is, with respect to symmetric fission, less damped [3]. Such a behaviour has been predicted in ref. [6].
We have empirically found that the TKE measured for binary fragmentations can be rather accurately described over the broad range of R and for nuclei of very different mass (A) and atomic number (Z) by the parametrization given in eq. 1 (fig. 1).

$$TKE = (0.2904 \pm 0.0075) \cdot \frac{Z^2}{A_1^{1/3} + A_2^{1/3} - A^{1/3}} \cdot \frac{A_1 A_2}{A^2} \; MeV \qquad (1)$$

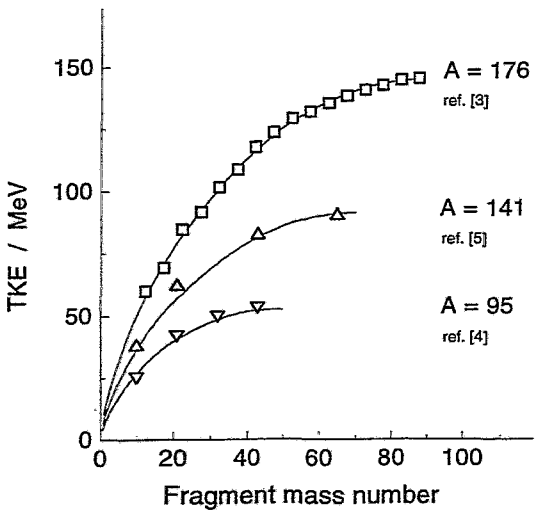

In the case of symmetric mass splitting, eq. 1 reduces to the analytic expression given in refs. [1, 2], but without the constant term and with a slightly different slope parameter. As an analysis showed, eq. 1 also well evaluates the available experimental TKE-data (cf. ref. [2]) over the whole range of the Coulomb parameter $\frac{Z^2}{A^{1/3}}$. Non-Coulomb components (e.g. thermal or rotational) which can contribute to the TKE are not explicitly considered.

Fig. 1 *Experimental TKE - data (symbols) compared with calculations using eq. 1 (lines).*

Although a specific calculation of the TKE in a binary fragmentation of a nuclear system can be performed by use of dynamial codes, eq. 1 may be useful for gross estimations.

References

[1] V.E. Viola, Jr., *Nucl. Data Tab.* A1 (1966) 391.
[2] V.E. Viola et al., *Phys. Rev.* C31 (1985) 1550.
[3] W. Wagner et al., in: "Advances in Nucl. Dynamics 2" (eds. W. Bauer and G.D. Westfall) Plenum Press, New York, 1996, p. 341.
[4] R.J. Charity et al., *Nucl. Phys.* A483 (1988) 371.
[5] R.J. Charity et al., *Nucl. Phys.* A511 (1990) 59.
[6] L.G. Moretto et al., in: "Progress in Part. and Nucl. Physics", vol. 21 (ed. A. Faessler) Pergamon Press, Oxford, 1988, p. 401.

Abstracts of publications

Effects of Nuclear Coulomb Field on Two-Meson Correlations
(Phys. Rev. C 53 (1996) 2536)

Barz, H.W.

Abstract: The influence of the nuclear Coulomb field on two-pion and two-kaon correlations is investigated for sources with charge number Z = 160. The source radii extracted from the correlation function determined in sideward and outward directions are remarkably affected for meson pairs with average momenta below 200 MeV/c.

Cluster Production and Correlations in Nuclear Molecular Dynamics
(Phys. Lett. B 382 (1996) 343)

Barz, H.W., J.P. Bondorf, D. Idier, I.N. Mishustin

Abstract: The formation of nuclear fragments in intermediate energy heavy ion reactions is studied within a molecular dynamics model, recently developed in Copenhagen. Observable characteristics such as fragment mass distributions, multiplicities of intermediate mass fragments (IMFs) and charged particles, fragment-fragment velocity correlations are calculated for Kr + Au and Au + Au reactions and compared with data at different bombarding energies. The data are well reproduced at beam energies above 100 MeV per nucleon. The sideward flow and the fragment-fragment correlations depend sensitively on the in-medium nucleon-nucleon cross section.

Analysis of Hard Two-Photon Correlations Measured in Heavy-Ion Reactions at Intermediate Energies
(Phys. Rev. C 53 (1996) R 553)

Barz, H.W., B. Kämpfer, Gy. Wolf, W. Bauer

Abstract: Recently reported measurements of hard photon correlations in the reactions ^{36}Ar on ^{27}Al at 95 AMeV, ^{86}Kr on ^{nat}Ni at 60 AMeV, and ^{181}Ta on ^{197}Au at 39.5 AMeV are analyzed. A Boltzmann-Ühling-Uhlenbeck transport model is used to describe the photon production by individual nucleon-nucleon collisions. In the lighter systems we find the best agreement with data when taking into account only photons from first-chance collisions of nucleons or photons produced during the passage of the nuclei, while the model predicts also a considerable late-time emission of photons, which leads to a depletion of the calculated correlation function. The accuracy of the present data does not allow firm conclusions on the reliability of this late-time evolution. Our investigations do not support a recently reported interference pattern in the heavy Ta + Au system.

Charge Pickup of ^{238}U at Relativistic Energies
(Phys. Rev. C 52 (1996) 993)

Rubehn, Th., R. Bassini, M. Begemann-Blaich, Th. Blaich, A. Ferrero, C. Groß, G. Imm, I. Iori, G.J. Kunde, W.D. Kunze, V. Lindenstruth, U. Lynen, T. Möhlenkamp, L.G. Moretto, W.F.J. Müller, B. Ocker, J. Pochodzalla, G. Raciti, S. Reito, H. Sann, A. Schüttauf, W. Seidel, V. Serfling, W. Trautmann, A. Trzcinski, G. Verde, A. Wörner, E. Zude, B. Zwieglinski

Abstract: Cross sections for the charge pickup of ^{238}U projectiles were measured at $E/A = 600$ and 1000 MeV for seven different targets (Be, C, Al, Cu, In, Au, and U). Events with two fission fragments with a sum charge of 93 in the exit channel were selected. Due to the significant excitation energy, the majority of the produced Np nuclei fission instead of decaying by evaporation to residues. The observed cross sections can be well reproduced by intranuclear-cascade-plus- evaporation calculations and, therefore, confirm recent results that no exotic processes are needed to explain charge-pickup processes.

Total and Nuclear Fission Cross Sections of ^{238}U at Relativistic Energies
(Phys. Rev. C 53 (1996) 3143)
Rubehn, Th., R. Bassini, M. Begemann-Blaich, Th. Blaich, A. Ferrero, C. Groß, G. Imm, I. Iori, G.J. Kunde, W.D. Kunze, V. Lindenstruth, U. Lynen, T. Möhlenkamp, L.G. Moretto, W.F.J. Müller, B. Ocker, J. Pochodzalla, G. Raciti, S. Reito, H. Sann, A. Schüttauf, W. Seidel, V. Serfling, W. Trautmann, A. Trzcinski, G. Verde, A. Wörner, E. Zude, B. Zwieglinski

Abstract: Total fission cross sections of ^{238}U projectiles were measured at bombarding energies of 0.6 and 1 GeV per nucleon for seven different targets (Be, C, Al, Cu, In, Au and U). It is found that all data points fall onto one curve, independent of bombarding energy, once the electromagnetic contribution to the total fission cross sections is subtracted. The abrasion-ablation model predicts a significantly weaker target dependence than observed, and underestimates the nuclear fission cross sections for the heavier targets.

Universality of Spectator Fragmentation at Relativistic Bombarding Energies
(Nucl. Phys. A 607 (1996) 457)

Schüttauf, A., W.D. Kunze, A. Wörner, M. Begemann-Blaich, Th. Blaich, D.R. Bowman, R.J. Charity, A. Cosmo, A. Ferrero, C.K. Gelbke, C. Groß, W.C. Hsi, J. Hubele, G. Immé, I. Iori, J. Kempter, P. Kreutz, G.J. Kunde, V. Lindenstruth, M.A. Lisa, W.G. Lynch, U. Lynen, M. Mang, T. Möhlenkamp, A. Moroni, W.F.J. Müller, M. Neumann, B. Ockere, C.A. Ogilvie, G.F. Peaslee, J. Pochodzalla, G. Raciti, F. Rosenberger, Th. Rubehn, H. Sann, C. Schwarz, W. Seidel, V. Serfling, L.G. Sobotka, J. Stroth, L. Stuttge, S. Tomasevic, W. Trautmann, A. Trzcinski, M.B. Tsang, A.Tucholski, G. Verde, C.W. Williams, E. Zude, B. Zwieglinski

Abstract: Multi-fragment decays of ^{129}Xe, ^{197}Au and ^{238}U projectiles in collisions with Be, C, Al, Cu, In, Au and U targets at energies between $E/A = 400$ and 1000 MeV have been studied with the ALADIN forward-spectrometer at SIS. By adding an array of 84 Si-CsI(Tl) telescopes the solid-angle coverage of the setup was extended to $\Theta_{lab} = 16°$. This permitted the complete detection of fragments from the projectile-spectator source.
The dominant features of the systematic set of data is the Z_{bound} universality that is obeyed by the fragment multiplicities and correlations. These observables are invariant with respect to the entrance channel if plotted as a function of Z_{bound}, where Z_{bound} is the sum of the atomic

numbers Z_i of all projectile fragments with $Z_i \geq 2$. No significant dependence on the bombarding energy nor on the target mass is observed. The dependence of the fragment multiplicity on the projectile mass follows a linear scaling law.
The reason for and the limits of the observed universality of spectator fragmentation are explored within the reals of the available data and with model studies. It is found that the universal properties should persist up to much higher bombarding energies than explored in this work and that they are consistent with universal features exhibited by the intranuclear cascade and statistical multifragmentation models.

Nuclear Structure Physics

This chapter comprises the progress reports of theoretical investigations as well as the results of the experimental nuclear spectroscopy group.

The main subject of the theoretical work is devoted to the further exploration of the new nuclear degree of freedom which is connected with the spin orientation. Considering initially the consequences of a non-principal axis rotation in nuclei with a deformed density distribution the detailed analysis of band structures in Pb isotopes with strong magnetic dipole transitions has shown that the concept of a tilted spin orientation can be extended to the nuclear current distribution where the deformation plays a minor role. The latter considerations implied the discovery of the phenomenon of magnetic rotation for which experimental evidence has now been collected by more precise life time measurements.

A further step is done by predicting another novel type of rotation, i.e. the chiral rotation for nuclei with a triaxial shape. According to this idea one expects to observe a pair of degenerate twin bands. A search for those interesting structures is planned in a EUROBALL experiment at the LNL Legnaro.

The investigation of an extra hexadecupole deformation aimed to find a microscopic explanation for the $\Delta I = 2$ staggering observed in some superdeformed bands. However, the calculated effect turned out to be too small. The origin of the staggering is still not unraveled.

The contribution concerning the supershell structure deals with non-nuclear finite Fermi systems: metal clusters and quantum dots. Interestingly, the calculation has the same background as the shell correction method in nuclei and, in addition, the supershell structure is unter study for the nuclear moments of inertia.

Another two contributions report on the theoretical studies referring the coupling of resonance states to continuum decay channels. The model considering the interference between doorway states and giant resonances describes qualitatively the observed gamma decay strength.

The experimental work in our spectroscopy group was dominated by the new possibilities provided with the γ-ray CLUSTER detectors. Altogether 7 CLUSTER systems were fin-

ished by various german groups and operated successfully in several Pre-EUROBALL experiments. The spectroscopy group participated in respective campaigns at the Heidelberg MP-tandem and at the Darmstadt UNILAC organized by the german EUROBALL collaboration.

The results of previous (γ, γ') experiments performed with the first CLUSTER in 1995 at the S-DALINAC were analysed and confronted with RPA calculations. The contribution concerning the measurements of dipole states in a chain of Te isotopes has shown that the high resolution power of the CLUSTER was crucial for identifying a new type of dipole states with two-phonon character. These excitations having a complex isoscalar-isovector structure are analogous to the scissors-mode in deformed nuclei.

In a common experiment with our partners a six CLUSTER arrangement built up at the Heidelberg tandem was used to investigate the level structure of ^{79}Br. The data evaluation is not finished but the main goal of this experiment to follow a magnetic dipole band up to high spin (37/2) was achieved. The life time analysis will later allow for a more quantitative comparison with the tilted cranking model. The dipole band in ^{79}Br is not a pure magnetic rotation.

The contribution concerning the level scheme of ^{81}Y shows the rich band structure and wealth of phenomena obtainable by using the efficiency of the modern γ-arrays as GAMMASPHERE or EUROBALL complemented with particle detectors. The rich experimental material is a challenge for the nuclear structure theory.

Chiral Rotation of Triaxial Nuclei

S. FRAUENDORF AND JIE MENG[1]

The Tilted Axis Cranking (TAC) theory is applied to the model of two particles coupled to a triaxial rotor. Comparing with the exact quantal solutions, the interpretation and quality of the mean field approximation is studied. For triaxial nuclei there appear two different types of solutions: The planar solutions, for which the axis of rotation lies in of one of the principal planes of the triaxial density distribution, represent $\Delta I = 1$ bands. The aplanar solutions, for which the rotational axis lies outside the principal planes, represent pairs of identical $\Delta I = 1$ bands with the same parity. The two bands differ by the chirality of the principal axes with respect to the angular momentum vector. (There is an analogy to the "chiral C - atoms" in optical active chemical compounds.) The transition from planar to chiral solutions is found in both the quantal and the mean field calculations. Chiral rotation appears for a high j proton and a high j neutron hole (or vice versa) coupled to a triaxial core. More complex configurations of the same type are also expected to show chiral rotation. It is not clear whether nuclei with the appropriate configurations can be sufficiently triaxial to show chiral rotation. A microscopic aplanar ("3D") TAC code has been developed, which is being used to search for possible nuclei with chiral rotation. So far, no experimental evidence for chiral sister bands has been reported.

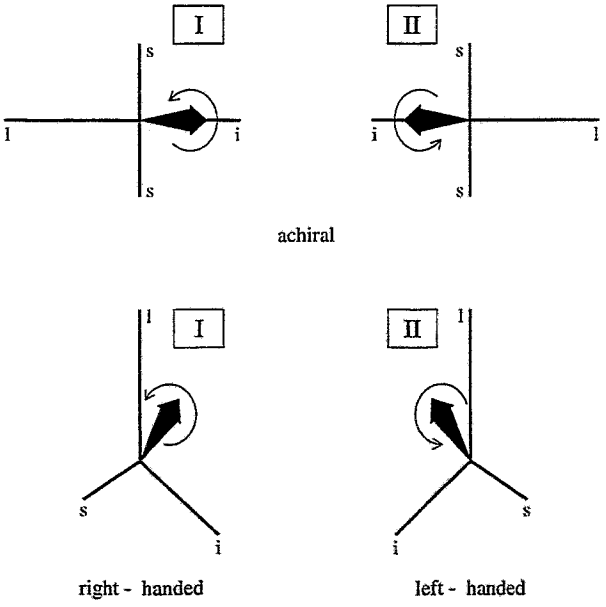

Fig. 1 *Planar (upper panel) and aplanar (lower panel) TAC solutions. The fat arrow represents the angular momentum $\vec{J}$. The labels s, i, and l denote, respectively, the short, intermediate and long principal axes of the triaxial nuclear density distribution. The chirality of the aplanar solution expresses the fact that the three different axes s, i, and l may form a left - handed or right - handed screw with respect to $\vec{J}$.*

[1] *Cyclotron Lab., Riken, Japan*

References

[1] S. Frauendorf, Jie Meng, Nucl. Phys. **A 615**, in print

Analysis of Experimental Evidence for Magnetic Rotation

S. FRAUENDORF

In the works [1 - 3] the concept of nuclear rotation has been extended to "Magnetic Rotation". In the case of the familiar rotation of deformed nuclei the deformed charge distribution rotates about the axis defined by the total angular momentum, emitting electric quadrupole radiation, the quanta of which connect the states of the band. In the case of magnetic rotation it is a magnetic dipole that goes round, emitting magnetic dipole radiation, whereas the mass and charge distributions are almost spherical. The apparent contradiction to the familiar concept that only well deformed nuclei show rotational bands has initiated experimental activities to test the new theory concept in a stringent way. Tilted Axis Cranking (TAC) calculations have been carried out in order to check whether these experiments agree with the theory or not.

A long standing discrepancy were the M1 transition rates in the Pb - isotopes. New life time data from GAMMASHPERE [4] have resolved this problem and confirmed the correctness of the theory. The predicted existence [2,3] of magnetic rotation in the mass 140 and 105 regions has been confirmed by experiments at GASP, measuring the M1 lifetimes in ^{139}Sm [5] and the spectrum of ^{105}Sn [6]. Magnetic rotation in the mass 80 region is being searched for by the spectroscopy group in our institute. A M1 band has been found in ^{79}Br, which has an intermediate character, showing a strong magnetic component and deformation as well [7].

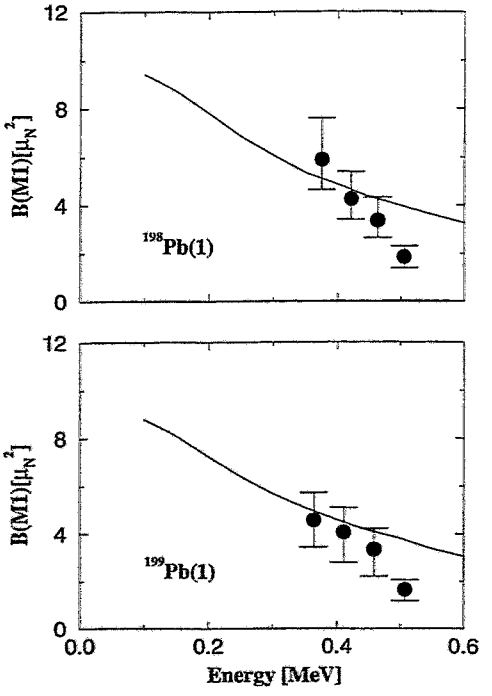

Fig. 1 *Experimental B(M1) values as deduced from DSAM lifetime measurements on GAMMASHPERE [4] compared to TAC calculations. The decrease of the B(M1) values with the rotational frequency is a consequence of the gradual alignment of the angular momenta of the excited $i_{13/2}, h_{9/2}$ protons and $i_{13/2}$ neutron holes with the total angular momentum $\vec{J}$ (shears mechanism). Early experiments gave constant or even increasing B(M1) values. The new, more accurate B(M1) values show the predicted decrease, demonstrating for first time the existence of the shears mechanism in a direct way.*

References

[1] S. Frauendorf, Nucl. Phys. **A 557** (1993) 259c
[2] S. Frauendorf, Proc. Workshop on Gammasphere Physics, 1995, Berkeley, p. 272
[3] S. Frauendorf, Z. Phys. **A**, in print
[4] R. M. Clark, et. al. and S. Frauendorf, Phys. Rev. Lett. **78** (1997) 1868
[5] F. Brandolini et al. and S. Frauendorf, Phys. Lett. **B 388** (1996) 468
[6] A. Gadea et al. and S. Frauendorf, Phys. Rev. **C**, in print
[7] T. Servene et. al., this annual report

Magnetic Dipole Bands in Odd Indium Isotopes

S. FRAUENDORF AND J. REIF

The structure of M1 bands in the odd isotopes $^{107-113}$In has been investigated by means of a shell-model calculation [1]. The configuration space consists of the proton $g_{9/2}$ and neutron $d_{5/2}$, $g_{7/2}$, $d_{3/2}$, $s_{1/2}$, $h_{11/2}$ orbitals outside the ^{100}Sn core. The calculation describes the experimental energies [2] well. In particular, the transition from irregular M1 sequences in the light isotope to regular ones in the heavy isotopes is reproduced,

The analysis of the wave functions reveals the presence of the intruder shears mechanism between the proton $g_{9/2}$ hole and the neutron $h_{11/2}$ pair. In contrast to the Pb isotopes, where the shears mechanism is the main source for the generation of angular momentum [2], in the In isotopes a substantial fraction of the angular momentum is generated by the normal parity neutrons. The In isotopes are an example that the concept of magnetic rotation [3] is more general than the shears bands model for the Pb isotopes [2], where it originated from. The mechanisms of generating the angular momentum are more divers (different couplings of the neutrons in the $d_{5/2}$ $g_{7/2}$ orbitals). However, the common feature of both cases consisting in the large B(M1) and the small B(E2) values indicates that the rotation is of magnetic type, i. e. it is the magnetic dipole that rotates whereas the charge distribution is nearly spherical. The strong M1 radiation is generated by the $g_{9/2}$ proton hole "antenna", which sticks out perpendicular to the rotational axis in order to keep large its density overlap with the neutron $h_{11/2}$ pair. In fact, the ratio of $B(M1)/B(E2) \sim 100(\mu_N/eb)^2$ predicted for the In isotopes points to a stronger prevalence of the magnetic character than in case of the Pb isotopes, where the ratio is $\sim 30(\mu_N/eb)^2$.

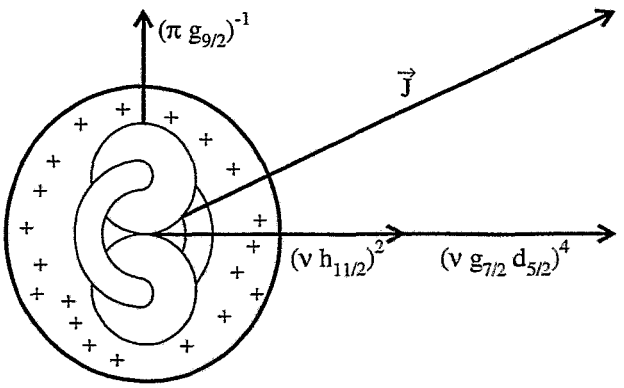

Fig. 1 *Composition of the angular momentum in the dipole bands of odd - A In isotopes. The dumbbell and the torus illustrate the density distribution of orbitals $\pi(g_{9/2})^{-1}$ and $\nu(h_{11/2})^2$, respectively, whereas the density distribution of the $d_{5/2}$ $g_{7/2}$ neutron orbitals is shown as the cloud of pluses. A substantial part of the angular momentum is generated by recoupling the neutrons in the $d_{5/2}$ $g_{7/2}$ orbitals. The $\pi(g_{9/2})^{-1}$ orbital forms the "magnetic antenna".*

References

[1] S. Frauendorf and J. Reif, Nucl. Phys. **A**, submitted
[2] P. Vaska Thesis, SUNY Stony Brook
[3] S. Frauendorf, Z. Phys. **A**, in print
[4] S. Frauendorf, Nucl. Phys. **A 557** (1993) 259c

Can Hexadecupole Deformation lead to $\Delta I = 2$ Staggering?

F. Dönau, S. Frauendorf and J. Meng[1]

The detailed analysis of the some superdeformed bands has shown that there exists a $\Delta I = 2$ staggering effect i.e. it occurs a small regular displacement (some hundred eV) between the two sequences $I = I_o, I_o + 4, \ldots$ and $I = I_o + 2, I_o + 6, \ldots$ in a given rotational band. The origin of this effect is still not clear. Among other explanations a phenomenological fourth order rotor term with inherent C_{4v}-symmetry has been studied [1] which indeed can generate such a staggering if the inertial parameter of this term is large enough. We tried to find out [2] whether such a rotor term can result from an superdeformed shape when an extra hexadecupole deformation term is added to the dominating quadrupole part. Such a shape is illustrated in Fig.1. The axial symmetry is reduced to C_{4v} which means invariance against 90 degree rotations about the z-axis. Therefore, in the corresponding bands appears K-mixing with $\Delta K = 4$.
The tilted cranking model enables one to estimate the inertial parameter of the C_{4v} rotor term modeled in [1] for describing such a K-mixing. The calculation was done for a typical superdeformed case $\varepsilon_2 = 0.42$ with a substantial hexadecupole deformation as in Fig.1. It turned out that the resulting size of the C_{4v} rotor term is far too small to give the $\Delta I = 2$ staggering observed in experiment.
The $\Delta I = 2$ staggering effect was also studied in odd-A nuclei within the core-quasiparticle coupling model. The question was investigated whether an odd high-j quasiparticle coupled to a C_{4v} rotor can amplify the staggering. We found, however, that a staggering appears only if the rotor core implies a fourth order term [1]. The hexadecupole shape of the core does not enhance the staggering. Thus, the appealing explanation that the $\Delta I = 2$ staggering is a consequence of the deformed shape with C_4-symmetry cannot be substantiated by our calculations.

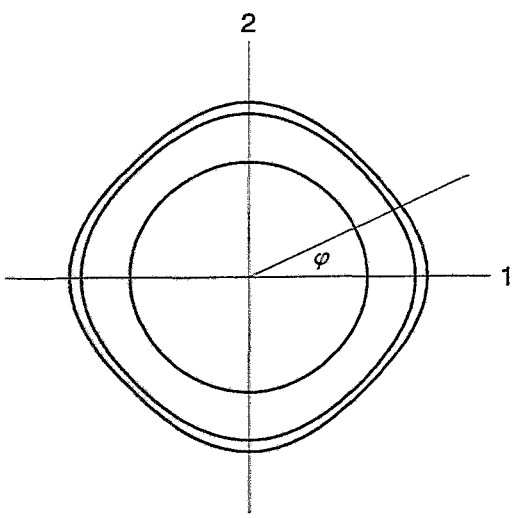

Fig.1
Shape of the deformed potential with C_{4v}-symmetry for $\varepsilon_2 = 0.42$ and $\varepsilon_{44} = 0.1$ (seen from the top). The equipotential lines at at z=0, z=±0.42 and z=±0.89 in units of the radius r($\varphi = \vartheta$=0, z=0) are shown. The corresponding nuclear shape resembles a double pyramid with rounded edges. The effect of the ε_{44} deformation is strongest at the waist z=0.

[1] *Cyclotron Lab., Riken, Japan*

References

[1] I. Hamamoto and B. R. Mottelson, Phys. Lett. **B333** (1994) 294
[2] F. Dönau, S. Frauendorf and J. Meng, Phys. Lett. **B387** (1996) 667

Super Shell Structure of the Magnetic Susceptibility of Metal Clusters and Quantum Dots[W]

S.FRAUENDORF, V.M.KOLOMIETZ[1], A. G. MAGNER[1] AND A. I. SANZHUR[1]

Supershell structure has been discovered in the abundances of alkali clusters [1]. It is understood as a quantum interference between electrons moving on triangular and square orbits in a spherical confining potential [2]. We studied the magnetic susceptibility of spherical metal clusters and circular quantum dots [3] and found a similar supershell pattern, the origin of which can be traced back to the same interference. Taking into account that the number of electrons is fixed, it is predicted that the supershell structure will survive averaging with respect to the electron number N over an interval of a few shells. It seems feasible to prepare ensembles of clusters embedded in frozen noble gas matrices and of quantum dots on AlGaAs-GaAS- semiconductor hetero structures such that N is specified with an accuracy of 10%. The susceptibility of such probes is predicted to show strong paramagnetism modulated by supershell quantum beats.

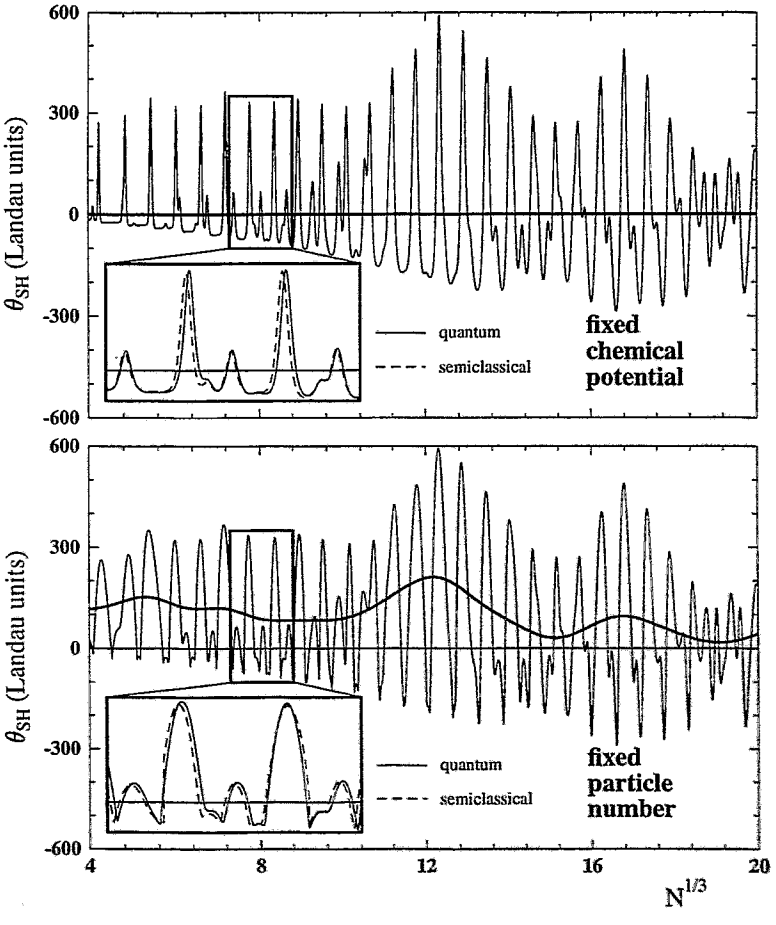

Fig. 1 *Finite size contribution to the magnetic susceptibility (in units of Landau diamagnetic susceptibility) of N electrons in a spherical cavity with the radius $R = r_s N^{1/3}$. The calculations are carried out for Na at $T = 5K$. The thin lines show the results without averaging over N. The fast oscillations represent the basic shell structure. The fat lines are obtained by averaging over a Gaussian distribution with the width of about one shell. The upper panel shows the results for the grand canonical ensemble. The averaging quenches the magnetism. The lower panel shows the susceptibility for (approximately) fixed N. Averaging wipes out the the fast oscillations, preserving the super shell quantum beats.*

[1] *Institute for Nuclear Research, 252028 Prospekt Nauki 47, Kiev-28, Ukraine*

References

[1] J. Pedersen et al., Nature, **353** (1991) 733
[2] R. B. Balian and C. Bloch, Ann. Phys. (N.Y.) **69** (1972) 76
[3] S.Frauendorf, V.M.Kolomietz, A. G. Magner and A. I. Sanzhur, Phys. Rev. Lett, subm.

Two-Phonon $J = 1$ States in ^{122}Te, ^{126}Te and ^{130}Te[B]

R. Schwengner, G. Winter, W. Schauer[1], M. Grinberg[2], F. Becker[3], P. von Brentano[3], J. Eberth[3], J. Enders[4], T. von Egidy[1], R.-D. Herzberg[3], N. Huxel[4], L. Käubler, P. von Neumann-Cosel[4], N. Nicolay[3], J. Ott[1], N. Pietralla[3], H. Prade, S. Raman[5], J. Reif, A. Richter[4], C. Schlegel[4], H. Schnare, T. Servene, S. Skoda[3], T. Steinhardt[3], C. Stoyanov[2], H.G. Thomas[3], I. Wiedenhöver[3] and A. Zilges[3]

Our study of the vibrational nuclei ^{122,126,130}Te in (γ,γ') experiments [1] revealed several $J = 1$ states at $E \approx 3$ MeV, where the occurrence of two-phonon states is expected. Quasiparticle-phonon-model calculations predict two states with $J = 1$ in this energy region: one 1^- state resulting from the coupling of the first quadrupole and the first octupole phonon $(2_1^+ \otimes 3_1^-)$ and one 1^+ state arising from coupling the first and the second quadrupole phonon which has mixed-symmetry (or isovector) character $(2_1^+ \otimes 2_{ms}^+)$. This 1^+ state represents a new type of two-phonon states with a complicated isoscalar-isovector structure. Based on the comparison of experimental and calculated level energies shown in figure 1 and transition strengths given in figure 2 a tentative correspondence between experimentally observed $J = 1$ states and the predicted two-phonon 1^- and 1^+ states is proposed.

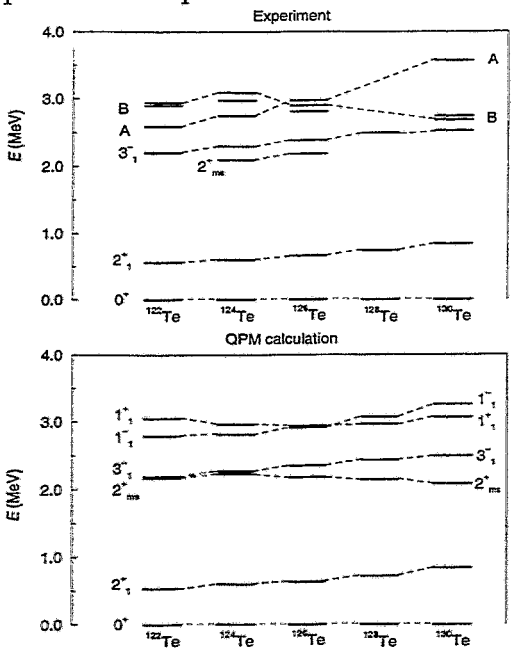

Fig. 1 *Experimental 2_1^+, 2_{ms}^+, 3_1^- and the three lowest $J = 1$ states (top), and calculated 2_1^+, 2_{ms}^+, 3_1^-, 1_1^- and 1_1^+ states (bottom) in $^{122-130}$Te. Experimental states tentatively supposed to be two-phonon $2_1^+ \otimes 3_1^-$ states or two-phonon $2_1^+ \otimes 2_{ms}^+$ states are labelled A or B, respectively.*

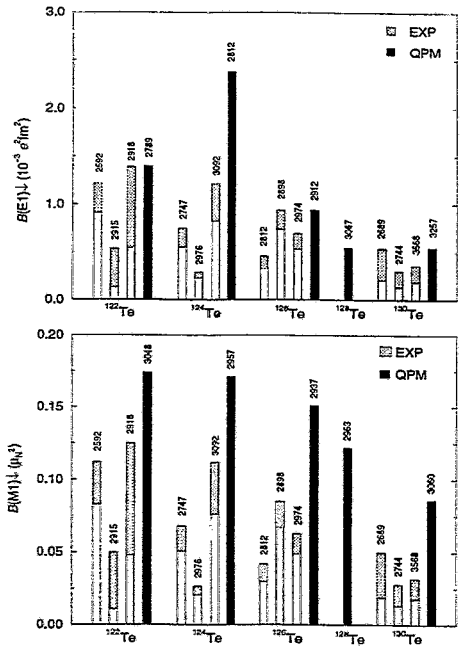

Fig. 2 *Top: experimental E1 strengths (π = -1 assumed for the experimental states) compared with QPM values for the $1_1^- \rightarrow 0^+$ transition. Bottom: experimental M1 strengths (π = +1 assumed) and QPM values for the $1_1^+ \rightarrow 0^+$ transition. Shaded area: experimental error bars.*

[1] *Physik Department, Technische Universität München, 85747 Garching*
[2] *Institute of Nuclear Research and Nuclear Energy, 1784 Sofia, Bulgaria*
[3] *Institut für Kernphysik, Universität zu Köln, 50937 Köln*
[4] *Institut für Kernphysik, Technische Hochschule Darmstadt, 64289 Darmstadt*
[5] *Physics Division, Oak Ridge National Laboratory, TN 37830, USA*

References

[1] R. Schwengner et al., Annual Report 1995, FZR-130 (1996) 81

Investigation of the Magnetic Dipole Band in ^{79}Br with EUROBALL Cluster Detectors [B]

T. SERVENE, J. REIF, H. SCHNARE, R. SCHWENGNER, H. PRADE, G. WINTER, L. KÄUBLER[1], J. EBERTH[2], H.G. THOMAS[2], F. BECKER[2], B. FIEDLER[2], S. FREUND[2], S. KASEMANN[2], S. SKODA[2], T. STEINHARDT[2], O. THELEN[2], T. HÄRTLEIN[3], CH. ENDER[3], F. KÖCK[3], P. REITER[3], D. SCHWALM[3],

We investigated the nucleus ^{79}Br in the reaction ^{76}Ge(^{7}Li,4n) at E(^{7}Li)=35 MeV at the Max-Planck-Institut für Kernphysik Heidelberg using a flat arrangement of six EUROBALL Cluster detectors. Details of the experimental setup are described in [1,2].
The coincidence data were sorted into a E_γ-E_γ matrix and a E_γ-E_γ-E_γ cube. From the analysis of the logical coincidences, a largely extended level scheme of ^{79}Br is proposed. In total, 32 new levels and 88 new γ transitions were found.
Multipole orders of the γ rays were deduced from directional correlations of coincident γ rays (DCO). In order to minimize the opening angle of the Cluster detectors only events detected in the middle rows of Cluster capsules at $\pm 40°$ and $90°$ were sorted into a DCO matrix. An efficiency correction was done for the $\pm 40°$ and $90°$ detectors separately. From the resulting DCO ratios level spins and mixing ratios were derived. In the level scheme of ^{79}Br, the $g_{9/2}$ band with signature α=+1/2 on top of the $9/2^+$ isomer could be extended up to spin $(37/2^+)$ and the $3/2^-$ ground state band based on the $p_{3/2}$ configuration was extended up to spin $(37/2^-)$.
The most interesting structure is the magnetic dipole band shown in Fig. 1. Here, four new dipole transitions were found and, for the first time, crossover transitions could be observed.
The examination of experimental B(M1)/ B(E2,ΔI = 2) ratios is a stringent test of the predictions of the tilted axis cranking model (TAC). The obtained experimental values of B(M1)/ B(E2,ΔI = 2) $\approx 10 - 20\,\mu_N^2/e^2b^2$ are consistent with the TAC calculations for this band [3].
The further analysis of the data applying the Doppler shift attenuation method in order to determine level lifetimes is in progress.

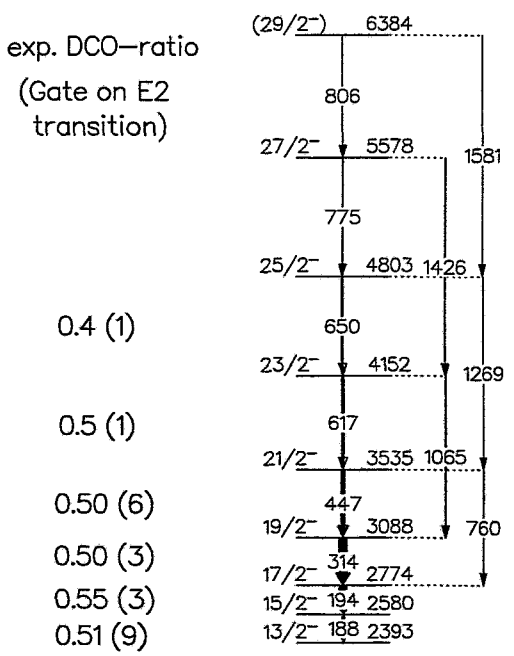

Fig. 1 *Magnetic dipole band in ^{79}Br (Interband transitions omitted). The experimental DCO ratios given on the left indicate the dipole character of the lowest six transitions.*

[1] *Institut für Kern- und Teilchenphysik, TU Dresden and Institut für Kern- und Hadronenphysik, FZR*
[2] *Institut für Kernphysik der Universität zu Köln*
[3] *Max-Planck-Institut für Kernphysik, Heidelberg*

References

[1] J. Eberth, Prog. Part. Nucl. Phys., **28** (1992) 495
[2] T. Servene et al., Annual Report 1995 FZR-130 (1996) 73
[3] R. Schwengner et al., Annual Report 1995 FZR-130 (1996) 71

Rotational Alignment and Band Termination in ^{81}Y [B]

H. Schnare, J. Reif, R. Schwengner, G. Winter, J. Döring[1], G.D. Johns[1], S.L. Tabor[1], C.J. Gross[2], C. Baktash[3], Y.A. Akovali[3], D.W. Stracener[3], F.E. Durham[4], D.G. Sarantites[5], M. Korolija[5], P.F. Hua[5], D.R. LaFosse[5], A. Macchiavelli[6], I.Y. Lee[6], W. Rathbun[6], A. Vander Mollen[7]

Nuclei in the mass region around $A = 80$ have been found to exhibit a rich variety of structural behavior at high spins. Theoretical calculations as well as experimental data have revealed properties like large deformation, shape coexistence and superdeformation.
The fusion-evaporation reaction ^{58}Ni(^{32}S,2αp) has been used to study the neutron-deficient isotope ^{81}Y. The combination of the GAMMASPHERE array for γ-ray detection and the simultaneous identification of emitted charged particles by the MICROBALL detector proved to be an essential tool for a detailed spectroscopy of this nucleus. Clean spectra have been achieved by selecting the desired reaction channel with the charged-particle detector. Furthermore a precise Doppler-shift correction has been applied to the γ-rays, deduced from an event-by-event determination of the nucleus recoil momentum. This leads to resolution-enhanced γ-lines in the spectra. (e.g. a resolution enhancement by a factor 2 is obtained for a 1 MeV γ-line [1]). The analysis of an $E_\gamma - E_\gamma$ matrix as well as a $E_\gamma - E_\gamma - E_\gamma$ cube resulted in the placement of more than 100 new γ-rays and 80 new levels in the decay scheme of ^{81}Y. Most of the new levels have been assigned to rotational bands, where 6 bands have been observed for the first time. Several bands have been extended up to an excitation energy of 17 MeV with the top most spin reaching I=($\frac{57}{2}$). The level scheme of ^{81}Y, based on the present work, is presented in Fig. 1.
At low excitation energy, all one quasiparticle excitations typical for Z=39 nuclei, have been identified. They are built on configurations involving the proton single-particle levels $[422]\frac{5}{2}^+$, $[301]\frac{3}{2}^-$, $[303]\frac{3}{2}^-$ and $[301]\frac{1}{2}^-$. The experimental evidence for a possible $[301]\frac{1}{2}^-$ level close to the ground state has been found for the first time in ^{81}Y.
With increasing rotational frequency the spin of the nucleus is predominantly built by the break-up of $g_{9/2}$ proton as well as $g_{9/2}$ neutron pairs and their alignment along the rotational axis. In the favored signature of the positive-parity yrast band (band A in Fig. 1) two of those alignments were observed. On the basis of systematics and results obtained in the neighboring nuclei ^{79}Rb and ^{83}Y the first alignment is attributed to $g_{9/2}$ neutrons and the second to $g_{9/2}$ protons. Regarding the negative-parity bands a gradual alignment of a proton $g_{9/2}$ pair is observed at low rotational frequencies. In addition an alignment of a $g_{9/2}$ neutron pair has been found for the favored signature of the negative-parity yrast band F. Band G is associated with a high moment of inertia ($J^{(1)} \approx 26\ \hbar^2/\mathrm{MeV}$). This value remains constant over a large frequency range and lies close to the moments of inertia deduced for superdeformed bands in the $A \approx 80$ nuclei. However, at variance to the Latter this band has been observed at a lower spin and excitation energy, compared to the superdeformed bands established in the neighboring nuclei. The bands A,C,H are found to exhibit the characteristic features of terminating bands. With increasing rotational frequency they show a successive decrease in their moment of inertia accompanied by an increasing "energy cost" for building spin units.

[1] *Department of Physics, Florida State University, Tallahassee, Florida, USA*
[2] *Oak Ridge Institute of Science and Education, Oak Ridge, Tennessee, USA*
[3] *Physics Division, Oak Ridge National Laboratory, Oak Ridge, Tennessee, USA*
[4] *Department of Physics, Tulane University, New Orleans, Louisiana, USA*
[5] *Chemistry Department, Washington University, St. Louis, Missouri, USA*
[6] *Nuclear Science Division, Lawrence Berkeley Laboratory, Berkeley, California, USA*
[7] *National Superconducting Cyclotron, Michigan State University, East Lansing, Michigan, USA*

References

[1] H. Schnare et al., Annual Report 1995, FZR-130 (1996)

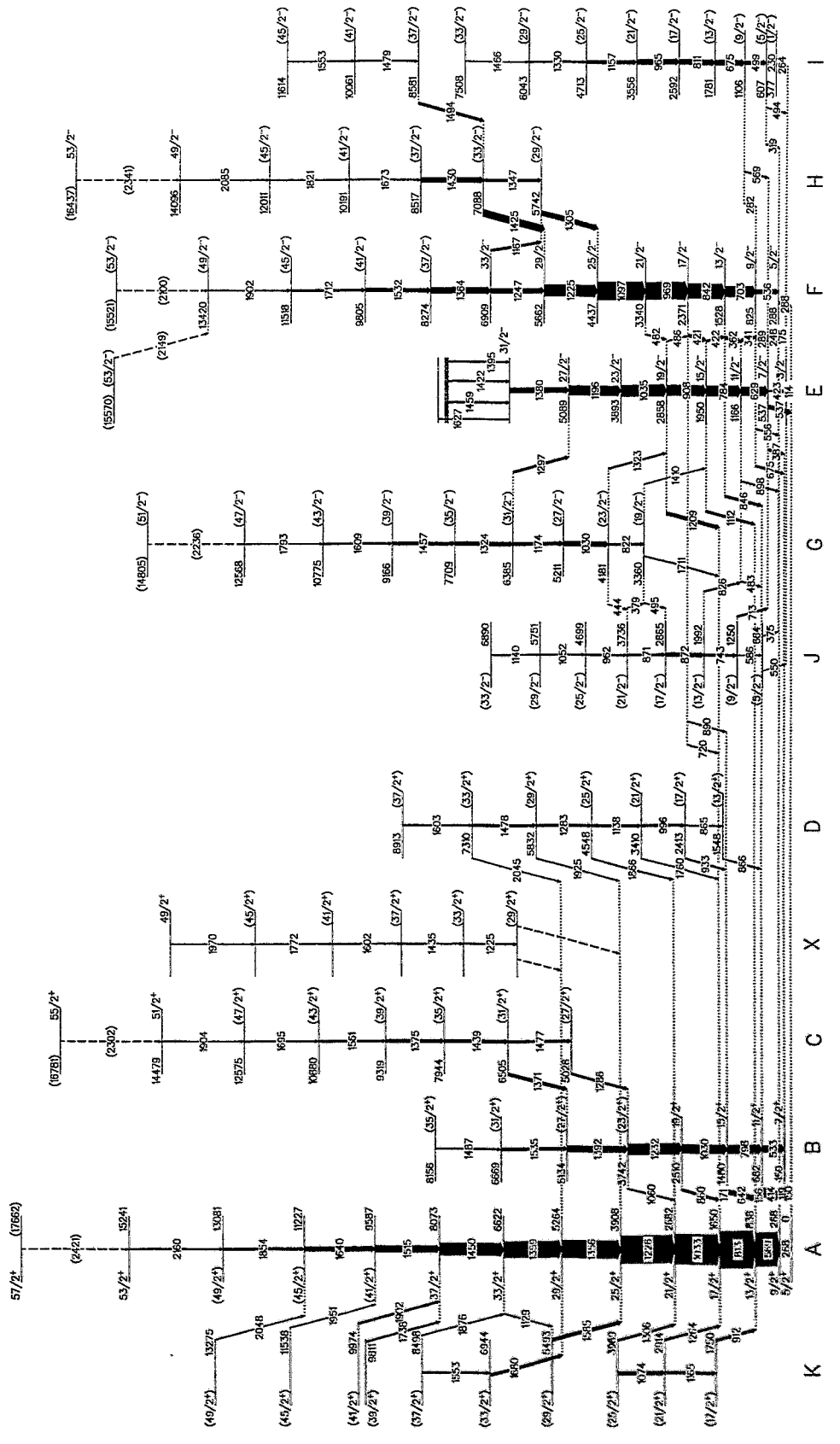

Fig. 1 *Level scheme of* ^{81}Y *deduced from the present work*

High-Spin States in the $N = 48$ Nucleus ^{87}Y

R. Schwengner, G. Winter, J. Reif, H. Schnare, T. Servene, H. Prade, M. Wilhelm[1], S. Kasemann[1], E. Radermacher[1] and P. von Brentano[1]

In our investigation of the $N = 48$ nuclei ^{83}Br and ^{85}Rb a variety of phenomena has been discovered [1]. At low spin regular level sequences with collective properties were observed while at high spin three- and five-particle excitations lead to a multiplet-like structure. The large M1 transition strengths between the states of the multiplets arise in the shell-model description from a recoupling of the spins of the involved proton and neutron orbits. This is an analogue of the shears mechanism described in the tilted-axis cranking model [2].

To extend the knowledge on $N = 48$ nuclei to nuclei with larger proton number we started the study of ^{87}Y. Excited states in this nucleus were populated in the ^{80}Se(^{11}B,4n) reaction at $E = 45$ MeV using the ^{11}B beam of the FN tandem accelerator of the University of Cologne. Gamma rays were detected with the six-detector array OSIRIS CUBE. A total of 2.9 $\times 10^8$ $\gamma\gamma$ coincidences was measured. Based on the coincidence measurement the level scheme of ^{87}Y known from previous work [3] could be extended up to $E \approx 7$ MeV. Some of the level assignments in [3] have been corrected. The preliminary level scheme deduced from the present work is shown in figure 1. Spin assignments are based on directional correlations of γ rays extracted from the present $\gamma\gamma$ coincidence measurement. The further analysis of the data is in progress. Special emphasis will be given to the determination of level lifetimes.

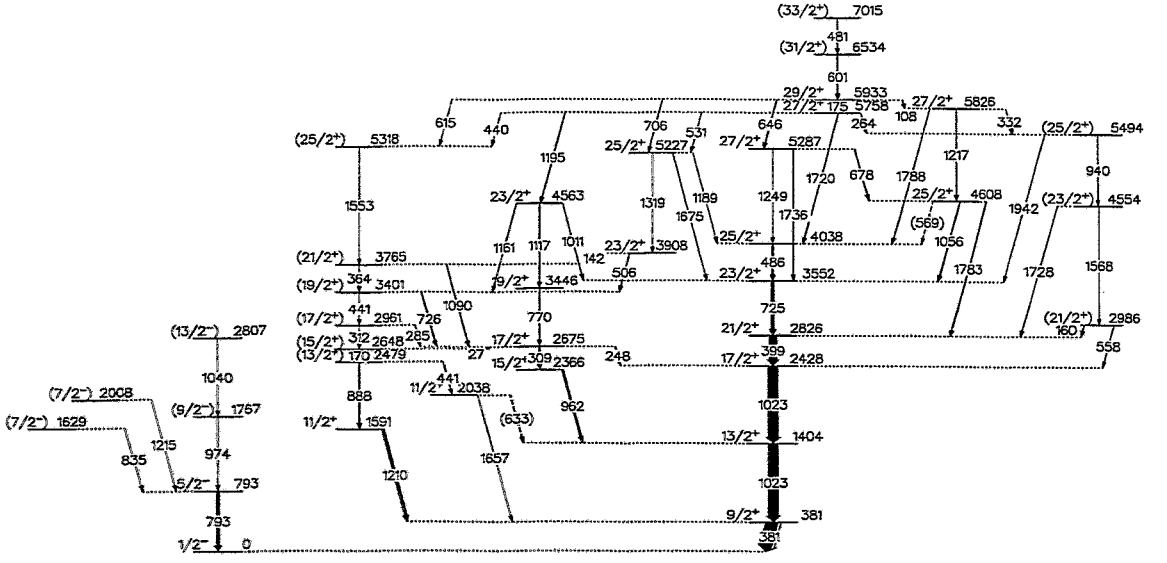

Fig. 1 *Preliminary level scheme of ^{87}Y deduced from the present work.*

[1] *Institut für Kernphysik, Universität zu Köln, 50937 Köln*

References

[1] R. Schwengner et al., Nucl. Phys. A 584 (1995) 159
[2] S. Frauendorf, Nucl. Phys. A 557 (1992) 259c
[3] C.A. Fields et al., Z. Phys. A 295 (1980) 365

Interfering Doorway States and Giant Resonances[D,W]

V.V. SOKOLOV[1], I. ROTTER[2], D.V. SAVIN[1] AND M. MÜLLER[3]

Using a phenomenological schematic model of multipole giant resonances we investigate analytically and numerically the effects of overlapping of their components. The Hamilton operator is

$$\mathcal{H} = H_0 + \mathbf{D}\mathbf{D}^{\mathbf{T}} - \frac{i}{2}AA^T = H - \frac{i}{2}AA^T$$

where H_0 is the unperturbed part containing N discrete levels and $\mathbf{D}\mathbf{D}^{\mathbf{T}}$ is the residual internal interaction of dipole-dipole type (real part H of $\mathcal{H} \leftrightarrow$ Brown-Bolsterli model). The external interaction via K common decay channels is described by the imaginary part $-\frac{i}{2}AA^T$.

If the states overlap, the interaction AA^T via the continuum of decay channels leads to interferences between the states. First, $N-K-1$ states become trapped and decouple almost fully from the continuum. Only $K+1$ doorway states (K channel states and 1 giant dipole resonance) remain relevant in studying the cross section pattern. In this case, the interference picture is determined mainly by the ratio λ of the strengths of external and internal interactions and by the angle between the dipole vector $\mathbf{D}$ and the K-dimensional subspace of decay vectors $\mathbf{A^c}$.

With increasing λ, the mixing of all the $K+1$ collective states leads to a restructuring of the total dipole strength in favour of the low-lying components and to an apparent quenching of the dipole strength [1]. The scenario is determined by mainly two of the doorway states: the giant dipole resonance with large internal collectivity and the channel state with the smallest width. The interference of these two resonance states is governed by the effect of avoided resonance crossing [2]. The dipole strengths of the two resonances behave very much like their positions in energy when considered as functions of λ. While the sums of the two resonance energies and of the two strengths remain constant, the corresponding differences decrease as functions of increasing λ up to certain minimum values. The widths of the two states increase first with increasing λ but bifurcate for large λ. As a result, the dipole state is shifted to lower energy and the channel state, acquiring an appreciable dipole strength, becomes trapped.

Thus, the mixing of the doorway components due to the interaction via the common decay channels influences significantly their multipole strengths, widths and positions in energy. The photoemission turns out to be most sensitive to the overlapping of the doorway states [3].

A saturation of the γ multiplicity is observed experimentally at about 250 MeV excitation energy in heavy nuclei [4,5]. The different existing theoretical approaches can only partly explain the situation observed [5]. The interference phenomena via the continuum, described well by the avoided resonance crossing of two states, show qualitatively the same features as those observed experimentally. Further investigations of this interesting question for concrete nuclei are necessary.

[1] *Budker Institute of Nuclear Physics, 6300090 Novosibirsk, Russia*
[2] *Institut für Theoretische Physik, TU Dresden, and Institut für Kern- und Hadronenphysik, FZR*
[3] *Centro Internacional de Ciencias, Cuernavaca, Mexico*

References

[1] V.V. Sokolov, I. Rotter, D.V. Savin and M. Müller, Preprint FZR-153 (October 1996)
[2] M. Müller, F.M. Dittes, W. Iskra and I. Rotter, Phys.Rev. E 52, 5961 (1995)
[3] V.V. Sokolov, I. Rotter, D.V. Savin and M. Müller, Preprint FZR-154 (October 1996)
[4] M. Thoennessen (ed.), Proceedings of the Gull Lake Nuclear Physics Conference on Giant Resonances, Nucl. Phys. A 569 (1964)
[5] T. Suomijärvi et al., Phys. Rev. C 53, 2258 (1996)

Width Distribution in Statistical Scattering[D,W]

T. Gorin[1], F.–M. Dittes, M. Müller[2], I. Rotter[1] and T. H. Seligman[2]

In [1] we investigate the distortion of regular motion by random coupling to few decay channels. The regular motion is described by means of a Poissonian ensemble (POE). Positions and widths of the resonances are given by the complex eigenvalues of an effective Hamiltonian. In the strong coupling regime, where K broad modes have segragated from the $N-K$ trapped ones [2,3] we found that there is a new distribution law for the widths: Whereas for the Gaussian orthogonal ensemble (GOE) one has a χ^2_K distribution as in the small coupling region, for the POE the variance of the width distribution is approximately double.

We derived an analytic expression for the width distribution at strong coupling in the one channel case, using a two level approximation [4]. From this we get width distributions for the POE and the GOE which turn out to be only asymptotically correct for $y \mapsto 0$, where $y = \Gamma/\langle\Gamma_{\mathrm{f}}\rangle$ is measured in units of the mean trapped width.

$$p_{\mathrm{POE}}(y) = \frac{\mathrm{e}^{y/\pi^2}}{4y} \mathrm{W}_{-1,0}\left(\frac{2y}{\pi^2}\right), \qquad p_{\mathrm{GOE}}(y) = \frac{1}{\sqrt{2\pi y}}\left(1+\frac{2y}{\pi}\right)^{-3/2}. \tag{1}$$

$W(z)$ is the Whitakker function [5]. Both distributions have a y^{-2} tail, in contrast to the rather exponential slope (cf. Fig. 1). Disregarding the tail the broadening is qualitatively reproduced.

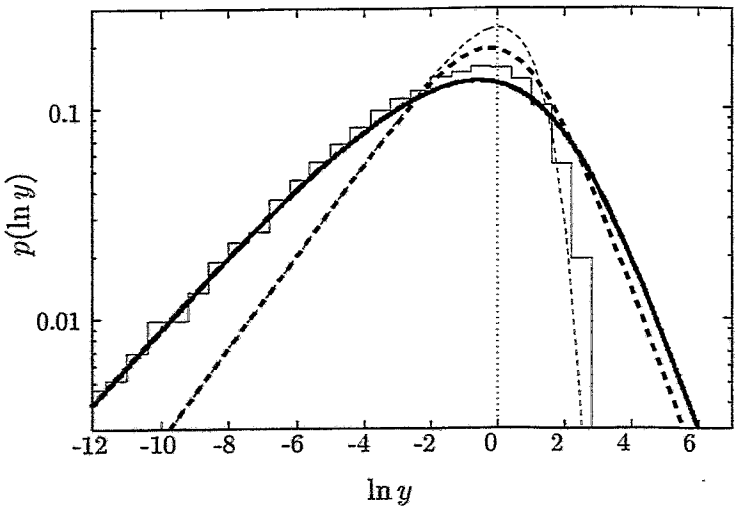

Fig. 1 *Distributions of the logarithms of the widths. The prediction of the two level approximation p_{POE} (solid bold line) is compared to the numerical result (histogram) produced by diagonalising the corresponding effective Hamiltonian. The two level GOE result p_{GOE} (dashed bold line) is compared to the known exact distribution, the Porter Thomas curve (dashed line).*

[1] *Institut für Theoretische Physik, TU Dresden and Institut für Kern- und Hadronenphysik , FZR*
[2] *Centro Internacional de Ciencias, Cuernavaca, Mexico*

References

[1] T. Gorin, F.–M. Dittes, M. Müller, I. Rotter, and T. H. Seligman. *Preprint FZR–162*, January 1997.
[2] F.–M. Dittes, I. Rotter, and T. H. Seligman. *Phys. Lett. A*, **158** 14, 1991.
[3] V. V. Sokolov, and V. G. Zelevinsky. *Nucl. Phys. A*, **504** 562, 1989.
[4] S. Albeverio, F. Haake, P. Kurasov, M. Kuś, and P. Šeba. *J. Math. Phys.*, 1997 (in press).
[5] M. Abramowitz, and I. A. Stegun, editors. *Handbook of mathematical functions.* , National Bureau of Standards, 1964.

Abstracts of publications

Shears Bands in ^{193}Pb
(Phys. Rev. C 54 (1996) 1106)

Baldsiefen, G., M.A. Stoyer, J.A. Cizewski, D.P. McNabb, W. Younes, J.A. Becker, L.A. Bernstein, M.J. Brinkman, L.P. Farris, E.A. Henry, J.R. Hughes, A. Kuhnert, T.F. Wang, B. Cederwall, R.M.Clark, M.A. Deleplanque, R.M. Diamond, P. Fallon, I.Y. Lee, A.O. Macchiavelli, J. Oliveira, F.S. Stephens, J. Burde, D.T. Vo, S. Frauendorf

Abstract: Four bands of enhanced dipole transitions, with weak crossovers, have been observed in ^{193}Pb. Three of these bands are connected to the spherical levels. In addition, the spherical level scheme has been extended. The nuclear spectroscopy was done with the early implementation of GAMMASPHERE and HERA arrays of Ge detectors. The nucleus ^{193}Pb was populated in the ^{174}Yb (^{24}Mg, $5n$) reaction at beam energies of 129, 131, and 134 MeV. The experimental results are compared to tilted-axis cranking calculations. The systematical behavior of the dipole bands in the heavier odd-A Pb isotopes, ^{195,197,199,201}Pb, is also discussed.

Lifetimes of a Shears Band in ^{139}Sm
(Phys. Lett. B 388 (1996) 468)

Brandolini, F., M. Ionescu-Bujor, N.H. Medina, R.V.Ribas, D. Bazzacco, M. De Poli, P. Pavan, C. Rossi Alvarez, G. de Angelis, S. Lunardi, D. De Acuna, D.R. Napoli, S. Frauendorf

Abstract: Lifetimes have been measured in ^{139}Sm with the DSAM method, using the reaction ^{62}Ni (^{81}Br,p3n)^{139}Sm at 350 MeV. In the negative-parity regular dipole band based on the $25/2^-$ state at 3325 keV values of 0.60(21), 0.40(14) and 0.25(8) ps were found for the 337, 409 and 473 keV transitions, respectively. The deduced B(M1) and B(E2) are in agreement with the predictions of the tilted axis cranking model, allowing a triaxial equilibrium shape for the assumed $\nu h_{11/2} \otimes \pi h^2_{11/2}$ configuration.

First Observation of the Scissors Mode in a γ-Soft Nucleus: The Case of ^{196}Pt
(Phys. Rev. Lett. 76 (1996) 2029)

Brentano, P. von, J. Eberth, J. Enders, L. Esser, R.-D. Herzberg, N. Huxel, H. Meise, P. von Neumann-Cosel, N. Nicolay, N. Pietralla, H. Prade, J. Reif, A. Richter, C. Schlegel, R. Schwengner, S. Skoda, H.G. Thomas, I. Wiedenhöver, G. Winter, A. Zilges

Abstract: A nuclear resonance fluorescence experiment with one of the newly developed highly efficient EUROBALL cluster detectors has been performed on the γ-soft nucleus ^{196}Pt. Magnetic dipole excitations were observed between 2 and 3.5 MeV excitation energy. They are interpreted as the main fragments of the scissors mode based on the measured excitation strengths and branching ratios. A strong γ decay, which we believe to be an $E2$ decay of the scissors mode to the 2^+_1 state, is observed. It allows an extraction of the effective boson quadrupole charges in the interacting boson model.

Can Hexadecapole Deformation Lead to ΔI=2 Staggering in Superdeformed Bands?
(Phys. Lett. B 387 (1996) 667)

Dönau, F., S. Frauendorf, J. Meng

Abstract: The possibility is investigated that a $C_{4\nu}$ -symmetric hexadecapole deformation causes the observed ΔI=2 staggering of rotational bands in even and odd-A nuclei. Calculating the energy as a function of intrinsic angular momentum components by means of the tilted cranking model, a rotor Hamiltonian with $C_{4\nu}$ -symmetry is derived, but the magnitude of the fourth order terms is found to be too small to generate a ΔI=2 staggering of the experimental size. Considering an odd-A system composed of a rotor and a high j-quasiparticle, the ΔI=2 staggering emerges only when the rotor core contains a $C_{4\nu}$-symmetric fourth order angular momentum term.

Shell-Model Study of Shears Bands in Light Pb Nuclei
(Nucl. Phys. A 601 (1996) 41)

Frauendorf, S., J. Reif, G. Winter

Abstract: Spherical shell-model calculations have been performed in the configuration space $(s_{1/2}\, h_{9/2}\, i_{13/2})$ and $(p_{1/2}\, p_{3/2}\, f_{5/2}\, i_{13/2})$ for protons and neutrons, respectively, in order to interpret the sequences of strong dipole transitions found in neutron-deficient Pb isotopes. Regular dipole bands are found if several high-j protons and high-j neutron holes are interacting with neutrons in the low-spin (fp) orbitals. The calculated B(M1) values are in the order of several μ_N^2 for the ΔJ=1 transitions, and the crossover E2 transitions are very weak. The mechanism generating the dipole bands is found to be the same as in the tilted axis cranking mean-field description.

Interpretation and Quality of the Tilted Axis Cranking Approximation
(Z. Phys. A 356 (1996) 263)

Frauendorf, S., J. Meng

Abstract: Comparing with the exact solutions of the model system of one and two particles coupled to an axial rotor, the quality of the semi classical tilted axis cranking approximation is investigated. Extensive comparisons of the energies and $M1$ and $E2$ transition probabilities are carried out for the lowest bands. Very good agreement is found, except near band crossings. Various recipes to take into account finite K within the frame of the usual principal axis cranking are included into the comparison. A set of rules is suggested that permits to construct the excited bands from the cranking configurations, avoiding spurious states.

General Axial Shapes of Sodium Clusters
(Ann. Physik 5 (1996) 34)

Frauendorf, S., V.V. Pashkevich

Abstract: The shell correction method is applied to calculate the shapes and binding energies of Na clusters. The axial equilibrium shapes are calculated by minimizing five deformation param-

eters simultaneously. Strong deviations from spheroidal shapes including reflection asymmetric ones are found. The influence of cluster deformation on the separation energies and ionization potentials and on the splitting of the photo - resonance are compared with the available experimental data. The N-dependence of the cluster shape and its relation to the N- and Z-dependences of the nuclear shape is discussed.

Shapes and Free Energies of Molten Sodium Clusters
(Surface Review and Letters 3 (1996) 241)

Frauendorf, S., V.V. Pashkevich

Abstract: The shell-correction method is formulated to calculate the shapes and free energies of hot alkali clusters. The equilibrium shapes of Na clusters with mass 100-700 are calculated by minimizing simultaneously with respect to two deformation parameters. For $T = 700°$ K strong deviations from spheroidal shape including reflection asymmetric shapes are found to survive in the center of the open shells. The second derivative of calculated free energy correlates with the derivative of the experimental cluster abundances, showing prominent spikes related to the change between spherical and deformed shape.

Magnetic Properties of Sodium Clusters
(Surface Review and Letters 3 (1996) 25)

Frauendorf, S., V.V. Pashkevich, S.M. Reimann

Abstract: Axial and triaxial shapes of Na clusters are determined by means of the shell-correction method. The orbital paramagnetism and the diamagnetism of small Na clusters are calculated. Odd axial clusters may have substantial orbital paramagnetic moments, which are quenched for triaxial shapes. Even clusters show diamagnetism, which is maximal for spherical and attenuated for deformed shape.

A New Type of Band Crossing at Large Deformation
(Phys. Lett. B 374 (1996) 277)

Harder, A., F. Dönau, K.P. Lieb, R.A. Cunningham, W. Gelletly, C.J. Groß, F. Hannachi, M.K. Kabadiyski, H.A. Roth, D. Rudolph, J. Simpson, Ö. Skeppstedt, B.J. Varley, D.D. Warner

Abstract: A detailed study of the positive parity yrast and yrare rotational bands in ^{77}Rb is presented. Using the reaction ^{40}Ca(^{40}Ca, $3p$) and the EUROGAM I spectrometer, $\gamma\gamma\gamma$ coincidences enabled us to follow both bands over a large spin range and to measure many $E2$ strengths. The moments of inertia and transition quadrupole moments indicate that a more deformed band ($\varepsilon_2 \approx 0.38$) is crossed by a less deformed one ($\varepsilon_2 \approx 0.29$). Since the yrare band starts at the extremely low spin value of I=9/2, the conventional band crossing mechanism of two aligning high-j quasiparticles is excluded. The frequency-dependent equilibrium shapes were calculated with Nilsson-Strutinsky type calculations using a diabatic tracing of configurations near the neutron Fermi level. This is the first observation of such a band crossing.

Collective Structures and Smooth Band Termination in ^{109}Sn
(Z. Phys. A 356 (1996) 235)

Käubler, L., H. Schnare, D.B. Fossan, A.V.Afanasjev, W. Andrejtscheff, R.G. Allat, J. de Graaf, H. Grawe, I.M. Hibbert, I.Y. Lee, A.O. Macchiavelli, N. O'Brien, K.-H. Mayer, E.S. Paul, H. Prade, I. Ragnarsson, J. Reif, R. Schubart, R. Schwengner, I. Thorslund, P. Vaska, R. Wadswoth, G. Winter

Abstract: Six rotational bands up to energies E_x=24.7 MeV and spins $J^\pi=(79/2^-)$ have been identified in ^{109}Sn using the GAMMASPHERE γ-detector array. Four of the bands show smoothly decreasing dynamic moments of inertia at rotational frequencies $\hbar\omega > 0.6$ MeV. The bands arise at medium spins from a coupling of a valence $d_{5/2}$, $g_{7/2}$ or $h_{11/2}$ neutron to the deformed 2p2h proton excitation of the Z=50 core ^{108}Sn. At very high $\hbar\omega$ these bands show the typical behaviour of smoothly terminating bands, i.e. a gradual alignment of the angular momenta of the valence particles and holes corresponding to a transition from high collectivity to noncollective states.

Particle-Number Projecting Method for Description of Pairing Effects in Metal Clusters
(Il Nuovo Cimento D 18 (1996) 645)

Kuzmenko, N.K., V.O. Nesterenko, S. Frauendorf, V.V. Pashkevich

Abstract: Particle-number projecting method for the description of pairing effects in metal clusters is proposed. In contrast with the Bardeen-Cooper-Schrieffer method (BCS) which does not conserve the particle number (thus not providing the necessary accuracy of calculations for small clusters) and has no solutions at sufficiently weak pairing, the projecting method can be applied to both small and large clusters with any pairing strength. As an example, the projection method is used to check the assertion on the pairing origin of the odd-even staggering (OES) in the ionization potentials (IP) of sodium clusters. Both effects of pairing and shape deformation are taken into account simultaneously. In general, the results obtained show that the existence of pairing in sodium clusters is doubtful.

Lifetimes of Shears Bands in ^{199}Pb
(Nucl. Phys. A 595 (1995) 499)

Neffgen, M., G. Baldsiefen, S. Frauendorf, H. Grawe, J. Heese, H. Hübel, H. Kluge, A. Korichi, W. Korten, K.H. Maier, D. Mehta, J. Meng, N. Nenoff, M. Piiparinen, M. Schönhofer, R. Schubart, U.J. van Severen, N. Singh, G. Sletten, B.V. Thirumala Rao, P. Willsau

Abstract: Lifetimes of states within the two strongest shears bands in ^{199}Pb have been measured using Doppler-shift techniques. The deduced B(M1) values confirm the proposed proton-particle neutron-hole structure of these bands. They show a decrease with increasing spin as expected within the tilted-axis cranking model. The B(E2) values confirm the low quadrupole collectivity and small deformation predicted by the calculations. The results give further support of the interpretation of the dipole bands in terms of the shears mechanism.

Decay Rates of Resonance States at High Level Density
(Phys. Rev. E 54 (1996) 3339)

Persson, E., T. Gorin, I. Rotter

Abstract: The time-dependent Schrödinger equation of an open quantum-mechanical system is solved by using the stationary biorthogonal eigenfunctions of the non-Hermitian time-independent Hamilton operator. We calculate the decay rates at low and high level densities in two different formalism. The rates are generally time dependent and oscillate around an average value due to the nonorthogonality of the wave functions. The decay law is studied disregarding the oscillations. In the one-channel case, it is proportional to t^{-b} with $b \approx 3/2$ in all cases considered, including the critical region of overlapping where the nonorthogonality of the wave functions is large. Starting from the shell model, we get $b \approx 2$ for two and four open decay channels and all coupling strengths to the continuum. When the closed system is described by a random matrix, $b \approx 1 + K/2$ for $K = 2$ and 4 channels. This law holds in a limited time interval. The distribution of the widths is different in the two models when more than one channel is open. This leads to the different exponents b in the power law. Our calculations are performed with 190 and 130 states, respectively, most of them in the critical region. The theoretical results should be proven experimentally by measuring the time behavior of deexcitation of a realistic quantum system.

Resonance Phenomena Near Threshold
(Phys. Rev. C 53 (1996) 3002)

Persson, E., M. Müller, I. Rotter

Abstract: The trapping effect is investigated close to the elastic threshold. The nucleus is described as an open quantum mechanical many-body system embedded in the continuum of decay channels. An ensemble of compound nucleus states with states below and above threshold is investigated in an energy-dependent formalism. It is shown that the states below threshold can trap the resonance ones and also that they can directly influence the scattering cross section.

The γ-Decay of Particle-Hole states in ^{208}Pb Using the Euroball Cluster Detector
(Nucl. Phys. A 597 (1996) 408)

Radermacher, E., M. Wilhelm, S. Albers, J. Eberth, N. Nicolay, H.G. Thomas, H. Tiesler, P. von Brentano, R. Schwengner, S. Skoda, G. Winter, K.H. Maier

Abstract: Neutron particle-hole states in the doubly magic nucleus ^{208}Pb were investigated using a Euroball Cluster detector and five usual HPGe detectors at the Osiris cube spectrometer in Cologne. 126 γ-ray transistions with energies up to 7.2 MeV could be detected, 14 of those for the first time. The states were excited with the ^{208}Pb $(p,p'\gamma)^{208}$Pb reaction via isobaric analogue resonances in ^{209}Bi at E $_p$ = 16.5, 17, 17.45, 17.5 and 18.5 MeV and through the subcoulomb ^{207}Pb $(d,p\gamma)^{208}$Pb reaction at E_d = 10 MeV. For most of the excited states assignments for the particle and/or the hole component of the configuration could be made, 22 of these are new.

Potential-Energy Surfaces of Sodium Clusters with Quadrupole, Hexadecapole, and Triaxial Deformations
(Surface Review and Letters 3 (1996) 25)

Reimann, S.M., S. Frauendorf

Abstract: Combining a modified Nilsson-Clemenger model with the shell-corrrection method, the potential-energy surfaces of sodium clusters with sizes of up to $N = 200$ atoms are calculated, including nonaxial deformations. For spherical clusters, the model potential is fitted to the single-particle spectra obtained from microscopically self-consistent Kohn-Sham calculations using the jellium model and the local-density approximation. Employing the Strutinsky shell-correction method, the surface energy of the jellium model is renormalized to its experimental value. The ground-state shapes are determined by simultaneous minimization of the deformation energies for quadrupole, hexadecapole, and triaxial cluster deformations.

Smooth Termination of Intruder Bands in Sb
(Phys. Rev. C 54 (1996) 1598

Schnare, H., D.R. LaFosse, D.B. Fossan, J.R. Hughes, P. Vaska, K. Hauschild, I.M. Hibbert, R. Wadswoth, V.P. Janzen, D.C. Radford, S.M. Mullins, C.W. Beausang, E.S. Paul, J. DeGraaf, I.-Y. Lee, A.O. Macchiavelli, A.V. Afanasjev, I. Ragnarsson

Abstract: Intruder rotational bands have been investigated to high frequency in $^{109}_{51}$Sb. Five decoupled (ΔI=2) bands extending to rotational frequencies above 1.4 MeV/$\hbar$ have been observed. At the highest frequencies, the $\mathcal{J}^{(2)}$ dynamic moments of inertia for four of these bands are seen to decrease steadily to unexpectedly low values. $\mathcal{J}^{(2)} \sim 10\,\hbar^2\mathrm{MeV}^{-1}$. These four bands, which are interpreted as being based on deformed 2p-2h proton excitations across the Z=50 closed-shell gap, achieve the so-called "smooth band termination" following alignment of the valence nucleons outside of ^{100}Sn. In addition, two strongly coupled (ΔI=1) bands have been observed, which are related to 1p-1h proton excitations across the gap.

Band Structure of the odd-even ^{125}La, ^{127}La Nuclei
(Phys. Rev. C 53 (1996) 137)

Starosta, K., Ch. Droste, T. Morek, J. Srebrny, D.B. Fossan, D.R. LaFosse, H. Schnare, I. Thorslund, P. Vaska, M.P. Waring, W. Satula and S.G. Rohoziski, R. Wyss, I.M. Hibbert, R. Wadsworth, K. Hauschild, C.W. Beausang, S.A. Forbes, P.J. Nolan, E.S. Paul

Abstract: Excited states of the ^{125}La and ^{127}La nuclei were populated following ^{112}Sn (^{16}O,p2n) and ^{112}Cd (^{19}F,4n) fusion-evaporation reactions, respectively, and investigated using methods of in-beam γ-ray spectroscopy. Five collective bands in ^{125}La, and eleven collective bands in ^{127}La were observed. The spin and/or parity assignments of excited states in these nuclei were based on angular-correlation and linear-polarization measurements. The experimental data are discussed and compared to the results of self-consistent total-Routhian-surface calculations including quadrupole pairing.

Intruder Bands in ^{114}Te: Smooth Band Termination
(Phys. Rev. C 52 (1995) R2839)

Thorslund, I., D.B.Fossan, D.R. LaFosse, H. Schnare, K. Hauschild, I.M. Hibbert, S.M. Mullins, E.S. Paul, I. Ragnarsson, J.M. Sears, P. Vaska, R. Wadsworth

Abstract: The nucleus ^{114}Te has been studied in heavy-ion γ-ray spectroscopy experiments performed with the early implementaton of the GAMMASPHERE multidetector array. Three rotational intruder bands have been observed up to high spins. The yrast band, involving the 4p2h $(h_{11/2})^2(g_{7/2})^2(g_{9/2})^{-2}$ proton configuration, reaches I = $48\hbar$ at an excitation energy of 30.3 MeV, the highest observed spin connected by γ rays in this mass region. The band properties are interpreted in the framework of smooth band termination.

Smooth Band Termination in ^{108}Sn
(Phys. Rev. C 53 (1996) 2763)

Wadsworth, R., C.W.Beausang, M. Cromaz, J. DeGraaf, T.E. Drake, D.B. Fossan, S. Flibotte, A. Galindo-Uribarri, K. Hauschild, I.M. Hibbert, G. Hackman, J.R. Hughes, V.P. Janzen, D.R. LaFosse, S.M. Mullins, E.S. Paul, D.C. Radford, H. Schnare, P. Vaska, D. Ward, J.N. Wilson, I. Ragnarsson

Abstract: Three rotational bands in ^{108}Sn have been investigated to high frequency via the ^{54}Fe (^{58}Ni,4p) reaction at 243 MeV. One of these bands is observed to undergo a band crossing at high spin. All three bands show a large decrease in their dynamic moments of inertia, to approximately one third of the rigid body value, as the rotational frequency approaches 1 MeV/$\hbar$.The structures of these bands are thought to be based on 2p-2h proton excitations across the Z=50 shell gap and their properties can be interpreted in terms of cranked Nilsson-Strutinsky calculations. Such calculations predict smooth band terminations for all three structures and a gradual shape change from collective prolate, at low spin, to noncollective oblate at high spin.

Biomedical Research

Research on applications of nuclear physics methods to other fields, especially to biology and medicine, has some tradition in Rossendorf. The most prominent example for this may be the introduction of positron emission tomography (PET), which can be considered as a continuous process starting in the 80th with a common effort of radiochemists, accelerator and nuclear physicists to establish PET at Rossendorf and finally cumulating in the recent installation of a PET-centre for medical diagnostics and research in the Institute of Bioanorganic and Radiopharmaceutical Chemistry of the FZR.

Another result of this development is presented in this Annual Report: In January 1996 a Positron Emission Tomograph has been installed at the treatment site for heavy ion tumour therapy at the Gesellschaft für Schwerionenforschung in Darmstadt (cf. W. Enghardt et al.). It is part of a novel cancer treatment facility that will utilize beams of ions, preferably ^{12}C, to irradiate precisely deep-seated, compact and radioresistant tumours in the vicinity of organs at risk. The results of preclinical tests of the tomograph indicate that PET may become a valuable tool for quality assurance in heavy-ion cancer therapy (cf. R. Hinz et al.). For this purpose the β^+-activity distributions which are created within the target volume by nuclear fragmentation as a by-product of any therapeutic irradiation with heavy ions and which are measured with the PET-scanner have to be compared with the predictions deduced from the treatment plan (cf. B.G. Hasch et al.). In contradiction to PET-scanners used in nuclear medicine the present tomograph is a limited angle device due to geometric constraints at the treatment site caused by the beam delivery and the patient positioning. Therefore, the filtered backprojection as the method of choice for reconstructing the source distributions from tomographic data cannot be applied and iterative algorithms have to be adapted to the special scanner geometry (cf. K. Lauckner et al.).

There is serious hope that the treatment facility at GSI will start its clinical operation in 1997. Then the potential and the benefit of the PET-technique for heavy ion therapy monitoring have to prove to be a success under realistic clinical conditions.

In parallel to this special PET application J. Pawelke et al. investigated PET-detectors of high spatial resolution. Such detectors are of considerable interest for the design of dedicated PET-scanners for biomedical and pharmacological research with small animals.

The Positron Emission Tomograph for Treatment Monitoring at the Heavy Ion Therapy Facility at GSI Darmstadt[B]

W. ENGHARDT[1], B.G. HASCH, R. HINZ, K. LAUCKNER, J. PAWELKE, M. SOBIELLA

The positron emission tomograph was completely transferred to GSI in Jan. 1996. The double-head positron camera was mounted at the medical beam line (Fig. 1), whereas the real-time data acquisition system and the workstation for controlling the whole system were installed in the therapy control room. Furthermore, the Monte Carlo code [1,2] for simulating the PET-imaging process on the basis of the treatment planning data (X-ray computed tomograms of the target volume, beam delivery control data set) became available in a first version. This progress allowed a series of in-beam PET-studies to be carried out, where different targets (lucite, tissue equivalent materials, ALDERSON head phantom) have been irradiated with ^{12}C-beams at therapeutically relevant energies ($E = 90 - 350\,A$ MeV). These experiments [3] were aimed at (i) system performance tests, (ii) investigations on the potential of the PET-imaging for quality assurance of heavy ion therapy [4], (iii) gathering realistic data as a base for the further refinement of the calculation of β^+-emitter distributions from the treatment planning [1,2], the adaption of tomographic reconstruction algorithms [5] and for development of software tools for clinical applications.

The results in summary seem to indicate that PET-imaging of the spatial distributions of β^+-radioactive nuclei produced as a byproduct of tumour irradiations with heavy ions should have a considerable value for quality assurance for this kind of therapy, especially with respect to a pre-therapeutic treatment plan verification, the retrospective dose localization for each therapy fraction and the check of patient positioning.

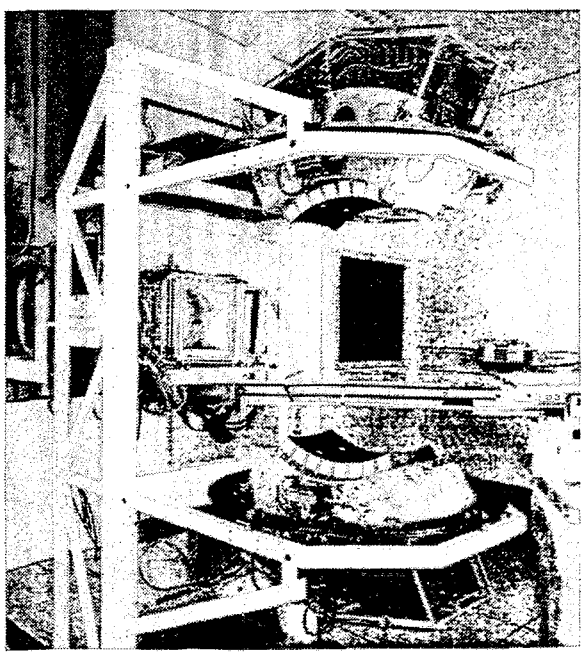

Fig. 1 *The double-head positron camera at the heavy ion tumour therapy facility at the GSI Darmstadt. The position sensitive BGO detectors are mounted below and above the patient couch. The horizontal beam enters the treatment site from the left and passes several detectors for beam diagnosis before hitting the patient. (Photo: A. Zschau, GSI)*

[1] *FZR* and *Uniklinikum der TU Dresden, Fetscherstr. 74, D-01307 Dresden, Germany*

References

[1] B.G. Hasch, PhD Thesis, TU Dresden, 1996
[2] B.G. Hasch et al., this Annual Report
[3] J. Pawelke et al., Proc. Nuclear Science Symposium and Medical Imaging Conference, Nov. 3-9, 1996 Anaheim, CA (in press)
[4] R. Hinz et al., this Annual Report
[5] K. Lauckner et al., this Annual Report

PET Imaging Modes for Quality Assurance of Tumour Treatment with Heavy Ion Beams [B]

R. HINZ, W. ENGHARDT[1], B. G. HASCH, K. LAUCKNER, J. PAWELKE, M. SOBIELLA

The PET scanner at the medical treatment place of GSI Darmstadt came into operation in January 1996 [1]. During the recent year a series of experiments has been carried out for investigating the capabilities of this novel therapy monitoring system that are essential for the clinical application. In the following results from two of these experiments are presented.
Fig. 1 shows the β^+-emitter distribution produced by irradiation of a spherical target volume of 4 cm diameter seated at a mean depth of 8 cm in a PMMA phantom with a dose of 3 Gy. These are typical parameters for a clinical radiotherapeutical application. The intensity controlled raster scanner delivered the dose contour by means of a pencil-like $^{12}C^{6+}$ beam of energies from 292.5 to 243 AMeV in steps of 1.5 AMeV which was deflected horizontally and vertically by magnetic fields. The comparision of this measured distribution with the β^+-emitter distribution obtained from the computer simulation [2] leads to in-situ dose localisation. This way the correspondence between the irradiation and the treatment plan can be verified *after* each therapy fraction.
In Fig. 2 another mode of PET imaging for treatment plan verification is demonstrated. This experiment has been aimed at determining the minimum dose necessary for generating β^+-emitters sufficient for deducing the range of the primary projectiles and the Bragg Peak, respectively. One pulse of approx. 300,000 carbon ions with an energy of 160.5 AMeV was shot into the phantom which corresponds with a Bragg Peak dose of 174 mGy. This is less than a tenth of a commonly applied dose fraction. The PET profile obtained from a 20 minutes decay scan shows the maximum shortly before the dose peak. This in-situ measurement of the range of monoenergetic ions at a prominent position before starting the therapeutic irradiation will be applied particularly to treatments very close to organs of risk e.g. brain or spinal cord. It gives a verification of treatment plan to the therapist *before* the treatment is started.

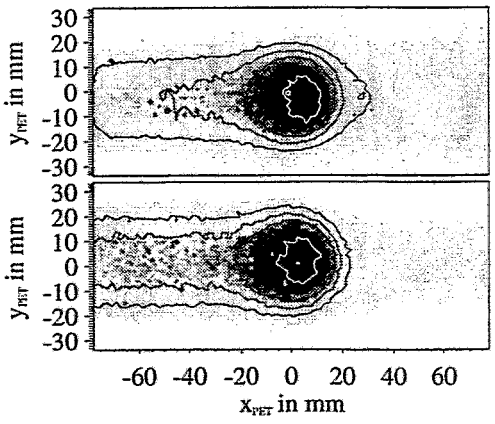

Fig. 1 *Back projection midplane of the β^+-emitter distribution. Above: experiment, below: simulation.*

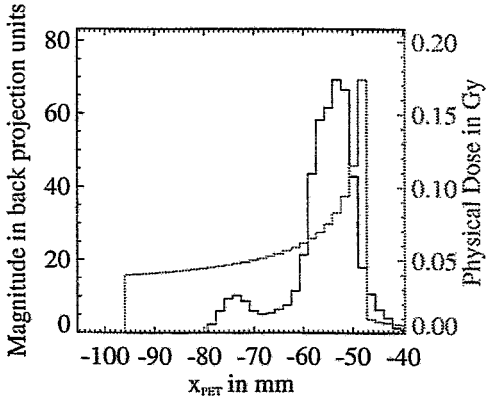

Fig. 2 *Depth profiles of β^+-activity (solid) and dose (dotted) from a low dose monoenergetic pulse of ^{12}C ions.*

[1] *FZR* and *Uniklinikum der TU Dresden, Fetscherstr. 74, D-01307 Dresden, Germany*

References

[1] W. Enghardt et al., this Annual Report
[2] B. G. Hasch et al., this Annual Report

The Simulation of the Positron Emitter Production by ^{12}C Irradiation of Extented Inhomogeneous Target Volumes[B]

B.G. Hasch, W. Enghardt[1] and J. Wetzel[2]

The control of dose localization at heavy ion tumour therapy by means of positron emission tomography requires the comparison between the measurement and a model calculation of the distribution of positron emitting fragments. In [1] we have shown that our Monte Carlo model calculations are in very good agreement with measurements for the special case of homogeneous targets and the irradiation with a non-deflected, pencil-like, monoenergetic beam. Naturally, the target volume which will be irradiated in heavy ion tumour therapy is inhomogeneous and because of its extension a set of beam energies has to be used. The model calculation for this more general case is founded on a database of the spatial distribution of the positron emitting fragments for each initial beam energy used in the therapy. These data are calculated for a plastic phantom (PMMA) assuming an irradiation with a non-deflected pencil-like beam of gaussian shaped profile (1 cm FWHM). According to the raster scan control data and the water equivalent path length in the phantom, which are derived from X-ray computed tomograms, a subset of these precalculated distributions is superimposed. The control data of the raster scanner resulting from the treatment planning define the number of particles and the initial energy for each irradiated point of the target. In a last step the β^+-decay of the fragments, the annihilation of the positrons, the interaction of the annihilation quanta with the phantom and their detection is simulated. The time regime of irradiation and measurement is taken into account.

An experiment was carried out applying the PET scanner [2] at the treatment place of GSI Darmstadt to test and improve the agreement between these calculations und measurement for an inhomogeneous phantom. The Fig. 1 shows the measured and simulated back projection of the annihilation points for a homogeneously irradiated plane of about 28×40 cm^2 tilted in respect to the beam line. The inhomogenous phantom was made up of different tissue or water equivalent plastic slabs. The relative yield of β^+-emitting target fragments is for the shown result of the calculation only determined from a path length equivalent weighting factor derived from the computed tomograms.

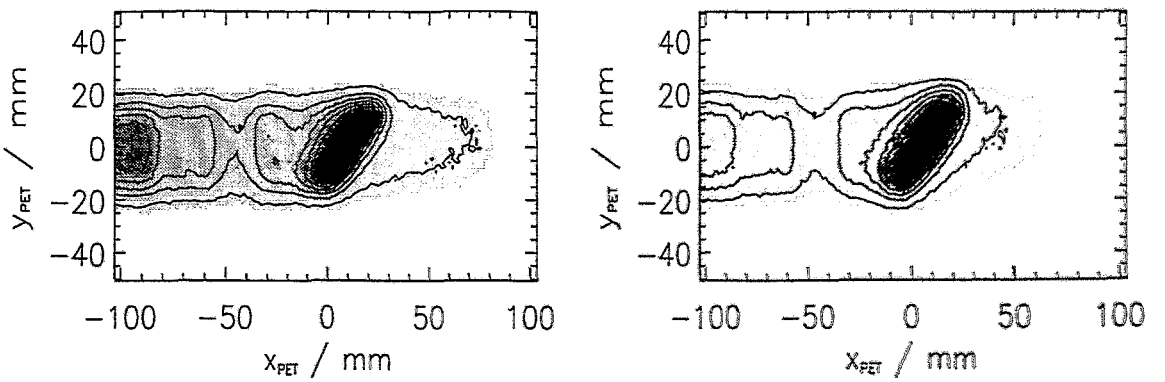

Fig. 1 *Midplane of back projection of the measured (left) and calculated (right) annihilation point distribution of β^+-emitting fragments for the homogeneous irradiation of a tilted plane in an inhomogeneous phantom. The energies of the ^{12}C beam range from 273.0 to 300.0 A·MeV.*

[1] *FZR and Uniklinikum der TU Dresden*
[2] *Strahlenzentrum der Justus-Liebig-Universität Gießen, Zell- und Strahlen-Biophysik*

References

[1] B.G. Hasch, PhD Thesis, TU Dresden 1996
[2] W. Enghardt et al., this Annual Report

Iterative Reconstruction Algorithms For Limited Angle PET [B]

K. LAUCKNER, W. ENGHARDT[1], R. HINZ, J. PAWELKE

At GSI Darmstadt the excellent physical and biological properties of heavy ions will be used to perform a precision radiation therapy that restricts the therapeutical effect only to the local tumour while saving surrounding healthy tissue substantially. With the feasibility of applications to local tomours nearby organs at risk an in-situ verification of the treatment plan is highly desired. A double-head positron camera has been installed in order to measure β^+-distributions produced during interactions of the therapy beam in tissue by fragmentation reactions.
Due to the limited angle tomography and the poor counting statistics encountered in this special PET application the reconstruction problem is notoriously ill-conditioned. We have adapted the image space reconstruction algorithm (ISRA) [1] and maximum likelihood algorithm (MLE) [2] and investigated the robustness of this stochastic reconstruction methods against incomplete data. The following modifications have been done: Modelling of the complicated shape of all line of response functions (LSF) arising from the nonlinear sampling of the camera due to the spherical geometry of the detector heads as well as modelling the shift variant point spread function (PSF), caused by the limited angle geometry and correction of parallaxe errors, because of the 3D aquisition mode.
A typical β^+-distribution was reconstructed both with ISRA in 40 iteration steps and MLE in 20 iteration steps. Because of their specific implementation, ISRA uses voxel driven and MLE projection driven methods, significant differences are shown in Fig. 1. Necessarily a crystal identification has to be performed when using a projection driven method. This results in a more precise modelling of detector granularity. Thus the images produced with MLE depict essential less artefacts. Further investigations are now concentrated to perform the attenuation correction.

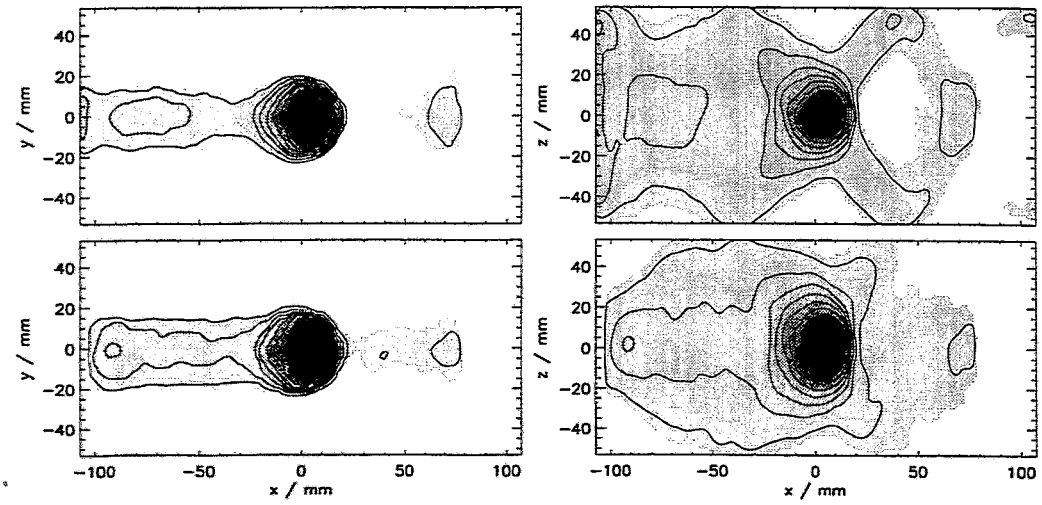

Fig. 1 *Reconstruction of a homogeneous spherical dose distribution (3 Gy) with ISRA (upper images) and MLE (lower images). A ^{12}C ion beam has been stopped in a PMMA-phantom. About 1.3 Mill coinicidences were measured in 24 min. The left side depicts the xy-slices which are parallel, the right side the xz-slices, which are perpendicular to the detector surfaces.*

[1] *FZR and Uniklinikum der TU Dresden, Fetscherstr. 74, D-01307 Dresden, Germany*

References

[1] M. Daube-Witherspoon, G. Muehllehner, IEEE Trans. Med. Imaging, MI-5 (1986) 61
[2] L. A. Shepp, Y. Vardi, IEEE Trans. Med. Imaging, MI-1 (1982) 113

Comparison of YAP and BGO for High Resolution PET Detectors[B]

J. PAWELKE, M. KAPUSTA[1] AND M. MOSZYŃSKI[2]

In [1] we report on a PET detector which consists of a scintillator matrix of 18×18 BGO crystals ($3\times3\times20$ mm^3) coupled to a position sensitive PMT. An improvement of the detector properties (especially spatial and timing resolution) is required to study for example the biodistribution or organ function in small animals as mices and rats and expected by replacing BGO with the recently proposed new inorganic scintillator YAP [2]. We investigated this by directly comparing the scintillator properties of $3\times3\times20$ mm^3 commercially available crystals of YAP (Preciosa Corp., Turnov, Czech Republic) with those of BGO. For this, the light yield, energy resolution, detection efficiency and timing properties have been measured for 511 keV γ-rays of a ^{22}Na source following the methods described in [3], whereby one of the 3×3 mm^2 crystal plane was coupled with a XP2020Q PMT. The results show an about 600 % greater light yield for YAP and good energy and time resolution (table 1). Note, that replacing the rather expensive optical reflector paint provided by the manufacturer with white teflon tape increases the number of photoelectrons given in table 1 by about a factor of two for both scintillators. However, due to the lower photo peak fraction the expected advantages of a YAP based PET detector over BGO associated with the higher light yield are not fully useable. This is confirmed by a comparison of the intrinsic spatial response obtained with a ^{22}Na flat source for a YAP and BGO matrix based detector, respectively (Fig. 1). Mainly an improved crystal identifiation at the edge of the sensitive detector area is given for YAP. Additionally the properties of the position sensitive PMT as well as the signal forming scheme of the detector (energy and time signals were obtained from the anode signals) limits the detector performance (cf. table 1 and 2).

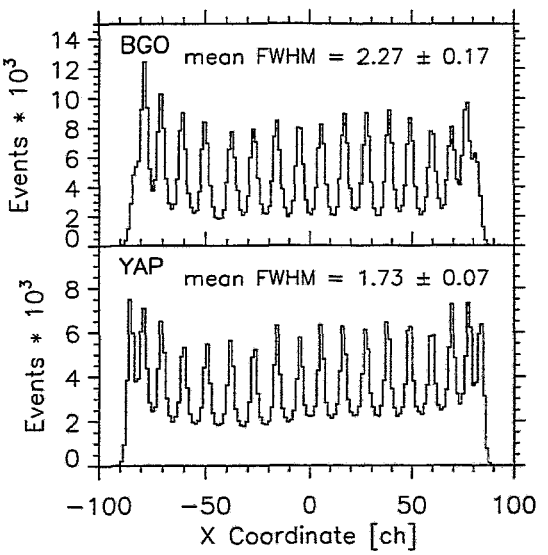

Fig. 1 *Intrinsic spatial response of the BGO and YAP based detector.*

Table 1 *Main crystal parameters*

	BGO	YAP
Photoelectron yield [phe/MeV]	221.9±1.7	1409.6±9.5
Energy resolution (FWHM) [%]	26.6±0.2	9.4±0.1
Time resolution (FWHM) [ns]	7.7±0.3	0.5±0.1
Detection efficiency[a]		
E_{thr}[b]= 0 keV	19.4±0.3	11.4±0.2
E_{thr}[b]=400 keV	8.5±0.1	1.0±0.0

[a]) relative values [b]) low energy threshold

Table 2 *Main detector parameters*

	BGO	YAP
Mean crystal energy resolution (FWHM) [%]	39.5±5.2	21.9±6.0
Time resolution (FWHM) [ns]	25.2±0.4	4.8±0.2

[1] *Institute of Experimental Physics, University of Warsaw, PL-00-681 Warsaw, Poland*
[2] *Soltan Institute for Nuclear Studies, Dept. of Nuclear Electronics, PL-05-400 Otwock-Świerk, Poland*

References

[1] J. Pawelke et al., Phys. Med. Biol. **41**(1996)279
[2] S.I. Ziegler et al., IEEE Transact. Nucl. Sci. **NS40**(1993)194
[3] M. Moszyński et al., Nucl. Instrum. Methods **A345**(1994)461

Abstracts of publications

Positronen-Emissions-Tomographie bei der Schwerionentherapie
(Phys. Bl. 52 (1996) 874)

Enghardt, W.

Abstract: Bei einer Tumorbehandlung mit schweren Ionen, z. B. Kohlenstoff, entstehen durch nukleare Wechselwirkungen des Therapiestrahles mit dem Gewebe positronenemittierende Nuklide. Ihr Nachweis mit Hilfe der Positronen-Emissions-Tomographie (PET) erlaubt Rückschlüsse auf die räumliche Verteilung der applizierten Dosis im Körper des Patienten und bietet damit die Möglichkeit, die korrekte Position des bestrahlten Volumens zu überwachen.

The Investigation of Different Cameras for In-Beam PET Imaging
(Phys. Med. Biol. 41 (1996) 279)

Pawelke, J., L. Byars, W. Enghardt, W.D. Fromm, H. Geissel, B.G. Hasch, K. Lauckner, P. Manfraß , D. Schardt, M. Sobiella

Abstract: *In situ* and *in vivo* treatment plan verification and beam monitoring as well as dose control during heavy-ion tumour therapy can be performed in principle by measurements of range distributions of β^+-emitting nuclei by means of PET techniques. For this purpose the performance of different types of positron camera as well as the results of in-beam PET experiments using beams of β^+-active heavy ions (^{15}O, ^{17}F and ^{19}Ne with energies of 300-500 AMeV) are presented. Following the deduced performance requirements a PET scanner that is designed for clinical use in experimental heavy-ion therapy at GSI Darmstadt has been built. This limited angle tomograph consists of two large-area detector heads based on position sensitive BGO detectors and is predicted to perform the measurement of the end point of a β^+-emitting ion beam for the verification of a treatment plan with a precision better than 1 mm. The maximum dose applied in the patient thereby is of the magnitude of 10 mGy.

Technical and Methodic Developments

The lack of an in-house experimental facility compels the Rossendorf nuclear physicists to join collaborations, to build up detector components and integrate them into experimental setups at remote accelerators as well as to evaluate data measured there. This section of the Annual Report comprises such activities and has, therefore, a heterogeneous structure.

The paper of Dshemuchadse et al. reports on the effort for completing the time-of-flight spectrometer TOF at COSY Jülich with the barrel hodoscope for identifying the reaction products of p+p collisions at energies larger than 1 GeV and for determing their trajectories. A technical solution for equipping one section of about 3 m length and 3 m diameter of the TOF-vessel with 96 plastic scintillator barrels has been elaborated. The detector could be assembled to a large extent (see the cover picture). Without any doubt, this detector is the largest one that has been ever built in Rossendorf so far and was, apart from the technical and physical problems, a logistic challenge to the staff involved. Methodic preparations of experiments with this device have been carried out by R. Geyer et al. studying the influence of target contaminations to COSY-TOF experimental results.

The Rossendorf contributions to the magnetic particle spectrometer ANKE at COSY comprise the complete development of the start and stop multi-wire chambers (MWC) and extensive technical support for the installation of the particle telescopes (cf. C. Schneider et al. and T. Grande et al., respectively). The two start MWC with a sensitive area of 130 x 35 cm^2 have been completely built up and tested in the detector laboratory of the institute, whereas the manufacturing of the much larger stop MWC (196 x 60 cm^2) has been initiated. For the particle telescope consisting of E, ΔE, veto and Čerenkov counters photo multiplier shieldings against magnetic fields and a LED-based monitoring system has been delivered. The capability of the 4π Si-detector array EuroSiB for light particle discrimination could be further improved by introducting a new electronics for signal processing (cf. G. Pausch et al.). EuroSiB will be applied in nuclear structure studies with the EUROBALL γ-ray detectors for reaction channel selection by means of the identification of light charged particles (protons and alphas).

Two reports of this section are devoted to refined off-line data analysis methods:
For heavy ion collision data of $^{96}Ru + ^{96}Ru$ at a bombarding energy of 1.69 AGeV taken with the FOPI-detector system at GSI C. Plettner et al. show that the combination of the data measured by the axial drift chambers and the scintillator barrels of FOPI results in a clean separation of the week Kaon signal from the much stronger background of protons and pions. Andronenko et al. propose an off-line restoration of Bragg ionization chamber pulses sampled with flash ADC. This procedure requiring considerable computer capacity is expected to lead to an impressive improvement of the energy resolution for intermediate mass fragments produced via 1 GeV proton-nucleus collisions. Finally, F.M. Dittes presents a new method for the solution of global optimization problems by using a simultaneous optimization of the energy or likelihood of the total system and of subsystems of arbitrary size.
A central role with respect to methodic developments is played by the detector laboratory and the electronic group of the institute. This staff mainly supported the experimentalists involved in collaborations at COSY (ANKE), GSI (heavy ion therapy) and EUROBALL. Furthermore, they took part in the installation of the electron gun test facility for ELBE. The detector laboratory has been extended by four new rooms of 85 m^2 total area including a dedicated laboratory for radiation physics to meet the requirements of future experiments at ELBE.

Set-Up of the One-Layer COSY-TOF Barrel Hodoscope [B,K]

S. Dshemuchadse, P. Michel, K. Möller[1] A. Schamlott, A. Schülke,
H. Angermann, K.-Th. Brinkmann[1], H. Freiesleben[1], B. Hübner[1], E. Kuhlmann[1],
M. Würschig-Pörsel[1] for the COSY-TOF-Collaboration

In the course of completing the COSY Time-of-Flight spectrometer TOF in 1995 intense work was performed to find a final solution for the construction of the COSY-TOF barrel hodoscopes resulting in the decision that one barrel section out of the three barrels planned for TOF should be built up on the basis of the one-layer barrel concept [1]. The year 1996 was devoted mainly to elaborate further technical details of the one-layer concept, to order the various components and to prepare the assembly of the barrel hodoscope. In the course of this work quite a lot of further improvements of the original concept was found leading to substantial simplifications of the assembly procedure. A sketch of the basic components of the barrel is shown in fig. 1.

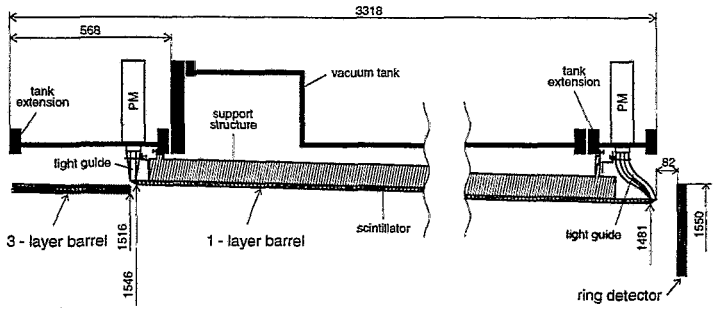

Fig. 1 *Sketch of the components of the one-layer barrel*

After delivery of the scintillator strips and the light guides prior to assembling the whole barrel one barrel module was assembled and installed in the tank section. For comparison with prototype measurements [2] this module was tested with respect to time and position resolution (fig. 2). In prototype measurements NE 110A-type scintillators were used whereas the actual barrel is equipped with BC 412-type scintillators, since NE 110A scintillators are no longer available. As illustrated in fig. 3 by now the set-up of the barrel hodoscope is nearly complete.

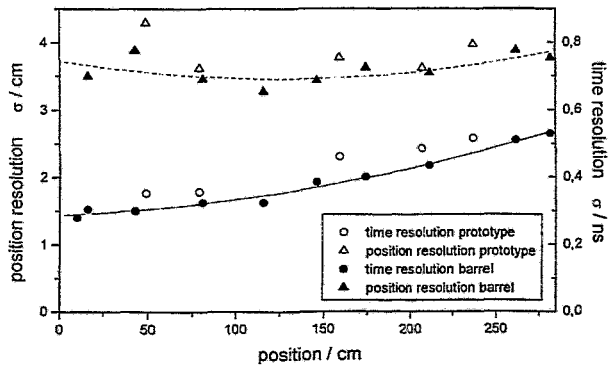

Fig. 2 *Time and position resolution of barrel modules*

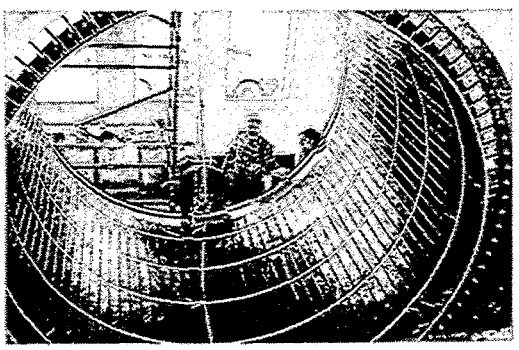

Fig. 3 *The one-layer barrel section in the set-up phase*

[1] *Institut für Kern- und Teilchenphysik, TU Dresden*

References

[1] K.-Th. Brinkmann et al., Review: "The barrel scintillator hodoscope for the COSY-TOF spectrometer" RU Bochum, TU Dresden, FZ Rossendorf

[2] P. Michel et al., Annual Report 1995, IKP, Jül-3200, p. 21-23

Investigation of the Target Contamination of the COSY-TOF-Spectrometer[B]

R. GEYER[1], B. NAUMANN, L. NAUMANN AND THE COSY-TOF-COLLABORATION

The contamination of the liquid hydrogen target [1] has been studied with data from proton-proton scattering at beam momentum 0.88 GeV/c. We analyzed missing mass (M_x) spectra of two prong events for two different cuts in phase space (β-cut: $\beta < 0.42$; Θ-cut: $\Theta > 23.7°$) to eliminate all $pn\pi^+$ and $d\pi^+$ events. For both data sets the time dependence of (p,2p) events is in good agreement. For the β-cut the M_x-spectra were normalized by the $pp\pi^0$ peak. To normalize the M_x-spectra by time duration of each run we assumed a constant beam intensity for the Θ-cut.

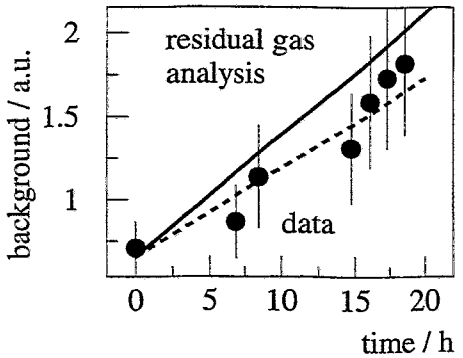

Fig. 1 *Relative growth of (p,2p)-events in dependence on the target exposition time.*

Fig. 1 shows a comparision of the time dependent relative growth of (p,2p) events for data from the β-cut and the growth of residual gas molecules on 2 μm thick cold target foils at vacuum pressure of 10^{-6} mbar [2]. There is a good agreement between the data fit and our residual gas approximation.
The influence of target foils and other materials is shown in the hatched area of fig. 2. The two superimposed spectra are normalized by $pp\pi^0$ events. The upper line represents events from the run after target heating without condensate contamination on the foils and the lower line shows the full target M_x-spectrum after an empty target background subtraction. The influence on the M_x-spectrum of the time averaged condensate growth for nearly one day is shown in fig. 3. The hatched area represents the difference between the summarized M_x-spectrum without background subtraction and the M_x-spectrum of the run after target heating (no condensate on the foils).

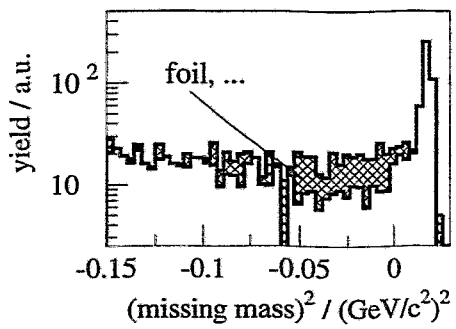

Fig. 2 *Squared missing mass spectrum for the pp-hypothesis; the hatched area shows the influence of target foils and other construction materials.*

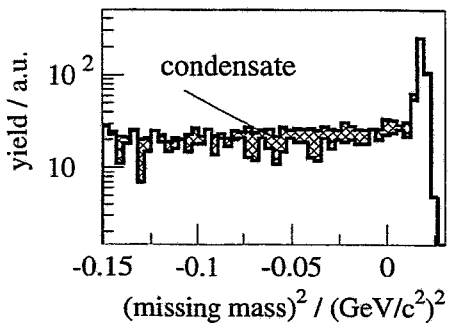

Fig. 3 *Squared missing mass spectrum for the pp-hypothesis; the hatched area shows the influence of condensate on target foils.*

The target contamination by foils and condensate superimposed the bremsstrahlung events is expected around $M_x = 0$. The background can be minimized by better vacuum ($p \leq 10^{-7}$mbar), thinner target foils ($d < 1\mu$m) and a frequent elimination of the ice layers (fast heating). In our second run on pp-bremsstrahlung in October 1996 target foils of thickness $d = 0.9$ μm and a fast heating device were used.

[1] *Institut für Kernphysik, FZ Jülich*

References

[1] V. Jaeckle et al., Nucl. Instr. and Meth. **A349** (1994) 15
[2] R. Klein et al., Annual Report 1994, Jül-3035 (1995) 17

Particle Telescopes for ANKE[B]

TH. GRANDE[1], R. ESSER[1], A. SCHNEIDER[1], H. OHM[1], B. PRIETZSCHK AND B. RIMARZIG

The particle telescopes at ANKE serve mainly for the identification of protons, pions and K-mesons. For low momenta they consist of stop, ΔE and veto counters. At higher momenta, in addition Ĉerenkov counters are included, see fig. 1. For the whole range of momenta degraders in front of the ΔE counters will be used in order to optimize the ratio of energy losses between pions and kaons. Additional degraders between the ΔE and the veto counters avoid that kaons, which are not completely stopped in the ΔE counters, enter into the veto counters. In total 15 telescopes will be used. The telescopes are individual modules which are assembled and tested separately and then mounted in their common frame. Scintillation counters consist of BC-408 with twisted light guides made out of Plexiglas GS-233. For the Ĉerenkov counters extended bars of UV-transmitting Plexiglas GS-218 are used which include the light guides. All joints between scintillators, light guides and photomultiplier tubes are glued which is expected to guarantee stable longterm operation. For the scintillators and Ĉerenkov counters PM tubes Philips XP 2020 (2") and XP 2312 (3"), respectively, are used. The narrow geometry in the ANKE side detector demands that magnetic PM shields are used which are smaller than the commercial ones. The corresponding components have been developed at FZR. In the installation phase the frame is located in the COSY hall outside the ring so that access is possible independently of the operation of the accelerator. Light emitting diodes are mounted in the center of each paddle for monitoring the performance of the detectors and in order to be able to adjust the fast trigger. Ultrabrigth LEDs HP HLMA KH-00 are used. They have been pre-aged with a constant current over 100 hours. The temperature dependence of the LEDs has been measured. In addition to the LED system temperature monitoring at various positions of the detector system will be done with Pt precision resistors. Furthermore, the light output of some LEDs will be monitored by coupling them directly with PIN-photodiodes which are known to have a very stable pulse-height response. The LEDs are operated with fast pulse generators which have been developed at FZR [1]. The trigger pulse is taken from a precision pulse generator which delivers two signals. The telescopes are being assembled one after another and tested with β-particles from ^{90}Sr and with cosmic rays using CFD discriminators and meantimers which have been developed for use at ANKE [2]. The telescope which is designed for the momentum range 138-163 MeV/c has been completed and is ready for installation in the frame. It consists of a stop, ΔE and veto counter with the respective thickness of 3, 5 and 10 mm. The length of the paddles is 540 mm. Pulse height spectra have been recorded with cosmic rays and light from the LED, see fig. 2. A timing resolution of 565 ps FWHM has been achieved which fulfills the requirements for the πK separation by time-of-flight.

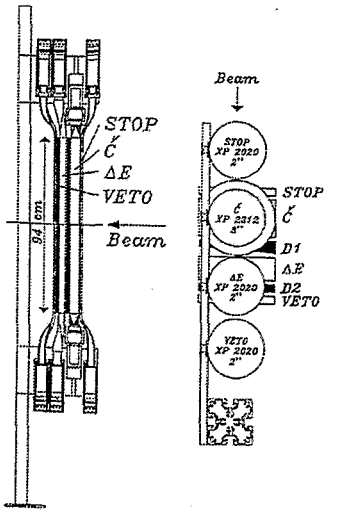

Fig. 1 *Telescope for the momentum range 334-366 MeV/c.*

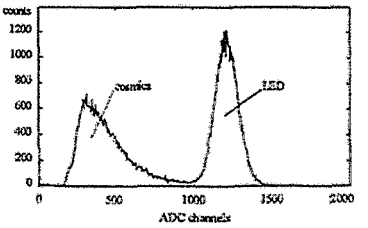

Fig. 2 *Pulse-height distribution of the stop counter.*

[1] *Institut für Kernphysik, FZ Jülich*

References

[1] B. Prietzschk et al., IKP 1995 Annual Report, KFA (1996) p. 64
[2] R. Schleichert et al., IKP 1995 Annual Report, KFA (1996) p. 65

Effects of Inclined Particle Tracks on the Operation Behaviour of a Multi-Wire Chamber[B]

Ch. Schneider, T. Kirchner, L.v. Horn[1], V. Kruglov[2]

At the ANKE spectrometer the ejectile momenta will be measured by using the central dipole magnet D2. Since the deflection of a charged particel in a magnetic field depends on its momentum this quantitiy can be determined from a position measurement of the track behind the magnet. At ANKE the tracks will be measured by two multi-wire chambers (MWC) on either deflection side of the magnet. In spite of an optimal positioning of the chambers they will be crossed by the particles up to an angle of $\sim 60°$. For these inclined trajectories one can expect a different operation behaviour for a MWC compared to 0°.
The main task for the chambers is to achieve a maximum momentum resolution. To fulfill this requirement the chambers have a designed position resolution of about $\sigma \approx 0.75$ mm [1]. This resolution should also be achievable in the more complicated situation of inclined trajectories. Therefore an investigation of this problem was performed at the BIG KARL spectrometer at COSY Jülich.
The situation expected from a pure geometrical consideration is shown in Fig. 1. Here a schema of one detection layer of anode wires between two cathodes is shown. The inclined tracks crossing the gas volume between the two cathodes can lead to the response of more than one wire, e.g. for the 50° trajectory there are six wires. So for every particle passing the chamber under larger angles one expects signals from a number of neighbouring wires labelled in the following as wire group.

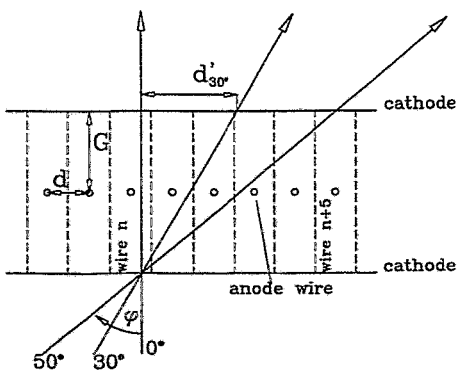

Figure 1: *Schema of a layer of a multi wire chamber*

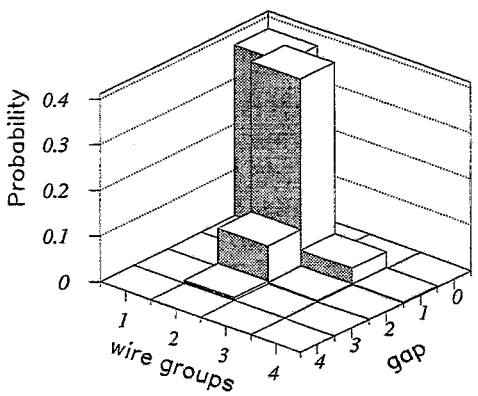

Figure 2: *Probability for different event types for an angle of incidence of 50°*

The deviation from this simple geometrical description are caused by the operation mechanism of a MWC. The energy loss from a particle traversing a gas volume is characterized by a Landau distribution. But clearly the amplitude hight in the proportional mode depends also on the number of interaction points with the gas. Since the particles flight path through the chamber-gas volume is longer for inclined crossing the amount of primary and therefore total deposited charge is larger compared to perpendicular tracks. On the other hand, the total charge is shared between more wires and, thus, the mean signal from one wire is smaller. Furthermore it is necessary to consider the development of the signals. In any case the negative signal on one wire induces a positive signal on the neighbouring wires. If more than one wire responds we have a complicated situation of mutual influences of the signals in amplitude and time development. For

a specific chamber geometry and gas it is therefore necessary to investigate the signal patterns which result from this dynamical process.
How the pattern will look like for an angle of 50°, a specific voltage and amplifier threshold can be deduced from Fig. 2. Here the number of detected wire groups for a single particle event is plotted against the gap in units of wires between these wire groups. The z axis gives the probability. There are the expected events with one-wire group but with the same probability there are events with two-wire groups separated by a gap of one wire. Furthermore there are events with a gap of two or three wires as well as three-wire groups each separated by a gap of one wire. In spite of a detection efficiency of 100% some of the signal amplitudes in between the expected one-wire group are lower than the threshold and split up these events in more than one-wire group.
If one compares the resolution of these split events with the resolution of the primary one-wire group events one achieves a better resolution for the restored split events. This can be explained as follows: The measured position of a particle track is determined from the center of gravity of the wire group. Therefore the resolution is very sensitive to correct identification of the boundary wires of the wire group because, if one of these wires is lost, the resolution is wrong by half a wire distance. The dynamical signal development leads to two main types of patterns. One are primary one-wire groups with high signal amplitudes in the middle and lower amplitudes at the boundary wires. That's why it is very likely that the signals from the boundary wires are below threshold and result in a worse position measurement. The other type of patter has low amplitudes in the middle which leads to split wire groups,but high amplitudes on the boundary wires. Here the width of the wire group and therefore the position of the particle track is very well defined.
From the above considerations one can expect that these effects depend strongly on the amplifier threshold as can be seen from Fig. 3. Here the resolution of particle tracks with an angle of 0° (perpendicular) and 30° is independent of the threshold in the displayed range. For large angles of incident like 50° it is necessary to operate the chamber with a low threshold to achieve the proposed resolution, in this application a value of $\sigma \approx 0.75$ mm.

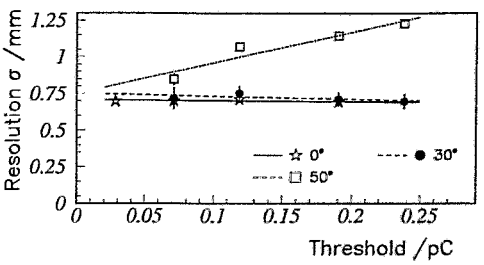

Figure 3: *Dependence of the chamber resolution from the amplifier threshold*

[1] *Institut für Kernphysik, KFA Jülich, Germany*
[2] *Laboratory of Nuclear Problems, JINR Dubna, Russia*

References

[1] Ch. Schneider. Untersuchung der Subschwellenerzeugung von Kaonen am COSY-ANKE-Spektrometer - Detektorentwicklung, Modell- und Simulationsrechnungen. Ph.D. thesis, Fakultät Mathematk und Naturwissenschaften der Technischen Universität Dresden (1997)

About the Capability of the FOPI-Detector to Extract K^+–Mesons Produced in Heavy-Ion Collisions of ^{96}Ru + ^{96}Ru at 1.69 A·GeV[B,G]

C. Plettner, R. Kotte, W. Neubert, D. Wohlfarth,
and the FOPI Collaboration

In September of 1996 the reaction 1.69 A·GeV ^{96}Ru + ^{96}Ru has been measured by the FOPI collaboration with the 4π-detector system [1] at the SIS accelerator at GSI. This system consists of two axial symmetric drift chambers (CDC, Helitron), which are placed inside of a superconducting solenoid (0.6T), and several time-of-flight scintillation detectors (Barrel, outer and inner Plastic Wall). Charged particles emitted between $\Theta_{lab} = 35°$ and 135° are measured with the CDC/Barrel, and those emitted between 8° and 27° are measured with the outer Plastic Wall/Helitron combination. The velocity information of the Barrel surrounding the CDC is used to improve particle identification of the CDC. With only the CDC information kaons could not be separated from the background of protons and π mesons.

The Barrel detector does not cover the CDC completely, thus for kaon analyses the angular acceptance is limited to $\Theta_{lab} = 40° - 135°$ (see Fig.1). Results of investigations [2] of K^+-production rates of the system ^{58}Ni + ^{58}Ni at 1060, 1450 and 1930 A·MeV, which rely solely on CDC/Barrel data, will be published soon ([3]). Now with the Helitron running the region around midrapidity ($Y^0 \equiv \left(\frac{Y}{Y_{proj}}\right)_{cm} = 0$, cp. Fig.1) is accessible. Thus we expect that in the near future we can present first results of the ^{96}Ru+^{96}Ru data comprising a major part of the phase space populated in this reaction.

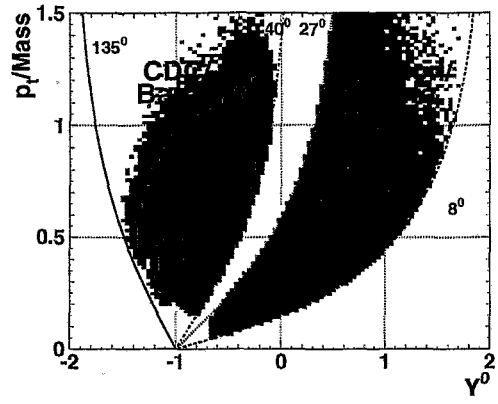

Fig. 1 *Uncorrected count rate in a log. scaled $p_t/Mass$ vs. Y^0 representation.*

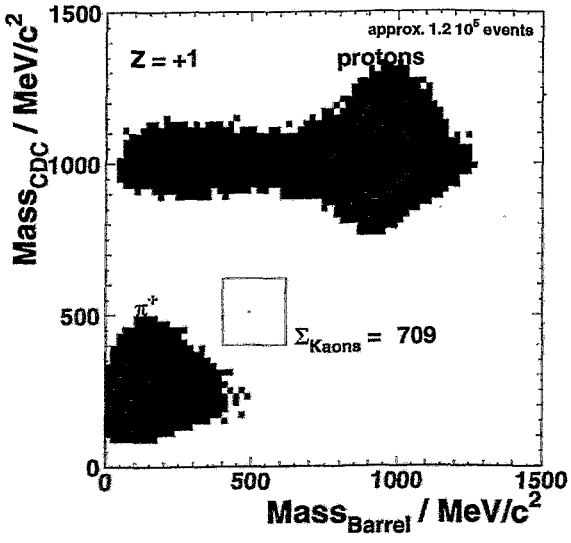

Fig. 2 *The mass from the CDC alone vs. the mass from the CDC momentum and the velocity information of the Barrel. The plot comprises about 2% of the available data.*

Up to date kaon separation of CDC/Barrel data has been performed. Fig.2 shows a mass plot where a surplus yield is indicated around the kaon mass of 494 MeV/c^2. The mass called $Mass_{CDC}$ is determined from the dependence of the mean energy loss of a particle on its laboratory momentum p. The velocity information of the CDC/Barrel matching provides the so called Barrel mass $m \equiv Mass_{Barrel}$ via the relation $p = mc\gamma\beta$. Due to the decreasing mass resolution with increasing momentum the laboratory momentum p is limited here to $p < 500$ MeV/c.

References

[1] J. L. Ritman for the FOPI collaboration, Nucl. Phys. **B** - Proc. Suppl. 44, 708 (1995)
[2] D. Best, PhD thesis, Universität Heidelberg, 1996
[3] D. Best et al., to be submitted to Nucl. Phys. **A**

Acceptance Tests of the Frontend Electronics and Detectors for EuroSiB

G. Pausch, M. Moszyński[1], D. Wolski[1], W. Bohne[2], H. Grawe[3], H. Prade, G. Röschert[2], and R. Schubart[3]

EuroSiB – a compact 4π Si-array for charged-particle detection – will be operational in 1997 [1]. The efforts to optimize electronics and detectors for best possible particle discrimination with the pulse-shape (PSD) method [2] have been continued.

A substantial improvement could be achieved with a modified electronics, considering the experience from previous tests [1]. A new preamplifier developed at Swierk is characterized by an internal rise time of 20 ns and a load resistor of only 2 MΩ, which increases the particle separation and eliminates the sensitivity to the load- and temperature-dependent detector current [3]. An additional bipolar output of the compact PSD electronics solved the problem of baseline restoration in case of high rates and strong background [1]. The new electronics was tested at ISL Berlin, using a 2-5 pnA beam of 150 MeV ^{36}Ar ions and 2 mg/cm^2 Ni targets for particle production. EuroSiB detectors from serial production were mounted at all angles and distances which correspond to the EuroSiB geometry. Almost full p/α-discrimination was achieved at all angles (Fig. 1a), in spite of the detector inhomogeneities which have been reported on [1,3]. We conclude that α counting down to a threshold of 2 MeV is possible with the existing detectors and electronics. Meanwhile, the serial production of the frontend electronics is almost finished. Measured detector maps indicate that the detector inhomogeneities result from the floating-zone process of Si-crystal production (see [3] and Fig. 1b). Therfore we intend to equip the critical backward hemisphere of EuroSiB with 300 μm detectors of neutron-transmutation doped Si. First detectors of this type have already been delivered and will be tested in spring '97.

A first test of $\approx$ 2 mm $\times$100 mm^2 Si(Li) detectors produced at Swierk, performed with the source technique described in [3], demonstrated their excellent capability for PSD. However, the thickness of the rear contact (dead layer of $\approx$ 5-10 μm) is still too large for applications where extremely low detection and discrimination thresholds are of importance.

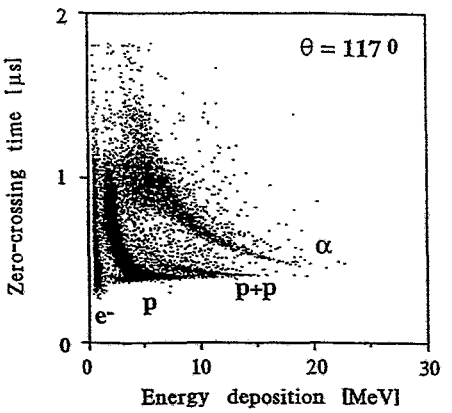

Fig. 1 *PSD plot of a EuroSiB detector measured with the new electronics;*

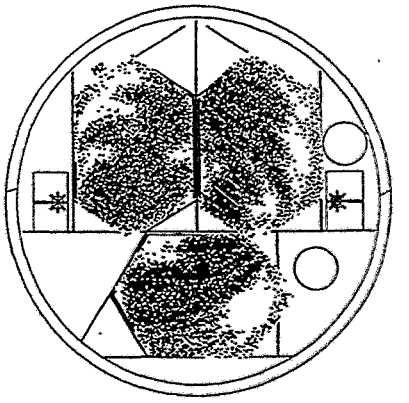

Fig. 2 *"Resistivity maps" of three EuroSiB detectors showing the structure of the inhomogeneities [3].*

[1] *Soltan Institute for Nuclear Studies, Swierk, Poland*
[2] *Hahn-Meitner-Institut Berlin, Bereich F*
[3] *GSI Darmstadt*

References

[1] G. Pausch et al., Annual Reports 1995, FZR-130 (1996), pp. 135-142
[2] G. Pausch et al., IEEE Transact. Nucl. Sci. **43**, No. 3 (1996), pp. 1097-1101
[3] G. Pausch et al., Paper presented at the IEEE Nuclear Science Symposium '96, Anaheim, California, November 1996 (submitted to IEEE Transact. Nucl. Sci.)

Status Report on Off-line Data Analysis for Fragment Identification using Bragg Ionization Chambers [W]

M.N.ANDRONENKO[1], L.N.ANDRONENKO[1], W.NEUBERT, D.M.SELIVERSTOV[1], L.A.VAISHNENE[1]

Bragg Ionization Chambers have been used to detect Intermediate Mass Fragments (IMF) produced in 1 GeV proton-nucleus collisions. The experimental data were received from CAMAC FADC's (20 MHz, 8 bit) via a PC interface [1]. In previous experiments [2] a limited disk memory capacity prevented the storage of the complete pulse shape provided by the FADC's. Therefore, the data were stored on disk using an on-line PC routine which allowed to reduce about 500 sample Bragg curves per sec.. If the particle is stopped in the active chamber volume, this routine calculates the integral, the maximum, the duration and a partial integral of the sample pulse. In a recent experiment the full information

In a recent experiment the full information including the complete pulse shapes was stored on Exabyte tapes. The further analysis becomes feasible only if large computer facilities with sufficient disk space memory are available. On that account, the existing software was installed at the CONVEX C-3220 at FZR and linked with the CERN library, the PAW and the BUFIO packages. Here we demonstrate partly the availability of the software with data obtained with calibration sources of ^{241}Am and ^{244}Cm. The α-energies are separated by 406 keV due to the different energy losses in the window foils.Fig.1 shows some steps of the off-line data analysis.

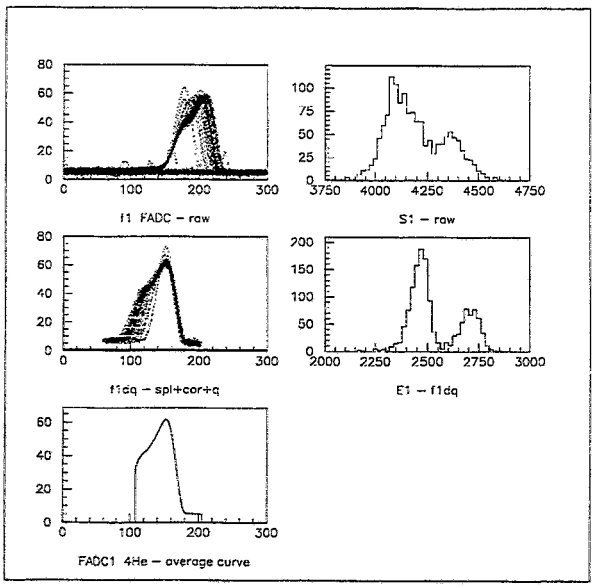

Figure 1: *Pulse shapes and energy resolution*

The upper panels show raw pulse-shapes and the corresponding raw energy spectrum denoted as *S1 raw*. In the first step the pulse shape was splined and corrected for the pulse height defect. Already these corrections lead to an improved energy resolution as shown in the panel labeled *E1-f1dg*. In the following step we generated an *averaged reference signal* by shifting the different Bragg signals each to other to their common flank side (as shown in the bottom). The disposal of this *reference* signal is useful to reject distorted signal shapes which are caused by pile-up's and the offset jitter.

[1] *St.Peterburg Nuclear Physics Institute, 188350 Gatchina, Russia*

References

[1] L.N.Andronenko et al., Nucl.Instr.Meth. **A312** (1992) 467
[2] L.N.Andronenko et al., Preprint PNPI **NP-38** (1994) Nr.1980

Numerical Tests for Democratic Optimization

F.-M. DITTES

Global optimization problems arise in many areas of physics. Typical examples are the determination of ground state energies of disordered or strongly interacting systems with many degrees of freedom or the fitting of experimental data by trial functions depending on many parameters. A unified formulation of these problems can be achieved by considering the quantity to be optimized (e. g. the energy or likelihood) as a "landscape" over the high-dimensional space of parameters on which the system depends. Due to the non-linear coupling of the degrees of freedom characteristic for complex systems, such landscapes are typically characterized by a complicated, "rugged" structure with many local minima and maxima, and finding the *global* optimum of such multipeaked functions is a highly non-trivial task.

Various strategies have been proposed to solve global optimization problems. Most prominent examples are simulated annealing (based on the thermodynamically motivated Metropolis algorithm) and evolutionary or genetic algorithms imitating adaptive processes in biological systems. In a recent publication [1] a novel method for finding optimal solutions to such problems has been proposed. The approach is based on a *simultaneous* optimization of the energy or likelihood of the total system *and* of sub-systems of arbitrary size. Adjusting this simultaneous optimization process in a "democratic" way - so as to give a high weight to small sub-systems ("individuals") while preserving the dominance of global interests - results in an efficient and robust Monte-Carlo algorithm, often performing better than previously used techniques.

In ref. [2], a detailed investigation of the performance of the proposed algorithm for several classes of discrete and continuous-valued optimization problems is given. Concerning discrete systems, a number of *travelling salesman problems* has been investigated. For system sizes around 100, the algorithm turns out to significantly reduce the CPU time necessary for finding the global minimum (as compared to, e. g., simulated annealing). For larger systems, it quickly finds solutions deviating from the global optimum by less than 0.5%. *Spin glasses* form another class of discrete optimization problems. Here, 3 examples have been considered: The $N-k$ model, the low autocorrelation binary sequence model and the Coulomb glass. The typical system size chosen was $N = 500$ and the energies found improved the average energy of local minima by more than 7 standard deviations (of the distribution of energies of local minima).
As an example of continuous-valued problems the *optical multilayer system* (OMS) has been considered. The aim of an OMS is to minimize the reflection at a surface separating two homogeneus media by covering it with a sequence of thin optical layers with given refraction indices. Whereas for any individual wavelength of incoming radiation the reflection coefficient can be minimized by choosing a single $\lambda/4$ layer, low *average* reflection R over a wide range of wavelenghts requires an optimal choice of the widths of many layers. A widely used test example with obvious practical relevance is the design of an OMS for the transition from air to Germanium in the infrared region, for which standard optimization techniques were able to find values down to $R = 0.66\%$. Again, the algorithm proposed above was able to improve this value by more than 30%, finding complicated configurations with $R < 0.46\%$.

References

[1] F.-M. Dittes, Optimization on Rugged Landscapes: A New General Purpose Monte Carlo Approach, Phys. Rev. Lett. **76** (1996) 4651

[2] F.-M. Dittes, Democratic Optimization for Discrete and Continuous Systems, Springer Lecture Notes in Computer Science **1141** (1996) 646

Abstracts of publications

Optimization on Rugged Landscapes: A New General Purpose Monte Carlo Approach
(Phys. Rev. Lett. 76 (1996) 4651)

Dittes, F.M.

Abstract: A new strategy for finding optimal solutions to complex problems with many competing requirements is proposed. It consists in an alternating optimization of the energy, cost, or fitness function of the system itself, and of subsystems of all sizes with an appropriate weight function. For various spin glasses (the $N-k$ model, the low autocorrelation binary sequence model, and the Coulomb glass), and for traveling salesman problems, the corresponding Monte Carlo algorithm is shown to yield results superior to those obtained by previous optimization techniques.

Test of a Scintillating-Fiber Calorimeter for Photons with Energies below 1 GeV
(Nucl. Instruments and Methods in Phys. Research A 382 (1996) 413-418)

Hübner, B., K.-Th. Brinkmann, H. Freiesleben, J.S. Lange, B. Naumann, L. Naumann, A. Schülke

Abstract: An array consisting of scintillating fibers embedded in a lead matrix was tested for use as a calorimeter for showers induced by energetic photons (50 MeV $\leq E_\gamma <$ 1 GeV). Experimentally, its efficiency was found to equal 100% for photon energies in excess of 100 MeV, the energy resolution is $(\sigma/E) \approx 10\%/(E_\gamma/\mathrm{GeV})^{-1/2}$ over the full energy range. Extensive Monte Carlo studies show that the efficiency drops rapidly around $E_\gamma = 40$ MeV. The suitability of cosmic radiation for calibration purposes is demonstrated. Based on these studies design criteria for future arrays can be matched to experimental requirements.

Identification of Light Charged Particles and Heavy Ions in Silicon Detectors by Means of Pulse-Shape Discrimination
(IEEE TRANSACTIONS ON NUCLEAR SCIENCE 43 (1996) 1097)

Pausch, G., H.-G. Ortlepp, W. Bohne, H. Grawe, D. Hilscher, M. Moszyski, D. Wolski, R. Schubart, G. de Angelis, M. de Poli

Abstract: Pulse-shape discrimination with totally depleted Si-detectors in reverse mount has been investigated and shown to be an excellent method of charged-particle identification in the energy range of $\approx$ 2 to 20 AMeV. In test experiments with heavy-ion beams we obtained element identification up to Ti and isotope resolution even for elements heavier than carbon. The promising results and the simplicity of the electronics recommend this technique for applications in multidetector arrays. In particular, small and compact 4π Si balls with relatively low thresholds for charged-particle identification to be combined with 4π neutron detectors or γ arrays can be constructed.

The Response of the Euroball Cluster Detector to γ-Radiation up to 10 MeV
(Nucl. Instr. Meth. A 381 (1996) 462)

Wilhelm, M., J. Eberth, G. Pascovici, E. Radermacher, H.G. Thomas, P. von Brentano, H. Prade, R.M. Lieder

Abstract: The Euroball Cluster detector consists of seven closely packed hexagonal encapsulated germanium detectors which are mounted in a common cryostat and surrounded by a BGO suppression shield. By adding back the Compton scattered events between the seven germanium detectors the detector system behaves similar as a single germanium detector with a volume of 2000 cm^3. The response of this very large germanium detector to γ-rays up to 10 MeV has been measured using a short lived ^{24}Al source produced at the Cologne FN Tandem accelerator. At 10 MeV the efficiency of the Cluster detector is nearly one order of magnitude larger than that of a 30% germanium detector.

PUBLICATIONS AND TALKS

Publications

Baldsiefen, G., M.A. Stoyer, J.A. Cizewski, D.P. McNabb, W. Younes, J.A. Becker, L.A. Bernstein, M.J. Brinkman, L.P. Farris, E.A. Henry, J.R. Hughes, A. Kuhnert, T.F. Wang, B. Cederwall, R.M.Clark, M.A. Deleplanque, R.M. Diamond, P. Fallon, I.Y. Lee, A.O. Macchiavelli, J. Oliveira, F.S. Stephens, J. Burde, D.T. Vo, S. Frauendorf
Shears Bands in ^{193}Pb
(Phys. Rev. C 54 (1996) 1106)

Barz, H.W.
Effects of Nuclear Coulomb Field on Two-Meson Correlations
(Phys. Rev. C 53 (1996) 2536)

Barz, H.W., J.P. Bondorf, D. Idier, I.N. Mishustin
Cluster Production and Correlations in Nuclear Molecular Dynamics
(Phys. Lett. B 382 (1996) 343)

Barz, H.W., B. Kämpfer, Gy. Wolf, W. Bauer
Analysis of Hard Two-Photon Correlations Measured in Heavy-Ion Reactions at Intermediate Energies (Phys. Rev. C 53 (1996) R 553)

Brandolini, F., M. Ionescu-Bujor, N.H. Medina, R.V.Ribas, D. Bazzacco, M. De Poli, P. Pavan, C. Rossi Alvarez, G. de Angelis, S. Lunardi, D. De Acuna, D.R. Napoli, S. Frauendorf
Lifetimes of a Shears Band in ^{139}Sm
Phys. Lett. B 388 (1996) 468)

Brentano, P. von, J. Eberth, J. Enders, L. Esser, R.-D. Herzberg, N. Huxel, H. Meise, P. von Neumann-Cosel, N. Nicolay, N. Pietralla, H. Prade, J. Reif, A. Richter, C. Schlegel, R. Schwengner, S. Skoda, H.G. Thomas, I. Wiedenhöver, G. Winter, A. Zilges
First Observation of the Scissors Mode in a γ-Soft Nucleus: The Case of ^{196}Pt
(Phys. Rev. Lett. 76 (1996) 2029)

Brill, D., P. Beckerle, C. Bormann, E. Schwab, Y. Shin, R. Stock, H. Ströbele, P. Baltes, C. Müntz, H. Oeschler, C. Sturm, A. Wagner, R. Barth, M. Cielak, M. Debowski, E. Grosse, P. Koczo, M. Mang, D. Mikowiec, R. Schicker, P. Senger, B. Kohlmeyer, F. Pühlhofer, J. Speer, K. Völkel, W. Waluś
Study of the Out-Of-Plane Emission of Protons and Light Fragments in Symmetric Heavy-Ion Collisions
(Z. Phys. A 355 (1996) 61)

Büscher, M., R. Eßer, A. Franzen, L. v. Horn, D. Kopyto, H. Ohm, H. Seyfarth, K. Sistemich, H. Müller, B. Prietzschk, B. Rimarzig, C. Schneider, C. Schneidereit, A. Akindinov, M. Chumakov, V. Demechin, V. Ergakov, A. Gerasimov, V. Goryachev, Y. Kiselev, V. Kostromin, A.A. Sibirtsev, V. Sopov, V. Tchernyshev, V. Kruglov, A. Petrus, V. Koptev, S. Mikirtychyants
K $^+$-Meson Production in pBe Interactions at $T_p = 2.9$ GeV
(Z. Phys. A 355 (1996) 93)

Debowski, M., R. Barth, M. Boivin, Y. Le Bornec, M. Cieślak, M.P. Comets, P. Courtat, R. Gacougnolle, E. Grosse, T. Kirchner, J.M. Martin, D. Miśkowiec, C. Müntz, E. Schwab, P. Senger, C. Sturm, B. Tatischeff, A. Wagner, W. Waluś, N. Willis, R. Wurzinger, J. Yonnet, A. Zghiche
Subthreshold K^+ Production in Proton-Nucleus Collisions
(Z. Phys. A 356 (1996) 313)

Dittes, F.M.
Optimization on Rugged Landscapes: A New General Purpose Monte Carlo Approach
(Phys. Rev. Lett. 76 (1996) 4651)

Dönau, F., S. Frauendorf, J. Meng
Can Hexadecapole Deformation Lead to ΔI=2 Staggering in Superdeformed Bands?
(Phys. Lett. B 387 (1996) 667)

Elmér, R., M. Berg, L. Carlén, B. Jakobsson, B. Norén, A. Oskarsson, G. Ericsson, J. Julien, T.-F. Thorsteinsen, M. Guttormsen, G. Løvhøiden, V. Bellini, E. Grosse, C. Müntz, P. Senger, L. Westerberg
K^+ Emission in Symmetric Heavy Ion Reactions at Subthreshold Energies
(Phys. Rev. Lett. 77 (1996) 4884)

Enghardt, W.
Positronen-Emissions-Tomographie bei der Schwerionentherapie
(Phys. Bl. 52 (1996) 874)

Frauendorf, S., J. Reif, G. Winter
Shell-Model Study of Shears Bands in Light Pb Nuclei
(Nucl. Phys. A 601 (1996) 41)

Frauendorf, S., J. Meng
Interpretation and Quality of the Tilted Axis Cranking Approximation
(Z. Phys. A 356 (1996) 263)

Frauendorf, S., V.V. Pashkevich
General Axial Shapes of Sodium Clusters
(Ann. Physik 5 (1996) 34)

Frauendorf, S. , V.V. Pashkevich
Shapes and Free Energies of Molten Sodium Clusters
(Surface Review and Letters 3 (1996) 241)

Frauendorf, S., V.V. Pashkevich, S.M. Reimann
Magnetic Properties of Sodium Clusters
(Surface Review and Letters 3 (1996) 25)

Freudenberger, J., M. Galemann, H. Genz, L. Groening, P. Hoffmann-Stascheck, V.L. Morokhovskii, V.V. Morokhovskii, U. Nething, H. Prade, A. Richter, J.P.F. Sellschop, R. Zahn
Experimental Determination of the Linewidth of Parametric X-ray Radiation at Electron Energies Below 10 MeV
(Nucl. Instr. Meth. B 115 (1996) 408)

Freudenberger, J., H. Genz, L. Groening, P. Hoffmann-Stascheck, W. Knüpfer, V.L. Morokhovskii, V.V. Morokhovskii, U. Nething, A. Richter, J.P.F. Sellschop
Channeling Radiation and Parametric X-radiation at Electron Energies below 10 MeV
(Nucl. Instr. Meth. in Phys. Res. B 119 (1996) 123)

Genz, H., L. Groening, P. Hoffmann-Stascheck, A. Richter, M. Höfer, J. Hormes, U. Nething, J.P.F. Sellschop, C. Toepffer, M. Weber
Channeling Radiation of Electrons in Natural Diamond Crystals and their Coherence and Occupation Lengths
(Phys. Rev. B 53 (1996) 8922)

Goldenbaum, F., W. Bohne, J. Eades, T. v. Egidy, P. Figuera, H. Fuchs, J. Galin, Ye.S. Golubeva, K. Gulda, D. Hilscher, A.S. Iljinov, U. Jahnke, J. Jastrzebski, W. Kurcewicz, B. Lott, M. Morjean, G. Pausch, A. Péghaire, L. Pienkowski, D. Polster, S. Proschitzki, B. Quednau, H. Rossner, S. Schmid, W. Schmid, P. Ziem Heating of Nuclei with Energetic Antiprotons
(Phys. Rev. Lett. 77 (1996) 1230)

Gulamov, T.I., A.I. Titov, B. Kämpfer
Asymmetry of the Dielectron Emission Rate in an Isospin-Asymmetric Pion Medium
(Phys. Lett. B 372 (1996) 187)

Gulamov, T.I., A.I. Titov, B. Kämpfer
Neutral ρ-Meson Properties in an Isospin-Asymmetric Pion Medium (Yad. Fiz. 59 (1996) 727)

Harder, A., F. Dönau, K.P. Lieb, R.A. Cunningham, W. Gelletly, C.J. Groß, F. Hannachi, M.K. Kabadiyski, H.A. Roth, D. Rudolph, J. Simpson, Ö. Skeppstedt, B.J. Varley, D.D. Warner
A New Type of Band Crossing at Large Deformation
(Phys. Lett. B 374 (1996) 277)

Hübner, B., K.-Th. Brinkmann, H. Freiesleben, J.S. Lange, B. Naumann, L. Naumann, A. Schülke
Test of a Scintillating-Fiber Calorimeter for Photons with Energies below 1 GeV
(Nucl. Instruments and Methods in Phys. Research A 382 (1996) 413-418)

Kaptari, L.P., A.Yu. Umnikov, S.G. Bondarenko, K.Yu. Kazakov, F.C. Khanna, B. Kämpfer
Bethe-Salpeter Amplitudes and Static Properties of the Deuteron
(Phys. Rev. C 54 (1996) 986)

Käubler, L., H. Schnare, D.B. Fossan, A.V.Afanasjev, W. Andrejtscheff, R.G. Allat, J. de Graaf, H. Grawe, I.M. Hibbert, I.Y. Lee, A.O. Macchiavelli, N. O'Brien, K.-H. Mayer, E.S. Paul, H. Prade, I. Ragnarsson, J. Reif, R. Schubart, R. Schwengner, I. Thorslund, P. Vaska, R. Wadswoth, G. Winter
Collective Structures and Smooth Band Termination in ^{109}Sn
(Z. Phys. A 356 (1996) 235)

Kolomeitsev, E.E., D.N. Voskresensky, B. Kämpfer
Hot and Dense Pion Gas with Finite Chemical Potential
(Acta Physica Polonica B 27 (11) (1996) 3263)

Kolomeitsev, E.E., D.N. Voskresensky and B. Kämpfer
The Impact of Kaon Polarization in Nuclear Matter on the K^- Production in Heavy-Ion Collisions
(Int. J. Mod. Phys. E5 (1996) 313)

Kuzmenko, N.K., V.O. Nesterenko, S. Frauendorf, V.V. Pashkevich
Particle-Number Projecting Method for Description of Pairing Effects in Metal Clusters

(Il Nuovo Cimento D 18 (1996) 645)

Müller, H.
Are Missing-Mass Measurements the Key for Understanding Subthreshold Particle Production?
(Z. Phys. A 355 (1996) 223)

Neffgen, M., G. Baldsiefen, S. Frauendorf, H. Grawe, J. Heese, H. Hübel, H. Kluge, A. Korichi, W. Korten, K.H. Maier, D. Mehta, J. Meng, N. Nenoff, M. Piiparinen, M. Schönhofer, R. Schubart, U.J. van Severen, N. Singh, G. Sletten, B.V. Thirumala Rao, P. Willsau
Lifetimes of Shears Bands in ^{199}Pb
(Nucl. Phys. A 595 (1995) 499)

Pausch, G., H.-G. Ortlepp, W. Bohne, H. Grawe, D. Hilscher, M. Moszyski, D. Wolski, R. Schubart, G. de Angelis, M. de Poli
Identification of Light Charged Particles and Heavy Ions in Silicon Detectors by Means of Pulse-Shape Discrimination
(IEEE TRANSACTIONS ON NUCLEAR SCIENCE 43 (1996) 1097)

Pawelke, J., L. Byars, W. Enghardt, W.D. Fromm, H. Geissel, B.G. Hasch, K. Lauckner, P. Manfraß , D. Schardt, M. Sobiella
The Investigation of Different Cameras for In-Beam PET Imaging
(Phys. Med. Biol. 41 (1996) 279)

Peshier, A., B. Kämpfer, O.P. Pavlenko, G. Soff
Massive Quasiparticle Model of the SU(3) Gluon Plasma
(Phys. Rev. D 54 (1996) 2399)

Persson, E., T. Gorin, I. Rotter
Decay Rates of Resonance States at High Level Density
(Phys. Rev. E 54 (1996) 3339)

Persson, E., M. Müller, I. Rotter
Resonance Phenomena Near Threshold
(Phys. Rev. C 53 (1996) 3002)

Radermacher, E., M. Wilhelm, S. Albers, J. Eberth, N. Nicolay, H.G. Thomas, H. Tiesler, P. von Brentano, R. Schwengner, S. Skoda, G. Winter, K.H. Maier
The γ-Decay of Particle-Hole states in ^{208}Pb Using the Euroball Cluster Detector
(Nucl. Phys. A 597 (1996) 408)

Reimann, S.M., S. Frauendorf
Potential-Energy Surfaces of Sodium Clusters with Quadrupole, Hexadecapole, and Triaxial Deformations
(Surface Review and Letters 3 (1996) 25)

Rubehn, Th., R. Bassini, M. Begemann-Blaich, Th. Blaich, A. Ferrero, C. Groß, G. Imm, I. Iori, G.J. Kunde, W.D. Kunze, V. Lindenstruth, U. Lynen, T. Möhlenkamp, L.G. Moretto, W.F.J. Müller, B. Ocker, J. Pochodzalla, G. Raciti, S. Reito, H. Sann, A. Schüttauf, W. Seidel, V. Serfling, W. Trautmann, A. Trzcinski, G. Verde, A. Wörner, E. Zude, B. Zwieglinski
Total and Nuclear Fission Cross Sections of ^{238}U at Relativistic Energie
(Phys. Rev. C 53 (1996) 3143)

Rubehn, Th., R. Bassini, M. Begemann-Blaich, Th. Blaich, A. Ferrero, C. Groß, G. Imm, I. Iori, G.J. Kunde, W.D. Kunze, V. Lindenstruth, U. Lynen, T. Möhlenkamp, L.G. Moretto, W.F.J. Müller, B. Ocker, J. Pochodzalla, G. Raciti, S. Reito, H. Sann, A. Schüttauf, W. Seidel, V. Serfling, W. Trautmann, A. Trzcinski, G. Verde, A. Wörner, E. Zude, B. Zwieglinski
Charge Pickup of ^{238}U at Relativistic Energies
(Phys. Rev. C 52 (1996) 993)

Roderburg, E., R. Bilger, A. Böhm, K.-T. Brinkmann, H. Clement, P. Cloth, M. Dahmen, M. Dellert, V. Drüke, H. Dutz, W. Eyrich, H. Freiesleben, D. Filges, M. Fritsch, R. Geyer, A. Hassan, J. Hauffe, J. Hays, P. Hermanowski, B. Hübner, P. Jahn, K. Kilian, H. Koch, R.A. Kraft, J. Krug, J. Kress, E. Kuhlmann, S. Lange, H. Matthäy, A. Metzger, W. Meyer, P. Michel, K. Möller, M. Moosburger, H.P. Morsch, C. Nake, B. Naumann, L. Naumann, N. Paul, M. Rogge, C. Rohloff, A. Schamlott, A. Schülke, T. Sefzick, E. Sinde, R. Sperl, M. Steinke, F. Stinzing, P. Turek, G.J. Wagner, D. Wallom, S. Wirth, U. Zielinsky
Studies of *pp* and *pd* Interactions with the Time of Flight Spectrometer at COSY
(Acta Physica Polonica B Vol.27 (1996))

Schnare, H., D.R. LaFosse, D.B. Fossan, J.R. Hughes, P. Vaska, K. Hauschild, I.M. Hibbert, R. Wadswoth, V.P. Janzen, D.C. Radford, S.M. Mullins, C.W. Beausang, E.S. Paul, J. DeGraaf, I.-Y. Lee, A.O. Macchiavelli, A.V. Afanasjev, I. Ragnarsson
Smooth Termination of Intruder Bands in Sb
(Phys. Rev. C 54 (1996) 1598

Schüttauf, A., W.D. Kunze, A. Wörner, M. Begemann-Blaich, Th. Blaich, D.R. Bowman, R.J. Charity, A. Cosmo, A. Ferrero, C.K. Gelbke, C. Groß, W.C. Hsi, J. Hubele, G. Immé, I. Iori, J. Kempter, P. Kreutz, G.J. Kunde, V. Lindenstruth, M.A. Lisa, W.G. Lynch, U. Lynen, M. Mang, T. Möhlenkamp, A. Moroni, W.F.J. Müller, M. Neumann, B. Ockere, C.A. Ogilvie, G.F. Peaslee, J. Pochodzalla, G. Raciti, F. Rosenberger, Th. Rubehn, H. Sann, C. Schwarz, W. Seidel, V. Serfling, L.G. Sobotka, J. Stroth, L. Stuttge, S. Tomasevic, W. Trautmann, A. Trzcinski, M.B. Tsang, A.Tucholski, G. Verde, C.W. Williams, E. Zude, B. Zwieglinski
Universality of Spectator Fragmentation at Relativistic Bombarding Energies
(Nucl. Phys. A 607 (1996) 457)

Starosta, K., Ch. Droste, T. Morek, J. Srebrny, D.B. Fossan, D.R. LaFosse, H. Schnare, I. Thorslund, P. Vaska, M.P. Waring, W. Satula and S.G. Rohoziski, R. Wyss, I.M. Hibbert, R. Wadsworth, K. Hauschild, C.W. Beausang, S.A. Forbes, P.J. Nolan, E.S. Paul
Band Structure of the odd-even ^{125}La, ^{127}La Nuclei
(Phys. Rev. C 53 (1996) 137)

Thorslund, I., D.B. Fossan, D.R. LaFosse, H. Schnare, K. Hauschild, I.M. Hibbert, S.M. Mullins, E.S. Paul, I. Ragnarsson, J.M. Sears, P. Vaska, R. Wadsworth
Intruder Bands in ^{114}Te: Smooth Band Termination
(Phys. Rev. C 52 (1995) R2839)

Titov, A.I., T.I. Gulamov, B. Kämpfer
ρ-Meson Self-Energy and Dielectron Emissivity in an Isospin-Asymmetric Pion Medium
(Phys. Rev. D 53 (1996) 3770)

Titov, A.I., B. Kämpfer, B.L. Reznik, V. Shklyar
The Reaction $NN \to NN \to_\gamma$ in the 1 GeV Region within an Effective One-Boson Exchange Model
(Phys. Lett. B 372 (1996) 15

Wadsworth, R., C.W.Beausang, M. Cromaz, J. DeGraaf, T.E. Drake, D.B. Fossan, S. Flibotte, A. Galindo-Uribarri, K. Hauschild, I.M. Hibbert, G. Hackman, J.R. Hughes, V.P. Janzen, D.R. LaFosse, S.M. Mullins, E.S. Paul, D.C. Radford, H. Schnare, P. Vaska, D. Ward, J.N. Wilson, I. Ragnarsson
Smooth Band Termination in ^{108}Sn (Phys. Rev. C 53 (1996) 2763)

Wilhelm, M., J. Eberth, G. Pascovici, E. Radermacher, H.G. Thomas, P. von Brentano, H. Prade, R.M. Lieder
The Response of the Euroball Cluster Detector to γ-Radiation up to 10 MeV
(Nucl. Instr. Meth. A 381 (1996) 462)

Conference Contributions and Laboratory Reports

Baldsiefen, G., M.A. Stoyer, J.A. Cizewski, D.P. McNabb, W. Younes, J.A. Becker, L.A. Bernstein, M.J. Brinkman, L.P. Farris, E.A. Henry, J.R. Hughes, A. Kuhnert, T.F. Wang, B. Cederwall, R.M. Clark, M.A. Deleplanque, R.M. Diamond, P. Fallon, I.Y. Lee, A.O. Macchiavelli, J. Oliveira, F.S. Stephens, J. Burde, D.T. Vo, S. Frauendorf:
Shears Banden im ^{193}Pb;
Verhandl. DPG (VI), 31 (1996) 978

Barz, H.W.,:
Effects of Nuclear Coulomb Field on Two-Meson Correlations;
FZR-125 (1996)

Barz, H.W., J.P. Bondorf, D. Idier, I.N. Mishustin:
Fragment-Fragment Correlations and Fragment Flow in Heavy Ion Collisions Described within Molecular Dynamics;
Proc. of CRIS'96, 1st Catania Relativistic Ion Studies, Acicastello, Italy, May 1996, World Scientific "Critical phenomena and collective observables", 1996, p. 305

Barz, H.W., D. Idier, J.P. Bondorf, I.N. Mishustin:
Beschreibung von Fragment-Fragment-Korrelationen in Schwerionenstößen bei mittleren Energien in einem molekulardynamischen Modell; Verhandl. DPG (VI), 31 (1996) 915

Beinker, M.W., B. Kämpfer, G. Soff:
Erzeugung von SUSY-Teilchen in ultrarelativistischen Schwerionenstößen; Verhandl. DPG (VI), 31 (1996) 985

Biegansky, J., R. Kotte, J. Mösner, W. Neubert, D. Wohlfarth:
Geschwindigkeitsverteilungen geladener Teilchen aus zentralen Kollisionen schwerer Ionen bei Strahlenergien im Bereich von 100 bis 2000 AMeV;
Verhandl. DPG (VI), 31 (1996) 914

Bohne, W., J. Eades, T. von Egidy, P. Figuera, H. Fuchs, J. Gallin, F. Goldenbaum, Ye.S. Golubeva, K. Gulda, F.J. Hartmann, D. Hilscher, A.S. Iljinov, U. Jahnke, J. Jastrzebski, W. Kurcewicz, B. Lott, M. Morean, G. Pausch, A. Peghaire, L. Pienkowski, D. Polster, S. Proschitzki, B. Quednau, H. Rossner, S. Schmid, W. Schmid, P. Ziem:
Excitation of Heavy Nuclei with Energetic Antiprotons;
Verhandl. DPG (VI), 31 (1996) 952

Bunakov, V.E., I. Rotter:
Conditions of resonance trapping in nuclei;
Proc. of the Int. Symp. on Interaction of Neutrons with Nuclei, Dubna, Russia, May 1996

Büscher, M., R. Esser, A. Franzen, L. v. Horn, D. Kopyto, H. Ohm, H. Seyfarth, K. Sistemich, H. Müller, B. Prietzschk, B. Rimarzig, C. Schneider, C. Schneidereit, A. Akindinov, M. Chumakov, V. Demechin, V. Goryachev, Y. Kiselev, V. Kostromin, V. Sopov, V. Tchernyshev, V. Kruglov, A. Petrus, A. Sibirtsev, V. Koptev, S. Mikirtychyants:
K^+-Meson Production in pBe Interactions at $T_p = 2.9$ GeV;
Verhandl. DPG (VI), 31 (1996) 1014

Büttig, H., F. Dönau, F. Gabriel, P. Gippner, W. Glaser, E. Grosse, H. Guratzsch, U. Nething, F. Pobell, H. Prade, D. Pröhl, K.D. Schilling, R. Schlenck, W. Seidel, P. vom Stein, R. Zahn:
The Project of a Far-Infrared FEL at the Rossendorf Electron Source ELBE;

Poster, 18th Int. Free Electron Laser Conf., Rom, Italy, Aug. 1996, Book of Abstracts

Dönau, F., A. Harder, K.P. Lieb, D. Rudolph:
Die Bandenkreuzung in ^{77}Rb - ein ungewöhnlicher Fall;
Verhandl. DPG (VI), 31 (1996) 903

von Egidy, T., P. Figuera, J. Galin, F. Goldenbaum, M. Hasinoff, D. Hilscher, U. Jahnke, M. Krause, V. Kurcewicz, X. Ledoux, B. Lott, M. Manrique de Lara, G. Pausch, L. Pienkowski, B. Quednau, W. Schott, U. Schröder, J. Toke:
Measurement of Inclusive n Spectra Produced by Fast $\bar{p}$ Annihilation at Nuclei;
Verhandl. DPG (VI), 31 (1996) 952

Enders, J., P. von Brentano, J. Eberth, R.-D. Herzberg, N. Huxel, P. von Neumann-Cosel, N. Nicolay, N. Pietralla, H. Prade, J. Reif, A. Richter, C. Schlegel, R. Schwengner, S. Skoda, H.G. Thomas, I. Wiedenhöver, G. Winter, A. Zilges:
Anregung eines $|2^+ \otimes 3^-; 1^-\rangle$ Zweiphonon-Zustandes in ^{52}Cr mit resonanter Photonenstreuung;
Verhandl. DPG (VI), 31 (1996) 87

Enghardt, W., B.G. Hasch, K. Lauckner, J. Pawelke, M. Sobiella, L. Byars:
A Positron Emission Tomograph for In-Situ Monotoring of Heavy Ion Tumour Therapy;
ECAT Technical Users Meeting, Stockholm, Sweden, apr. 1996, Book of Abstracts, p. A-42

Frauendorf, S.:
Residual Interaction and Spin Orientation in Rotating Nuclei;
Proc. of the Workshop on Gammssphere Physics, Ernest Orlando Lawrence Berkeley National Laboratory, Dec. 1995, World Scientific Pub. (1996) p. 27)

Frauendorf, S., V.V. Pashkevich:
Thermodynamics and Decay of Liquid Alkali Clusters;
Proc. of the NATO Advanced Study Institute, Int. School of Solid State Physics, 6th Course: Large Clusters of Atoms and Molecules, Erice, Sicily, June 19 - 29, 1995, Kluwer Acad. Publ, NATO ASI Series E, vol. 313 (1996) p. 201

Freudenberger, J., H. Genz, V.L. Morokhovskii, V.V. Morokhovskii, U. Nething, A. Richter, J.P.F. Sellschop, R. Zahn:
Intensität parametrischer Röntgenstrahlung;
Verhandlungen DPG (VI), 31 (1996) 1030

Gorin, T., F.-M. Dittes, M. Müller, I. Rotter:
Intensitätsgewichtete Maße für Spektren offener Quantensysteme;
Verhandl. DPG (VI), 31 (1996) 878;
Poster, Frühjahrstagung Arbeitskreis Festkörperphysik, Regensburg, Mar. 1996

Gorin, T., F.M. Dittes, M. Müller, I. Rotter:
Intensitätsgewichtete Maße für Spektren offener Quantensysteme;
Frühjahrstagung Arbeitskreis Festkörperphysik, Regensburg, Mar. 1996, p. 1281

Gorin, T., F.M. Dittes, M. Müller, I. Rotter:
Correlations in the Spectra of Open Quantum Systems;
164. WE-Heraeus-Seminar Quantum Chaos and Dissipation, Günzburg, Germany, Sep. 1996, p. 4 and Poster

Gorin, T., F.M. Dittes, M. Müller, I. Rotter:
Intensity Weighted Measures for Spectra of Open Quantum Systems;
European Research Conf. Nuclear Physics: Chaotic Phenomena in Nuclear Physics, Crete (Greece), Sep./Oct. 1996, Contributions, p. 24 and Poster

Grosse, E., B. Kämpfer:
Internal Workshop on Kaon Production;
FZR-150 (1996)

Harder, A., T.D. Johnson, A. Jungclaus, D. Kast, K.P. Lieb, D. Rudolph, M. Weiszflog, G. Winter und die NORDBALL-Kollaboration:
Messung von Lebensdauern und Sidefeeding-Zeiten in der Reaktion ^{40}Ca(^{40}Ca,3p)^{77}Rb;
Verhandl. DPG (VI), 31 (1996) 903

Hentschel, M., B. Kämpfer, O.P. Pavlenko, K. Redlich, G. Soff:
Diphoton Rates from Thermalized Matter Resulting in Ultra-Relativistic Heavy-Ion Collisions;
FZR-142 (1996)
GSI-Preprint-96-37 (1996)

Herbach, C.-M., H.-G. Ortlepp, P. Gippner, D.V. Kamanin, A. Matthies, G. Pausch, Yu.E. Penionzhkevich, G. Renz, K.D. Schilling, W. Wagner (für die FOBOS-Kollaboration):
Spaltung nach unvollständiger Fusion im Fermi-Energie-Bereich;
Verhandl. DPG (VI), 31 (1996) 849

Herbach, C.-M., H.-G. Ortlepp, P. Gippner, D.V. Kamanin, Yu.E. Penionzhkevich, G. Renz, K.D. Schilling, O.V. Strekalovsky, V.G. Tichtchenko, W. Wagner and the FOBOS-collaboration:
Decay Study of Hot Nuclei below the Multifragmentation Threshold with the FOBOS Detector at Dubna;
Int. Research Workshop "Heavy Ion Physics at Low, Intermediate and Relativistic Energies Using 4 Detectors;
Poiana Brasov, Romania, Oct. 1996

Herbach, C.-M., H.-G. Ortlepp, P. Gippner, D.V. Kamanin, Yu.E. Penionzhkevich, G. Renz, K.D. Schilling, O.V. Strekalovsky, V.G. Tichtchenko, W. Wagner and the FOBOS-collaboration:
Decay Study of Hot Nuclei below the Multifragmentation Threshold with the FOBOS Detector at Dubna;
ZfK-159 (1996)

Herzberg, R.-D., P. von Brentano, J. Eberth, J. Enders, L. Esser, R. Fischer, C. Fransen, N. Huxel, T. Klemme, H. Meise, P. von Neumann-Cosel, N. Nicolay, M. Phillip, N. Pietralla, H. Prade, J. Reif, A. Richter, C. Schlegel, R. Schwengner, S. Skoda, O. Stuch, H.G. Thomas, I. Wiedenhoever, G. Winter, A. Zilges:
Photonenstreuung an ^{140}Ce mit einem EUROBALL CLUSTER Detektor;
Verhandl. DPG (VI), 31 (1996) 995

Hinz, R., L. Byars, W. Enghardt, B.G. Hasch, K. Lauckner, J. Pawelke, M. Sobiella:
A Method for In-Vivo Treatment Plan Verification of Heavy-Ion Tumour Therapy by Positron Emission Tomography;
V. Int. Conf. on Application of Physics in Medicine and Biology, Trieste, Italy, International Centre of Theoretical Physics, Sep. 1996

Physica Medica XII (1996) 157

von Horn, L., D. Gotta, H. Ohm, Th. Kirchner, H. Müller, C. Schneider, V. Kruglov:
Clustering Phenomena and the Effect on the Position Resolution of a Muliwire Proportional Chamber to be Used at the ANKE Spectrometer at COSY Jülich;
Verhandl. DPG (VI), 31 (1996) 868

Hübner, B., K.-Th. Brinkmann, H. Freiesleben, J.S. Lange, B. Naumann, L. Naumann:
Test eines Spaghetti-Kalorimeters für den Photonennachweis am COSY-TOF-Spektrometer;
Verhandl. DPG (VI), 31 (1996) 1000

Huxel, N., P. von Brentano, J. Eberth, J. Enders, R.-D. Herzberg, von Neumann-Cosel, N. Nicolay, N. Pietralla, H. Prade, J. Reif, A. Richter, C. Schlegel, R. Schwengner, S. Skoda, H.G. Thomas, I.V. Denhöver, G. Winter, A. Zilges:
Die Scissors Mode in den ungeraden Kernen ^{165}Ho und ^{169}Tm;
Verhandl. DPG (VI), 31 (1996) 976

Imme, G., V. Maddalena, C. Nociforo, G. Raciti, G. Riccobene, F.P. Romano, A. Saija, C. Sfienti, G. Verde, M. Begemann-Blaich, S. Fritz, C. Grofl, U. Kleinevofl, U. Lynen, M. Mahl, W.F.J. Müller, B. Ocker, T. Odeh, M. Schnittker, C. Schwarz, V. Serfling, W. Trautmann, A. Wörner, H.Xi, T. Möhlenkamp, W. Seidel, W.D. Kunze, A. Schüttauf, J. Pochodzalla, G.J. Kunde, S. Gaff, R. Bassini, I. Iori, A. Moroni, F. Petruzzelli, A. Trzcinski, B. Zwieglinski:
Last Minute from ALADIN: Temperature Measurements in Au + Au Reactions at Relativistic Energies;
GSI-Preprint-96-30 (1996)

Jahnke, U., W. Bohne, J. Eades, T. v. Egidy, P. Figuera, H. Fuchs, J. Galin, F. Goldenbaum, Ye.S. Golubeva, K. Gulda, F.J. Hartmann, D. Hilscher, A.S. Iljinov, J. Jastrzebski, W. Kurcewicz, B. Lott, M. Morjean, G. Pausch, A. Pèghaire, L. Pienkowski, D. Polster, S. Proschitzki, B. Quednau, H. Rossner, S. Schmid, W. Schmid:
Production and Decay of Hot Nuclei Following Antiproton Annihilation at Rest and in Flight;
III Int. Conf. on Nucleon-Antinucleon Physics (NAN '95), Inst. of Theoret. and Experim. Physics (ITEP), Moscow, Sep. 1995

Kacharava, A.K., V.I. Komarov, A.V. Kulikov, M.S. Nioradze, G.G. Macharashvili, Z.R. Menteshashvili, H. Müller, A.Yu. Petrus, H. Seyfarth:
Simulation of Deuteron Break-Up at $T_p = 2.5$ GeV for ANKE Facility;
Dubna-Preprint E1-96-270 (1996)

Kamanin, D.V., C.-M. Herbach, H.-G. Ortlepp, W. Wagner:
Spectroscopy of Light Charged Particles at the FOBOS Set-Up;
Third Int. Conf. on Dynamical Aspects of Nuclear Fission, Casta-Papirnicka, Slovak Republic, Aug./Sep. 1996

Kämpfer, B.:
Evidence for Low Freeze-Out Temperature and Large Transverse Flow in Central Collisions of Pb + Pb at 158 AGeV;
FZR-149 (1996)

Kämpfer, B., O.P. Pavlenko, A. Peshier, M. Hentschel, G. Soff:
Estimates of Electromagnetic Signals from Deconfined Matter Produced in Ultrarelativistic

Heavy-Ion Collisions;
FZR-128 (1996)

Kämpfer, B., O.P. Pavlenko:
Thermal Dilepton and Open Charm Signals Versus Hard Initial Yields in Heavy-Ion Collisions at RHIC and LHC Energies;
FZR-144 (1996)

Kämpfer, B., A. Peshier, M. Hentschel, G. Soff, O.P. Pavlenko:
Electromagnetic Signals from Deconfined Matter Resulting from Ultrarelativistic Heavy-Ion Collisions;
FZR-136 (1996)

Kaptari, L.P., A.Yu. Umnikov, S.G. Bondarenko, K.Yu. Kazakov, F.C. Khanna, B. Kämpfer:
Bethe-Salpeter Amplitudes and Static Properties of the Deuteron;
FZR-134 (1996)

Kaptari, L.P., B. Kämpfer, S.M. Dorkin, S.S.Semikh:
Relativistic Description of Exclusive Deuteron Break-up Reactions;
FZR-161 (1996)

Käubler, L., H. Schnare, D.B. Fossan et al., J. de Graaf, A. Macchiavelli et al., E.S. Paul et al., J. Reif, R. Schwengner, R. Wadswoth et al.:
Search for Smooth Band Termination in ^{109}Sn;
Verhandl. DPG (VI), 31 (1996) 927

Kirchner, T.:
Meson Production in the $\vec{p}$+d$\rightarrow^3$He+X Reaction at SPES 3 at E_{inc} = 1450 MeV;
Proc. of MESON '96 Workshop, Cracow, Poland, May 1996,
APOBB B 27 (11) (1996) p. 2949

Kirchner, T., H. Müller, C. Schneider, C. Schneidereit:
Anwendung des Rossendorf Collision Modells auf p, d und α induzierte K^+ Produktion an der Schwelle;
Verhandl. DPG (VI), 31 (1996) S. ?

Kolomeitsev, E., D. Voskresensky, B. Kämpfer:
Pionengas mit erhaltener Teilchenzahl;
Verhandl. DPG (VI), 31 (1996) 986

Kolomeitsev, E., D.N. Voskresensky, B. Kämpfer:
Hot and Dense Pion Gas with Finite Chemical Potential;
Proc. of the Int. Workshop MESON'96, Cracow, Poland, May 1996

Kotte, R., J. Biegansky, J. Mösner, W. Neubert, C. Plettner, D. Wohlfahrt and the FOPI Collaboration:
Proton-Proton Correlations in Central Collisions of Ni+Ni at 1.93AGeV and the Space-Time Extent of the Emission Source;
Proc. Int. Workshop on Heavy Ion Physics at Low, Intermediate and Relativistic Energies Using 4 Detectors, Poiana Brasov, Romania, Oct. 1996

Kotte, R., J. Biegansky, J. Mösner, W. Neubert, D. Wohlfarth:
Geschwindigkeitsverteilungen geladener Teilchen aus zentralen Kollisionen schwerer Ionen bei Strahlenergien im Bereich von 100 bis 2000 A GeV;
Verhandl. DPG (VI), 31 (1996) 914

Kotte, R., J. Biegansky, J. Mösner, W. Neubert, D. Wohlfarth and the FOPI collaboration:
Phase Space Distributions of Charged Particles from Central Collisions of Au+Au between 250 and 1050 MeV per nucleon;
GSI-Report-96-1 (1996) 38

Lane, G.J., D.B. Fossan, I. Thorslund, P. Vaska, R.G.Allat, E.S. Paul, I.M. Hibbert, N. O'Brien, R.Wadsworth, L. Käubler, H. Schnare, J. de Graaf, J. Simpson, I.Y. Lee, A.O. Macchiavelli, D.J. Blumenthal, C.N. Davids, C.J. Lister, D.Seweryniak, A.V.Afanasjev, I. Ragnarsson:
Excited States in ^{110}Sb and ^{111}Te: Intruders and Smooth Termination;
Abstract, Conf. on Nuclear Structure at the Limits, Argonne National Laboratory, Jul. 1996

Lane, G.J., D.B.Fossan, I. Thorslund, P. Vaska, I.M. Hibbert, N. O'Brien, R. Wadsworth, R.G. Allatt, E.S. Paul, L. Kubler, H. Schnare, J. de Graaf, J. Simpson, I.Y. Lee, A.O. Macchiavelli, D.J. Blumenthal, C.N. Davids, C.J. Lister, D.Seweryniak:
Intruder Bands in ^{110}Sb;
Meeting of the American Physical Society, Apr. 1996

Lauckner, K., W. Enghardt, B.G. Hasch, R. Hinz, J. Pawelke, M. Sobiella, R. Freyer:
Ein Verfahren zur in-vivo Kontrolle der Bestrahlungsplanung bei der Schwerionen-Tumortherapie mittels Positronen-Emissions-Tomographie;
Gemeinsame Jahrestagung der Deutschen, der Österreichischen und der Schweizerischen Gesellschaft für biomedizinische Technik, Zürich, Schweiz, Sep. 1996
Biomedizinische Technik 41 (1996) Ergänzungsband 1, 194-195

Lauckner, K., W. Enghardt, B.G. Hasch, R. Hinz, J. Pawelke, M. Sobiella:
Ein iterativer Rekonstruktionsalgorithmus für PET bei der in-vivo Kontrolle der Schwerionen-Tumortherapie;
Poster, Aachener Workshop Bildverarbeitung für die Medizin, Algorithmen-Systeme-Anwendungen, Aachen, Nov. 1996

Michel, P., K. Müller, A. Schamlott, A. Schülke und COSY-TOF-Kollaboration:
Methodische Untersuchungen zum Aufbau der COSY-TOF-Barrelsegmente;
Verhandl. DPG (VI), 31 (1996) 894

Mohren, S., G. Augustinski, G. Berek, A. Gobbi, K.H. Hermann, N. Herrmann, Z. Fodor, J. Keczkemeti, R. Kotte, Y. Leifels, M. Marquardt, J. Mösner, W. Neubert, C. Schröder, D. Schüll, Z. Seres, D. Wohlfahrt, J. Weinert and the FOPI collaboration:
New Results from the HELITRON Drift Chamber of the FOPI Detector;
GSI-Report-96-1 (1996) 183

Morokhovskii, V.L., J. Freudenberger, V. Gavrikov, H. Genz, V.V. Morokhovskii, U. Nething, A. Richter, J.P.F. Sellschop:
Special Features of Parametric X-Radiation Type B at Low Electron Energy;
Poster, 17th Int. Conf. on X-Ray and Inner-Shell Processes, Book of Abstracts, 1996

Morokhovskii, V.V., J. Freudenberger, M. Galemann, H. Genz, V.L. Morokhovskii, U. Nething,

A. Richter, J.P.F.Sellschop, R. Zahn:
Linewidth and Shape of Parametric X-Radiation at Low Electron Energy;
Poster, 17th Int. Conf. on X-Ray and Inner-Shell Processes, Book of Abstracts, 1996

Müller, H.:
A Quark Model for Hadron Production;
Proc. of MESON '96 Workshop, Cracow, Poland, May 1996,
APOBB B 27 (11) (1996) p. 3385

Müller, W.F.J., R. Bassini, M. Begemann-Blaich, Th. Blaich, H. Eming, A. Ferrero, S. Fritz, C. Grofl, G. Immè, I. Iori, U. Kleinevoß, G.J. Kunde, W.D. Kunze, V. Lindenstruth, U. Lynen, M. Mahi, A. Moroni, T. Möhlenkamp, B. Ocker, T. Odeh, J. Pochodzalla, G. Raciti, Th. Rubehn, H. Sann, M. Schnittker, A. Schüttauf, C. Schwarz, W. Seidel, V. Serfling, J. Stroth, W. Trautmann, A. Trzcinski, G. Verde, A. Wörner, E. Zude, B. Zwieglinski:
Determination of Critical Exponents in Nuclear Systems;
GSI-Preprint-96-29 (1996)

Müller, M., F.M. Dittes, I. Rotter:
Level Repulsion in the Complex Plane;
European Research Conf. Nuclear Physics: Chaotic Phenomena in Nuclear Physics, Crete (Greece), Sep./Oct. 1996, Contributions, p. 43

Naumann, B., Hassan A., P. Jahn, M. Rogge, M. Steinke, and R. Tölle :
Optimizing the COSY Beam Transport to the TOF-Spectrometer and Investigation of the Beam Properties near the Target;
Verhandl. DPG (VI), 31 (1996) 934

Naumann B., A. Hassan, P. Jahn, R. Maier, M. Rogge, R. Tölle and the COSY-TOF collaboration :
Beam Profile and Phase Space Measurements of the Beam Extracted from COSY;
Int. Workshop on Relativistic Nuclear Physics: from MeVs to TeVs , Sozopol, Bulgaria, 30.9.-5.10.1996

Naumann, L., for the COSY-TOF collaboration:
Experiments with the Magnetless 4π Time of Flight Spectrometer at COSY;
Int. Workshop on Relativistic Nuclear Physics: from MeVs to TeVs , Sozopol, Bulgaria, 30.9.-5.10.1996

Neubert, W., A. Botvina, J. Biegansky, R. Kotte, J. Mösner, D. Wohlfarth and the FOPI collaboration:
Test eines statistischen Modells am Beispiel von zentralen Au auf Au Kollisionen;
Verhandl. DPG (VI), 31 (1996) 914

Neubert, W., J. Biegansky, R. Kotte, J. Mösner, C. Plettner, D. Wohlfarth and the FOPI Collaboration:
Limits of Energy Equilibration in Central Au on Au Collisions in the Proejctile Energy Range from 150 AMeV to 1050 AMeV;
Proc. Int. Workshop Heavy Ion Physics at Low, Intermediate and Relativistic Energies Using 4π Detectors, Poiana Brasov, Romania, Oct. 1996

Oeschler, H., S.P. Avdeyev, W. Karcz, V.A. Karnaukhov, W.D. Kuznetsov, L.A. Petrov, V.K.

Radionov, A.S. Zubkevich, O.V. Bochkarev, L.V. Chulkov, E.A. Kuzmin, W. Neubert, E. Norbeck, A.S. Botvina, D.H.E. Gross:
Multifragmentation mit leichten Projektilen;
Verhandl. DPG (VI), 31 (1996) 851

Pausch, G.:
Limitations of the Pulse-Shape Technique for Particle Discrimination in Planar Si Detectors;
Poster, IEEE Nuclear Science Symposium, Anaheim, California, Nov. 1996

Pausch, G., M. Moszynski, W. Bohne, J. Cederkll, H. Grawe, W. Klamra, M.-O. Lampert, P. Rohr, R. Schubart, W. Seidel, D. Wolski:
Limitations of the Pulse-Shape Technique for Particle Discrimination in Planar Si Detectors;
IEEE Nuclear Science Symposium, Anaheim, California, Nov. 1996;
FZR-157 (1996)

Pausch, G., H. Prade, M.Sobiella, M. Freitag, H. Grawe, K.-H. Maier, M. Moszynski, D. Wolski, R. Schubart, A. Johnson, G. de Angelis:
Ein 4π-Siliziumball als Zusatzdetektor für geladene Teilchen im γ-Spektrometer EUROBALL;
Poster, Spring Meeting "Physik der Hadronen und Kerne", Stuttgart, Mar. 1996
Verhandl. DPG (VI), 31 (1996) 1002

Pausch, G., H. Prade, M. Sobiella, H. Grawe, K.-H. Maier, M. Moszynski, D. Wolski, A. Johnson, R. Schubart, G. de Angelis and the EUROBALL Ancillary Detectors Group:
EuroSiB - a 4π Silicon Ball for Charged Particle Detection in EUROBALL;
Project Description, Research Center Rossendorf, Mar. 1996

Pawelke, J., W. Enghardt, T. Haberer, B.G. Hasch, R. Hinz, M. Krämer, K. Lauckner, M. Sobiella:
In-Beam PET Imaging for the Control of Heavy Ion Tumour Therapy;
IEEE Medical Imaging Conference, Anaheim, CA, USA, Nov. 1996
Abstract Book of the IEEE Nuclear Science Symposium and Medical Imaging Conference, p. 201-205

Peiffer, A., B. Köhler, B.G. Hasch, W. Enghardt:
Sound Radiation Caused by Heavy Ions Stopping in Water and its Possibilities for Dose Distribution Monitoring in Modern Cancer Therapy;
Proc. of the 1995 World Congress on Ultrasonics, Berlin, p. 1095-1098

Persson, E., T. Gorin, I. Rotter:
Decay Rates of Resonance States at High Level Density;
FZR-139 (1996)

Persson, E., T. Gorin, I. Rotter:
Decay Rates of Resonance States at High Level Density;
164. WE-Heraeus-Seminar Quantum Chaos and Dissipation, Günzburg (Germany), Sep. 1996, p. 3 and Poster

Persson, E., T. Gorin, I. Rotter:
Decay Rates of Resonance States at High Level Density;
European Research Conf. Nuclear Physics: Chaotic Phenomena in Nuclear Physics, Crete (Greece), Sep./Oct. 1996, Contributions, p. 46 and Poster

Persson, E., T. Gorin, I. Rotter:
Onset of Chaos in Nuclei at High Level Density;
Poster, European Research Conf. Nuclear Physics: Chaotic Phenomena in Nuclear Physics, Crete (Greece), Sept./Oct. 1996

Persson, E., I. Rotter:
The Trapping Effect and the Optical Model;
Verhandl. DPG (VI), 31 (1996) 878

Peshier, A., B. Kämpfer, G. Soff:
Das SU(3)-Gluon-Plasma als Quasiteilchensystem;
Verhandl. DPG (VI), 31 (1996) 908

Pochodzalla, J., G. Immé, V. Maddalena, C. Nociforo, G. Raciti, G. Riccobene, F.P. Romano, A. Saija, C. Sfienti, G. Verde, M. Begemann-Blaich, S. Fritz, C. Grofl, U. Kleinevoß, V. Lindenstruth, U. Lynen, M. Mahl, W.F.J. Müller, B. Ocker, T. Odeh, T. Rubehn, H. Sann, M. Schnittker, C. Schwarz, V. Serfling, W. Trautmann, A. Wörner, E. Zude, T. Möhlenkamp, W. Seidel, W.D. Kunze, A. Schüttauf, G.J. Kunde, S. Gaff, H. Xi, R. Bassini, I. Iori, A. Moroni, F. Petruzzelli, A. Trzcinski, B. Zwieglinski:
The Nuclear Liquid-Gas Phase Transition: Present Status and Future Perspectives;
GSI-Preprint-96-31 (1996)

Pyatkov, Yu.V., V.V. Pashkevich, Yu.E. Penionzhkevich, V.G. Tichtchenko, A.V. Unzhakova, H.-G. Ortlepp, P. Gippner, C.-M. Herbach, W. Wagner:
Manifestation of Clustering in the ^{252}Cf (sf) and ^{249}Cf(n_{th},f) Reactions;
Third Int. Conf. on Dynamical Aspects of Nuclear Fission, Casta-Papirnicka, Slovak Republic, Aug./Sep. 1996

Reif, J., P. von Brentano, J. Eberth, J. Enders, R.-D. Herzberg, N. Huxel, P. von Neumann-Cosel, N. Nicolay, N. Pietralla, V.Yu. Ponomarev, H. Prade, A. Richter, C. Schlegel, R. Schwengner, T. Servene, S. Skoda, H.G. Thomas, I. Wiedenhöver, G. Winter, A. Zilges:
Photonenstreuung am halbmagischen Kern ^{89}Y;
Verhandl. DPG (VI), 31 (1996) 904

Rotter, I.:
Critical Phenomena at High Level Density;
European Research Conf. Nuclear Physics: Chaotic Phenomena in Nuclear Physics, Crete (Greece), Sep./Oct. 1996, Contributions, p. 49

Rotter, I., M. Müller, E. Persson:
Resonanzphänomene bei großer Niveaudichte in einem energie-abhängigen Formalismus;
Verhandl. DPG (VI), 31 (1996) 878

Rotter, I., M. Müller, V.V. Sokolov:
Critical Phenomena in Open Quantum Systems;
Poster, European Research Conf. Nuclear Physics: Chaotic Phenomena in Nuclear Physics, Crete (Greece), Sep./Oct. 1996

Rotter, I., E. Persson, T. Gorin:
Onset of Chaos in Nuclei at High Level Density;

European Research Conf. Nuclear Physics: Chaotic Phenomena in Nuclear Physics, Crete (Greece), Sep./Oct. 1996, Contributions, p. 50

Rubehn, Th., R. Bassini, M. Begemann-Blaich, Th. Blaich, A. Ferrero, C. Gross, G. Immè, I. Iori, G.J. Kunde, W.D. Kunze, V. Lindenstruth, U. Lynen, T. Möhlenkamp, L.G. Moretto, W.F.J. Müller, B. Ocker, J. Pochodzalla, G. Raciti, S. Reito, H. Sann, A. Schüttauf, W. Seidel, V. Serfling, W. Trautmann, A. Trzcinski, G. Verde, A. Wörner, E. Zude, B. Zwieglinski:
Total and Nuclear Fission Cross Sections of ^{238}U at Relativistic Energies;
GSI-Preprint-96-11 (1996)

Schleif, M., R. Wünsch:
Bestimmung der Masse des Nukleons in Kernmaterie basierend auf solitonische Konfigurationen des NJL-Modells bei endlicher Temperatur und Dichte;
Verhandl. DPG (VI), 31 (1996) 910

Schnare, H., J. Reif, R. Schwengner, G. Winter, Y.A. Akovali, C. Baktash, J. Döring, F.E. Durham, C. Gross, P.F. Hua, M. Korolija, D.R. Lafosse, I.Y. Lee, A. Machiavelli, W. Rathbun, D.E. Sarantites, D.W. Stracener, A. Vandermolen:
Resolution-Enhanced Spectroscopy of High-Spin States in ^{81}Y by Kinematic Doppler-Shift Correction;
Verhandl. DPG (VI), 31 (1996) 904

Schneider, C.:
Untersuchung der Ortsauflösung der Vieldrahtkammern für das ANKE-Spektrometer mit dem Protonenstrahl am COSY;
Verhandl. DPG (VI), 31 (1996) 868

Schüttauf, A., W.D. Kunze, A. Wörner, M. Begemann-Blaich, Th. Blaich, D.R. Bowman, R.J. Charity, A. Cosmo, A. Ferrero, C.K. Gelbke, C. Grofl, W.C. Hsi, J. Hubele, G. Immè, I. Iori, J. Kempter, P. Kreutz, G.J. Kunde, V. Lindenstruth, M.A. Lisa, W.G. Lynch, U. Lynen, M. Mang, T. Möhlenkamp, A. Moroni, W.F.J. Müller, M. Neumann, B. Ocker, C.A. Ogilvie, G.F. Peaslee, J. Pochodzalla, G. Raciti, F. Rosenberger, Th. Rubehn, H. Sann, C. Schwarz, W. Seidel, V. Serfling, L.G. Sobotka, J. Stroth, L. Stuttge, S. Tomasevic, W. Trautmann, A. Trzcinski, M.B. Tsang, A. Tucholski, G. Verde, C.W. Williams, E. Zude, B. Zwieglinski:
Universality of Spectator Fragmentation at Relativistic Bombarding Energies;
GSI-Preprint-96-26 (1996)

Schwengner, R., P. von Brentano, J. Eberth, J. Enders, T. von Egidy, R.-D. Herzberg, N. Huxel, P. von Neumann-Cosel, N. Nicolay, J. Ott, N. Pietralla, H. Prade, J. Reif, A. Richter, W. Schauer, C. Schlegel, H. Schnare, S. Skoda, H.G. Thomas, I. Wiedenhöver, G. Winter, A. Zilges:
Dipolanregungen in ^{122}Te, ^{126}Te und ^{130}Te;
Verhandl. DPG (VI), 31 (1996) 928

Schwengner, R., S. Frauendorf, J. Reif, G. Winter:
Magnetische Rotation in Kernen um $A = 80$;
Verhandl. DPG (VI), 31 (1996) 903

Senger, P., W. Ahner, R. Barth, D. Brill, M. Debowski, E. Grosse, P. Koczo, B. Kohlmeyer, F. Laue, M. Mang, D. Mikowiec, Ch. Müntz, H. Oeschler, F. Pühlhofer, E. Schwab, Y. Shin, J. Speer, R. Stock, H. Ströbele, Ch. Sturm, A. Wagner, W. Waluś:

Kaon Production in Relativistic Nucleus-Nucleus Collisions;
Int. Workshop on Meson Production (MESON '96), Cracow, Poland, May 1996,
Acta Physica Polonica B 27 (1996) 2993

Senger, P., R. Barth, D. Brill, M. Debowski, A. Förster, E. Grosse, P. Koczo, B. Kohlmeyer, F. Laue, M. Mang, H. Oeschler, F. Pühlhofer, E. Schwab, Y. Shin, J. Speer, H. Ströbele, C. Sturm, F. Uhlig, A. Wagner, W. Waluś:
Kaon Production in Hadronic Matter;
Int. Workshop on Strangeness in Hadronic Matter, Budapest, Hungaria, May 1996,
in Acta Physica Hungarica, New Series, Heavy Ion Physics 4 (1996) 317

Senger, P., R. Barth, D. Brill, M. Debowski, A. Förster, E. Grosse, P. Koczo, B. Kohlmeyer, F. Laue, M. Mang, H. Oeschler, F. Pühlhofer, E. Schwab, Y. Shin, J. Speer, H. Ströbele, C. Sturm, F. Uhlig, A. Wagner, W. Waluś:
Kaon Production in Hadronic Matter;
Int. Workshop on Hadrons in Dense Matter;
GSI Darmstadt, Jul. 1996

Senger, P., R. Barth, D. Brill, M. Debowski, A. Förster, E. Grosse, P. Koczo, B. Kohlmeyer, F. Laue, M. Mang, H. Oeschler, F. Pühlhofer, E. Schwab, Y. Shin, J. Speer, H. Ströbele, C. Sturm, F. Uhlig, A. Wagner, W. Waluś:
Kaon and Pion Production in Nuclear Collisions;
Int. Workshop on Meson Physics, Oberjoch, Sep. 1996

Senger, P., R. Barth, D. Brill, M. Debowski, A. Förster, E. Grosse, P. Koczo, B. Kohlmeyer, F. Laue, M. Mang, H. Oeschler, F. Pühlhofer, E. Schwab, Y. Shin, J. Speer, H. Ströbele, C. Sturm, F. Uhlig, A. Wagner, W. Waluś:
Kaon and Pion Production in Nuclear Collisions;
Int. Research Workshop "Heavy Ion Physics at Low, Intermediate and Relativistic Energies Using 4π Detectors", Poiana Brasov, Romania, Oct. 1996,
World Scientific 1996

Skoda, S., P. von Brentano, J. Eberth, J. Enders, R.-D. Herzberg, N. Huxel, L. Kubler, P. von Neumann-Cosel, N. Nicolay, N. Pietralla, H. Prade, J. Reif, A. Richter, C. Schlegel, R. Schwengner, T. Servene, H.G. Thomas, I. Wiedenhöver, G. Winter, A. Zilges:
Nachweis von Dipolanregungen in ^{154}Sm bei 6 MeV mit einem EUROBALL-CLUSTER-Detektor;
Verhandl. DPG (VI), 31 (1996) 955

Sokolov, V.V., I. Rotter, D.V. Savin, M. Müller:
Interfering Doorway States and Giant Resonances I: Resonance Energies, Widths and Dipole Strengths;
FZR-153 (1996)

Sokolov, V.V., I. Rotter, D.V. Savin, M. Müller:
Interfering Doorway States and Giant Resonances II: Cross Section Pattern;
FZR-154 (1996)

Vitko, I., A. Klein, K.-Th. Brinkmann, H. Freiesleben, D. Hilscher, G. Pausch:
Studium von Fusions-Spaltungs-Reaktionen von 220 MeV ^{20}Ne + ^{165}Ho mit LANCER;
Verhandl. DPG (VI), 31 (1996) 950

Wagner, W., C.-M. Herbach, H.-G. Ortlepp, A.A. Aleksandrov, I.A. Aleksandrova, L. Dietterle, V.N. Doronin, S. Dshemuchadse, P. Gippner, D.V. Kamanin, A. Matthies, G. Pausch, Yu.E. Penionzhkevich, G. Renz, K.D. Schilling, D.I. Shishkin, O.V. Strekalovsky, V.G. Tichtchenko, I.P. Tsurin, C. Umlauf, D.V. Vakatov, V.M. Vasko, M. Wilpert, V.E. Zuchko:
The Binary and Ternary Decay of Hot Heavy Nuclei Produced in the Reaction ^{14}N (34 AMeV) + ^{197}Au;
Third Int. Conf. on Dynamical Aspects of Nuclear Fission, Casta-Papirnicka, Slovak Republic, Aug./Sep. 1996,
FZR-163 (1997)

Wagner, W., H.-G. Ortlepp, P. Gippner, C.-M. Herbach:
The Binary Decay of Hot Heavy Nuclei: Fission, Evaporation, and also Flow?
FZR-133 (1996)

Wagner, W., H .-G. Ortlepp, P. Gippner, C.-M. Herbach:
The Binary Decay of Hot Heavy Nuclei: Fission, Evaporation, and also Flow?
XII Winter Workshop on Nuclear Dynamics, Snowbird, Utah, USA, Feb. 1996

Lectures and Seminars

Barz, H.W., F. Dönau, S. Frauendorf, B. Kämpfer, R. Wünsch:
Neue BMBF-Anträge;
Seminar, IKH/FZ Rossendorf, Jan. 1996

Barz, H.W.:
Beschreibung von Fragment-Fragment-Korrelationen in Schwerionenstößen bei mittleren Energien in einem molekulardynamischen Modell;
Spring Meeting "Physik der Hadronen und Kerne", Stuttgart, Mar. 1996

Barz, H.W.:
Zwei-Teilchen-Korrelationen und Coulomb-Korrekturen;
Seminar, IKH/FZ Rossendorf, May 1996

Barz, H.W.:
Fragment-Fragment Correlations and Fragment Flow in Heavy Ion Collisions Described within Molecular Dynamics;
CRIS '96 - 1^{st} Catania Relativistic Ion Studies, Acicastello, Italy, May 1996

Barz, H.W.:
Clustererzeugung in der Molekulardynamik;
Seminar, IKH/FZ Rossendorf, Nov. 1996

Dönau, F.:
Die Bandenkreuzung in ^{77}Rb - ein ungewöhnlicher Fall;
Spring Meeting "Physik der Hadronen und Kerne", Stuttgart, Mar. 1996

Dönau, F.:
Vom mittleren Feld zur Kollektivbewegung großer Amplituden in Atomkernen;
Seminar, TU Dresden, Jul. 1996

Dönau, F.:
The Positive Parity Band Crossing in ^{77}Rb - a Case of Deformation Alignment?
Seminar, Joint Institute of Heavy Ion Research, Oak Ridge, USA, Sep. 1996

Dönau, F.:
The Fall of the C4-Symmetry in Rotational Bands;
Seminar, Department of Physics, University of Tennessee, Knoxville, USA, Sep. 1996

Enghardt, W.:
A Positron Emission Tomograph for In-Situ Monitoring of Heavy Ion Tumour Therapy;
Seminar, ECAT Technical Users Meeting, Stockholm Sweden, Apr. 1996

Enghardt, W.:
Tumortherapie mit Strahlen schwerer Ionen;
Lecture Course, TU Dresden, Fakultät für Elektrotechnik, Institut für Biomedizinische Technik, Jun. 1996

Enghardt, W.:
Simultan-Kontrolle der Tumorbehandlung mit Strahlen schwerer Ionen durch Positronen-Emissions-Tomographie;
Seminar, TU Dresden, Nov. 1996

Frauendorf, S.:
Statistischer Zerfall von Alkali-Clustern;
Seminar, IKH/FZ Rossendorf, Feb. 1996

Frauendorf, S.:
Fragmentation of Hot Alkali Clusters;
ICW-96, Col de Port, France, Feb. 1996

Frauendorf, S.:
Kerne und Cluster;
Spring Meeting "Physik der Hadronen und Kerne", Stuttgart, Mar. 1996

Frauendorf, S.:
Magnetic Rotation;
NORDITA Study Weekend on EUROBALL Physics, Copenhagen, Danmark, May 1996

Frauendorf, S.:
Magnetismus in Clustern und Beziehungen zur Hochspinphysik;
Seminar, IKH/FZ Rossendorf, Jun. 1996

Frauendorf, S.:
Tilted Rotation of Weakly Deformed and Triaxial Nuclei;
Int. Conference on Nuclear Structure around the Turn of the Century, Crete, Greece, Jun./Jul. 1996

Frauendorf, S.:
Persistent Currents in Clusters and Nuclei;
Nuclear Physics Forum, Nuclear Science Division Colloquium, Lawrence Berkeley Laboratory, Berkeley, USA, Jul. 1996

Frauendorf, S.:
Magnetic Rotation;
Nuclear Physics Forum, Nuclear Science Division Colloquium, Lawrence Berkeley Laboratory, Berkeley, USA, Jul. 1996

Frauendorf, S.:
Tilted Cranking;
Congress Commemorating the 30th Anniversary of the Brasilian Physical Society, Aguas de Lindeois, Brasil, Sep. 1996

Frauendorf, S.:
Mesoscopic Aspects of Nuclei;
Fall Meeting of the American Physical Society, Division of Nuclear Physics, Massachusetts Institute of Technology, Cambridge, USA, Oct. 1996

Frauendorf, S.:
Tilted Rotation of Weakly Deformed and Triaxial Nuclei;
EUROBALL User Meeting, University of Padua, Italy, Oct. 1996

Frauendorf, S.:
High Spin Physics;
Graduiertenkolleg of the Department of Physics, University of Tübingen, Germany, Dec. 1996

Gorin, T.:
Intensitätsgewichtete Maße für Spektren offener Quantensysteme;
Spring Meeting "Physik der Hadronen und Kerne", Stuttgart, Mar. 1996

Gorin, T.:
Statistische Maße von offenen Quantensystemen;
Seminar, IKH/FZ Rossendorf, Apr. 1996

Gorin, T.:
Korrelationen zwischen Resonanzen in einem statistischen Streumodell;
Seminar, TU Dresden, Institut für Theoretische Physik, Nov. 1996

Grinberg, M.:
Low-Lying J = 1 Excited States in Spherical Even-Even Nuclei;
Seminar, IKH/FZ Rossendorf, Apr. 1996

Grinberg, M.:
Nuclear Vibrational Modes and the Problem of Self-Consistency;
Seminar, IKH/FZ Rossendorf, Nov. 1996

Grosse, E.:
Previous and Future Activities at Rossendorf;
FOBOS-Meeting, GSI Darmstadt, Nov. 1996

Grosse, E.:
High Brilliance e-Beams and FEL-Operation;
Seminar, Paul Scherrer Institute, Villigen, Switzerland, Sep. 1996

Herbach, C.-M.:
Decay Study of Hot Nuclei below the Multifragmentation Threshold with the FOBOS Detector at Dubna;
Seminar, IKH/FZ Rossendorf, Oct. 1996

Herbach, C.-M.:
Analysis of Fission Fragments Produced in the Reaction ^{14}N (53 AMeV) + ^{197}Au and ^{232}Th;
FOBOS-Meeting, GSI Darmstadt, Nov. 1996

Herbach, C.-M.:
Drei-Fragment-Zerfälle nach zentralen Stößen in den Reaktionen ^{14}N (53 AMeV) + ^{197}Au und ^{232}Th;
Seminar, HMI Berlin, Dec. 1996

Hinz, R.:
A Method for In-Vivo Treatment Plan Verification of Heavy-Ion Tumour Therapy by Positron Emission Tomography;
V. International Conference on Application of Physics in Medicine and Biology, Trieste, Italy, International Centre of Theoretical Physics, Sep. 1996

Kamanin, D.V.:
Results of the Light Particle Data Analysis;
FOBOS-Meeting, GSI Darmstadt, Nov. 1996

Kämpfer, B.:
Quantenelektrodynamik;
Lecture Course, TU Dresden, WS 1995/1996

Kämpfer, B.:
Kosmologie;
Lecture Course, TU Dresden, SS 1996

Kämpfer, B.:
Quantenchromodynamik;
Lecture Course, TU Dresden, WS 1996/1997

Kämpfer, B.:
Modelle zur Partonenevolution in ultrarelativistischen Schwerionenstößen;
Seminar, IKH/FZ Rossendorf, Jan. 1996

Kämpfer, B.:
Dileptons from Parton Matter Resulting in Ultrarelativistic Heavy-Ion Collisions;
12. Meeting on Nuclear Dynamics, Snowbird, USA, Feb. 1996

Kämpfer, B.:
Electromagnetic Signals from Deconfined Matter;
Seminar, LBL Berkeley, USA, Feb. 1996

Kämpfer, B.:
IMF Correlations in Central Collisions of Au + Au at 100 - 400 AMeV;
Seminar, LBL Berkeley, USA, Feb. 1996

Kämpfer, B.:
Real Photon and Dilepton Production in Expanding, Equilibrating and Hadronizing Parton Matter;
Int. Conference on Nuclear Physics at the Turn of the Millenium, Wilderness, Südafrika, Mar. 1996

Kämpfer, B.:
Dileptons;
Seminar, Uni Kapstadt, Südafrika, Mar. 1996

Kämpfer, B.:
Dileptons: HADES - ALICE;
Workshop HADES in Rez, CSSR, Jun. 1996

Kämpfer, B.:
$\gamma\gamma$- and IMF-IMF Correlations;
Seminar, ECT Trento, Italy, Sep. 1996

Kämpfer, B., P. Michel, K. Müller:
Assoziierte Strangenessproduktion - Diskussion eines zukünftigen TOF-Experimentes;
Seminar, IKH/FZ-Rossendorf, Dec. 1996

Lauckner, K.:
Ein Verfahren zur in-vivo Kontrolle der Bestrahlungsplanung bei der Schwerionen-Tumortherapie mittels Positronen-Emissions-Tomographie;
Gemeinsame Jahrestagung der Deutschen, der Österreichischen und der Schweizerischen Gesellschaft für biomedizinische Technik, Zürich, Schweiz, Sep. 1996

Kolomeitsev, E.E.:
Pionengasmodell;
Seminar, IKH/FZ Rossendorf, Jul. 1996

Müller, H.:
K^- - Production at COSY;
Spring Meeting of the Institute of Nuclear and Hadronic Physics, Holzhau, Mar. 1996

Müller, H.:
Diskussion zum ROC-Modell für Hadronenproduktion;
Seminar, IKH/FZ Rossendorf, Oct. 1996

Naumann B.,
Untersuchung des physikalischen Untergrundes bei Experimenten an COSY-TOF bei p=0.88 GeV/c;
COSY-TOF Analyse-Meeting, TU Dresden, 7./8.5.1996

Naumann L.,
Untersuchungen zur Bestimmung der Nachweiseffektivitäten einzelner Spektrometerelemente des COSY-TOF bei p=0.88 GeV/c;
COSY-TOF Analyse-Meeting, TU Dresden, 7./8.5.1996

Naumann L.,
Untersuchung des physikalischen Untergrundes bei bei 880 und 777 MeV/c;
TOF-Meeting, FZ Jülich, 14.6.1996

Naumann L.,
Gedanken zum Einsatz des Dresdner Neutronen-Detektors für das Bremsstrahlungsexperiment an der Pionenproduktionsschwelle;
COSY-TOF Arbeitstreffen, TU Dresden, 26./27.8.199

Nething, U.:
Erste Auslegung des Strahlführungssystems der ELBE-Quelle;
Seminar, IKH/FZ Rossendorf, Jan. 1996

Nething, U.:
Grundlagen der Channelingstrahlung;
Seminar, IKH/FZ Rossendorf, Jun. 1996

Nething, U.:
Neuartige Strahlungsquellen im Röntgenbereich;
Seminar, IKH/FZ Rossendorf, Nov. 1996

Ortlepp, H.-G.:
The FOBOS (and ARGUS) Detector and Recent Experiments;
FOBOS-Meeting, GSI Darmstadt, Nov. 1996

Pausch, G.:
Identification of Light Charged Particles and Intermediate-Mass Fragments in Silicon Detectors by Means of Pulse-Shape Discrimination: Test Experiments and Applications;
Seminar, GANIL, Caen, France, Mar. 1996

Pausch, G.:
Status of EuroSiB - a Silicon Ball for Charged-Particle Detection in EUROBALL;
Extended EUROBALL LCP Ancillary Detectors Meeting, C.E.N.B.G. Bordeaux Gradignan, France, May 1996

Pausch, G.:
EuroSiB - ein Siliziumball zum Nachweis geladener Teilchen in EUROBALL;
Seminar, LMU München, Beschleunigerlaboratorium, Garching, Jul. 1996

Pausch, G.:
EuroSiB - an Advanced Si-Ball for LCP Detection in EUROBALL;
EUROBALL Users Meeting, Padova, Italy, Oct. 1996

Pawelke, J.:
In-Beam PET Imaging for the Control of Heavy Ion Tumour Therapy;
IEEE Medical Imaging Conference, Anaheim, CA, USA, Nov. 1996

Persson, E.:
Decay Rates of Resonance States at High Level Density;
Seminar, IKH/FZ Rossendorf, Feb. 1996

Persson, E.:
Resonance Phenomena at High Level Density;
Spring Meeting "Physik der Hadronen und Kerne", Stuttgart, Mar. 1996

Peshier, A.:
The Gluon-Plasma as a Quasi-Particle System;
Seminar, TU Dresden, May 1996

Peshier, A.:
The Gluon-Plasma near T_c as a Quasi-Particle System;
Seminar, Universitt Regensburg, Jul. 1996

Pfitzner, A.:
Dynamik von Dichtefluktuationen im Kern;
Seminar, IKH/FZ Rossendorf, Dec. 1996

Prade, H.:
Das ELBE-Projekt in Rossendorf;
Seminar, Universitt Stuttgart, Jul. 1996

Reif, J.:
Photonenstreuung am halbmagischen Kern ^{89}Y;
Spring Meeting "Physik der Hadronen und Kerne", Stuttgart, Mar. 1996

Rotter, I.:
Synergetik;
Lecture Course, TU Dresden, WS 1996/1997

Rotter, I.:
Time Scales and Chaos in Quantum Mechanical Many-Body Systems;
Seminar, Max-Planck-Institut für Physik komplexer Systeme, Dresden, Jan. 1996

Rotter, I.:
Trappingeffekt und optisches Modell;
Spring Meeting "Physik der Hadronen und Kerne", Stuttgart, Mar. 1996

Rotter, I.:
Time Scales and Chaos in Quantum Mechanical Many-Body Systems;
The Russian-German Workshop Collective Modes in Fission: Regular and Chaotic Aspects, Dubna, Russia, Sep. 1996

Rotter, I.:
Kritische Phnomene in offenen Quantensystemen;
Seminar, IKH/FZ Rossendorf, Oct. 1996

Rotter, I.:
Kritische Phnomene in offenen Quantensystemen;
Seminar, TU Dresden, Institut für Theoretische Physik, Nov. 1996

Rotter, I.:
Critical Phenomena in Open Quantum Systems;
International Workshop on Nuclear Giant Resonances, Trento, Italy, Dec. 1996

Prade, H.:
Das Rossendorfer ELBE-Projekt;
Seminar, Institut für Strahlenphysik, Universitt Stuttgart, Jul. 1996

Schleif, M.:
Träge Masse des NJL-Solitons im Medium;
Spring Meeting "Physik der Hadronen und Kerne", Stuttgart, Mar. 1996

Schleif, M.:
Das NJL-Soliton im heißen Medium;
Seminar, IKH/FZ Rossendorf, Oct. 1996

Schleif, M.:
NJL-Soliton im Wärmebad;
Seminar, TU Dresden, Nov. 1996

Schnare, H.:
Resolution-Enhanced Spectroscopy of High-Spin States in ^{81}Y by Kinematic Doppler-Shift Correction;
Spring Meeting "Physik der Hadronen und Kerne", Stuttgart, Mar. 1996

Schwengner, R.:
Magnetische Rotation in Kernen um A = 80;
Spring Meeting "Physik der Hadronen und Kerne", Stuttgart, Mar. 1996

Schwengner, R.:
Dipolanregungen in ^{122}Te, ^{126}Te und ^{130}Te;
Spring Meeting "Physik der Hadronen und Kerne", Stuttgart, Mar. 1996

Schwengner, R.:
Experiments with EUROBALL CLUSTER Detectors;
Spring Meeting of the Institute of Nuclear and Hadronic Physics, Holzhau, Mar. 1996

Schwengner, R.:
Dipole Excitations in ^{122}Te, ^{126}Te and ^{130}Te – Nuclear Resonance Fluorescence Experiments at the S-DALINAC with One EUROBALL CLUSTER Detector –;
Int. Conference on Nuclear Structure Around the Turn of the Century, Kreta, Jun./Jul. 1996

Servene, T.:
Investigation of the Magnetic Dipole Band in ^{79}Br with EUROBALL CLUSTER Detectors;
Workshop on Experiments with German EUROBALL CLUSTER Detectors, Heidelberg, Nov. 1996

Wagner, W.:
Report on First Measurements with FOBOS;
12. Meeting on Nuclear Dynamics, Snowbird, USA, Febr. 1996

Wagner, W.:
Symmetric and Asymmetric Mass Splits in the Fission of Hot Nuclei – the ^{14}N (34 AMeV) on ^{197}Au Results;
FOBOS-Meeting, GSI Darmstadt, Nov. 1996

Wünsch, R.:
The Nambu-Jona-Lasinio Soliton in Hot Matter;
Seminar, IKH/FZ Rossendorf, Jul. 1996

Wünsch, R.:
The NJL Soliton in a Medium of Constituent Quarks;
Seminar, Univ. Bochum, Aug. 1996

Wünsch, R.
The NJL Soliton in a Heat Bath;
Seminar, Univ. Tübingen, Sep. 1996

Yanez, R.:
Theoretical Model Calculations of the Reaction ^{14}N (53 AMeV) + ^{197}Au;
FOBOS-Meeting, GSI Darmstadt, Nov. 1996

Zahn, R.:
Grundlagen der Parametrischen Röntgenstrahlung;
Seminar, IKH/FZ Rossendorf, Jun. 1996

Zahn, R.:
Neuartige Strahlungsquellen im Röntgenbereich;
Seminar, IKH/FZ Rossendorf, Nov. 1996

Talks of Visitors

Avakian, R.O., Jerevan:
Monoenergetic X-Ray Sources at the Crystaline Radiator;
Mar. 7, 1996

Christov, C.V., Bochum:
Baryons as Non-Topological Solitons;
Feb. 8, 1996

de Angelis, G., Legnaro:
New Experimental Results from the GASP Array (Legnaro);
May 6, 1996

Eyrich, W., Erlangen:
Assoziierte Strangeness-Produktion in pp- und $\bar{p}p$-Reaktionen;
Dec. 10, 1996

Geissel, H., Darmstadt:
Neue atom- und kernphysikalische Experimente mit relativistischen Schwerionen am FRS-ESR der GSI Darmstadt;
Aug. 29, 1996

Hammer, W., Stuttgart:
Schlüsselreaktionen im Helium-Brennen der Sterne
Aug. 12, 1996

Hansen, W., Dresden:
Zum Konzept eines beschleunigergetriebenen, unterkritischen Th^{232}/U^{233}–Brutreaktors zur Energiegewinnung;
Jun. 20, 1996

Hass, M., Rehovot:
Parity Non-Conservation in the Gamma Decay of Polarized $^{93}Tc(17/2^-)$;
Oct. 23, 1996

Heiss, W.D., Witwatersrand:
Chaotic Motion in the Modified Nilsson Model;
Jul. 1, 1996

Jolos, R.V., Köln:
Parity Splitting in Nuclei with Strong Octupole Correlations;
Apr. 10, 1996

Kruglov, V., Dubna:
A New High-Current Mode of Wire Chamber Performance;
Jul. 15, 1996

Kühn, W., Gießen:
Hadronische Materie unter extremen Bedingungen: Dileptonen-Spektroskopie mit HADES;
Nov. 4, 1996

Kvasil, J., Prag:
Residual Interaction in the Nuclear Hamiltonian and the Properties of Low-Lying States in Deformed Nuclei;
Oct. 25, 1996

Magner, A., Kiev:
Semiclassical Analysis of the Supershell Structure in Spherical Metal Clusters;
Apr. 22, 1996

Meng, J., München:
Relativistic Hartree - Bogoliubov Theory for Drip Line Nuclei;
Aug. 19, 1996

Nazmitdinov, R., Dubna:
Shell Effects in Mesoscopic Systems: Metallic Clusters, Quantum Dots;
Jun. 18, 1996

Nitta, H., Tokyo:
Effect of Dynamical Diffraction on Channeling Radiation;
Dec. 10, 1996

Polyakov, M.V., Petersburg:
Parton Distributions from the Chiral Soliton;
Oct. 16, 1996

Reinhardt, H., Tübingen:
Chirale Quark-Flavor-Dynamic;
Nov. 11, 1996

Sokolov, V.V., Novosibirsk:
Interfering Doorway States and Giant Resonances;
Jun. 24, 1996

Sujkowski, Z., Warschau:
Giant Resoances and the Compressibility of Nuclear Matter;
May 23, 1996

Yanez, R.A., Uppsala:
Fission and Heavy Fragment Formation in Intermediate-Energy Heavy-Ion Reactions;
Feb. 26, 1996

THE INSTITUTE OF NUCLEAR AND HADRON PHYSICS

Departments of the Institute

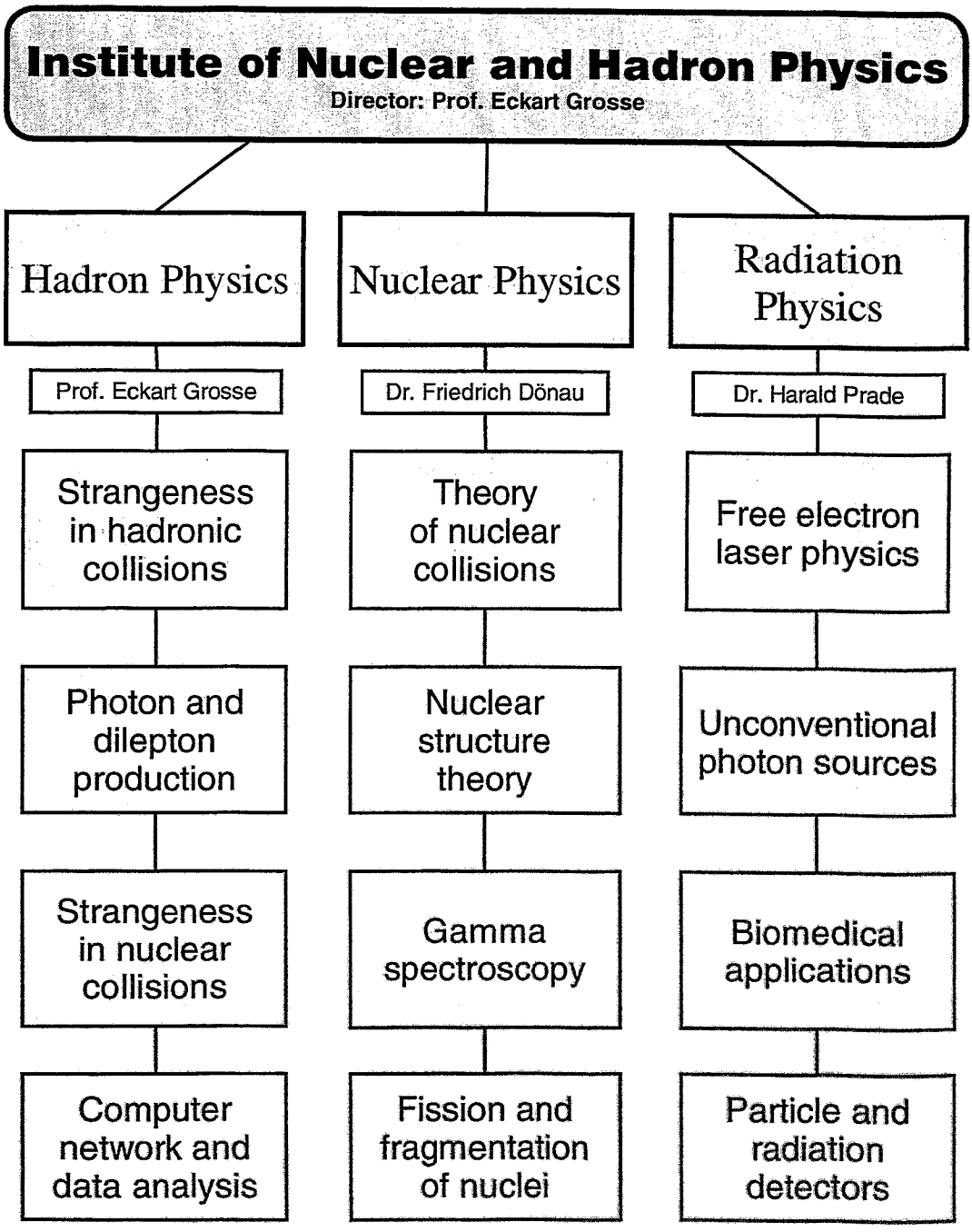

Personnel of the Institute for Nuclear and Hadron Physics

Director: Prof. E. Grosse[1]

Sientific Personnel

Dr. H.W. Barz [1]
L. Dietterle
Dr. F.M. Dittes
Dr. F. Dönau
Dr. S. Dshemuchadse
Dr. W. Enghardt[1]
Dr. S. Frauendorf
Dr. P. Gippner
Dr. C.-M. Herbach
Dr. B. Kämpfer[1]
Dr. L. Käubler[1]
Dr. Th. Kirchner
Dr. R. Kotte
Dr. A. Matthies
Dr. P. Michel
Dr. Th. Möhlenkamp
Dr. K. Möller[1]
Dr. J. Mösner
Dr. H. Müller
Dr. B. Naumann
Dr. L. Naumann
Dr. W. Neubert
Dr. U. Nething
Dr. H.-G. Ortlepp
Dr. G. Pausch
Dr. J. Pawelke
Dr. H. Prade
Dr. J. Reif
G. Renz
Prof. I. Rotter[1]
A. Schamlott
Dr. K.D. Schilling
Dr. H. Schnare
Dr. M. Schlett
Dr. R. Schwengner
Dr. W. Seidel
Dr. S. Skoda
Dr. W. Wagner
Dr. G. Winter
D. Wohlfarth
Dr. R. Wünsch
Dr. R. A. Yanez
Dr. R. Zahn

PhD Students

J. Biegansky
T. Gorin
B.G. Hasch
R. Hinz
D. Kamanin
E. Kolomeitsev
J. Krüger
K. Lauckner
E. Persson
A. Peshier
C. Plettner
M. Schleif
Chr. Schneider
A. Schülke
Th. Servene

Technical Personnel

M. Altus
H. Angermann
U. Baumann
J.U.Berlin
M. Boeck
M. Böse
J. Fiedler
R. Förster
M. Freitag
L. Göbel
K. Heidel
K.H. Hermann
J. Hutsch
J. Kerber
E. Kluge
M. Langer
B. Meier
M. Paul
B. Prietzschk
I. Prob
B. Rimarzig
H. Römer
M. Scheinpflug
Chr. Schneidereit
W. Schulze
M. Sobiella
A. Uhlmann
C. Umlauf

[1]also TU Dresden

Guest Scientists

Prof. W. Andrejtscheff	INRE Sofia
Prof R. Avakian	Universität
Ch.J. Chiara	University Stony Brook
Prof. D. Rostilav	VIK Dubna ,
K. Hansen	NBI Kopenhagen
Prof. D. Heiss	Universität Johannesburg
D. Jenkins	University of York
A. Kacharava	VIK Dubna
Dr. L. Kaptari	VIK Dubna
Dr. V. Kruglov	VIK Dubna
Dr. Y.N. Lobach	Inst. für Kernforschung Kiev
Dr. N. Kusmenko	Radiuminstitut St. Petersburg
Dr. A. Magner	Inst. f. Nuclear Research Kiev
P. Meier	Universität Regensburg
Prof. V. Michailov	Universität Petersburg
Prof. M. Moszynski	Soltan-Institute Swierk
Dr. R. Nazmitdinov	VIK Dubna
Prof. H. Nitta	Gakugei University Toky
Dr. V.V. Pashkevich	VIK Dubna
Dr. O. Pavlenko	Inst. F. Theor.Physik Kiev
St. Reimann	NBI Kopenhagen
Dr. A. Sanzhur	Inst. für Kernforschung Kiev
Prof. V.V. Sokolov	Inst. of Nuclear Physics Nowosobirsk
Dr. O.V. Strekalowskij	VIK Dubna
V.G. Tichtchenko	VIK Dubna
Prof. A.I. Titov	VIK Dubna
D. Wolski	Soltan Institute Swierk
Dr. N.I. Zhuravlev	VIK Dubna